12-2013

Decoding the `Nature Encoded' Messages for Wireless Networked Control Systems

Shuping Gong
University of Tennessee - Knoxville, sgong1@utk.edu

To the Graduate Council:

I am submitting herewith a dissertation written by Shuping Gong entitled "Decoding the `Nature Encoded' Messages for Wireless Networked Control Systems." I have examined the final electronic copy of this dissertation for form and content and recommend that it be accepted in partial fulfillment of the requirements for the degree of Doctor of Philosophy, with a major in Electrical Engineering.

Husheng Li, Major Professor

We have read this dissertation and recommend its acceptance:

Qing Cao, Seddik M. Djouadi, Xueping Li

Accepted for the Council:

Carolyn R. Hodges

Vice Provost and Dean of the Graduate School

(Original signatures are on file with official student records.)

Decoding the 'Nature Encoded' Messages for Wireless Networked Control Systems

A Dissertation Presented for the

Doctor of Philosophy

Degree

The University of Tennessee, Knoxville

Shuping Gong

December 2013

Acknowledgements

I would like to thank my advisor, Dr. Husheng Li, for his continous support and guidance throughput my Ph.D. studies, which allow me to develop my skills as a resercher. I would further like to thank the other members of my committee: Dr. Seddik M. Djouadi, Dr. Qing Cao, and Dr. Xueping Li. Their time and input to this dissertation is greatly appreciated.

I am very thankful to newton HPC program for providing me the simulation platform to verify my algorithms. In particular, I would like to thank Gerald Ragghianti for his help and support for me to run simulation with newton HPC program. Within my group, I would like to thank my fellow graduate labmates, Depeng Yang, Kun Zheng, Rukun Mao, Hannan Ma, Qi Zeng, Zhenghao Zhang, Yifan Wang, and Jingchao Bao. I enjoyed the conversations and discussions with them that have given me much insights about my research.

Finally, I would like to express my appreciation and love to my wife Fang Mao and my parents. They have always been proud and supportive of my Ph.D. studies.

Abstract

Because of low installation and reconfiguration cost wireless communication has been widely applied in networked control system (NCS). NCS is a control system which uses multi-purpose shared network as communication medium to connect spatially distributed components of control system including sensors, actuator, and controller. The integration of wireless communication in NCS is challenging due to channel unreliability such as fading, shadowing, interference, mobility and receiver thermal noise leading to packet corruption, packet dropout and packet transmission delay.

In this dissertation, the study is focused on the design of wireless receiver in order to exploit the redundancy in the system state, which can be considered as a 'nature encoding' for the messages. Firstly, for systems with or without explicit channel coding, a decoding procedures based on Pearl's Belief Propagation (BP), in a similar manner to Turbo processing in traditional data communication systems, is proposed to exploit the redundancy in the system state. Numerical simulations have demonstrated the validity of the proposed schemes, using a linear model of electric generator dynamic system.

Secondly, we propose a quickest detection based scheme to detect error propagation, which may happen in the proposed decoding scheme when channel condition is bad. Then we combine this proposed error propagation detection scheme with the proposed BP based channel decoding and state estimation algorithm. The validity of the proposed schemes has been shown by numerical simulations.

Finally, we propose to use MSE-based transfer chart to evaluate the performance of the proposed BP based channel decoding and state estimation scheme. We focus on two models to evaluate the performance of BP based **sequential** and **iterative** channel decoding and state estimation. The numerical results show that MSE-based transfer chart can provide much insight about the performance of the proposed channel decoding and state estimation scheme.

Table of Contents

List of Tables

List of Figures

Chapter 1

Introduction

1.1 Wireless Networked Control System

Networked control system (NCS), which uses multi-purpose shared network as communication medium to connect spatially distributed components of control system including sensors, actuator, controller, leads to flexible architecture of control system and generally reduces installation and maintenance cost for control system. Therefore, NCS has been applied in a wide range of areas such as chemical processes, power plants, airplanes, vehicles, mobile sensor networks, and remote surgery. As shown in Figure 1.1, a NCS includes a dynamic system, a sensor, an estimator, a controller and an actuator. The controller is used to monitor and control the dynamic system so as to make sure that the dynamic system runs toward the specified goal, such as stability, performance. The monitoring of the dynamic system is provided by the collaboration of sensor, network and estimator. The sensor measures the system state at given times; and then the information related to current system state measurement is sent over network and utilized by estimator to obtain estimate of current system state. The controlling actions made by controller is sent over network and imposed to the dynamic system by the actuator.

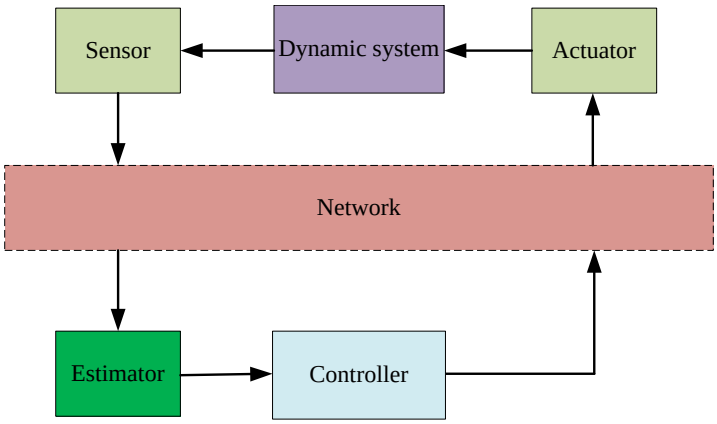

Figure 1.1: An illustration of networked control system (NCS)

Wireless networked control system (WNCS) uses wireless communication such as 802.15.4(Song et al., 2009)(Godoy et al., 2012)(Yen et al., 2013), 802.11 (Lee et al., 2008)(Boggia et al., 2008) (Refaat et al., 2010), 3G network (Chen et al., 2011), as networking technology. Comparing with other networking technologies, such as field bus, Ethernet and optical network, the advantage of wireless communication is faster deployment, lower installation and reconfiguration cost. Therefore, WNCS has been widely used in many areas such as agriculture (Kim et al., 2008),(Song, 2010),(Chen et al., 2011), bio-medicine (Chen et al., 2007)(Chen et al., 2009), power system (Han and Lim, 2010)(Kang et al., 2011), transportation (Chen et al., 2005)(Jing et al., 2007).

Although wireless communication has many advantages over other networking technologies, wireless communication has its own disadvantages due to time-varying channels, limited spectrum and transmission power, and interference. WNCS has the following challenges:

1. Limited data rate

   Limited data rate leads to low resolution of the transmitted data which introduces large quantization errors impinging on control performance. The causes for limited data rate include limited spectrum resources, limited transmission power, bad channel condition, and resource sharing among

multiple users. For example, the maximum data rate of IEEE 802.15.4 is 250kbps. Even if some wireless technologies such as IEEE 802.11 can provide high data rate transmission, with the increasing number of devices and applications in WNCS, the effectively allocated data rate for each device is still low.

2. Packet data corruption

   Packet data corruption can not only introduce communication noise to control system if packets with error are kept, but also increase packet transmission delay due to retransmission and packet dropout. The causes for packet data corruption are interference, fading, multi-path effects. For applications which are not sensitive to delay, packet data corruption can be compensated by retransmission. However, as pointed out by Mostofi and Murray (2009c) some applications has stringent delay requirement. For such applications retransmitted packets which miss deadline are useless.

3. Packet delay

   The control system is sensitive to packet delay due to real time requirement. However, the focus of research on communication side is the accuracy of data transmission instead of packet delay. Packet delay includes network access time (i.e., the interval between the transmitter receives the data and transmitter starts to transmit over network) and packet transmission time (i.e., the interval between transmitter starts to transmit the data and transmitter finish transmitting the data). The network access delay is due to resource competition during multiple users, and is not guaranteed during network congestion. The network transmission delay is due to transmission time over medium, transmission error leading to multiple transmission, and transmission over many hops.

4. Packet dropout

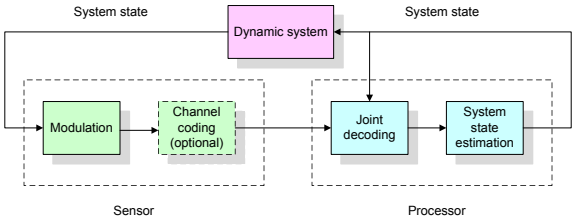

Figure 1.2: An illustration of the communication procedure and dynamic system.

Packet dropout is caused by transmission error, buffer overflow due to congestion and long transmission delay in which received packets are useless for controller.

1.2 Motivation

This dissertation focuses on packet data corruption issue on the condition that there is stringent delay requirement. In this context there are two challenges to design the decoding procedure at the wireless receiver. One challenge is that the conventional decoding procedure utilizing redundancy from channel coding does not work. This is because there is no or weak channel coding protection due to the timing requirement. The other challenge is that performance evaluation framework for system state estimation has to handle a hybrid system: continuous system state/observation and discrete information bits in wireless communication system. The performance of system state estimation is impacted by two parts: control system itself and the wireless system. For the control system, system state changes over time. In addition, system observation is impacted by observation noise. For the communication system, the transmitted information bits are quantized system observation. Therefore, a good performance evaluation framework should take into account both correlation of system state in time domain and performance of wireless system in discrete domain. Note that system performance evaluation plays significant role in designing a good system. This is because system performance evaluation can not only help evaluate the performance of the system but also help obtain much insights about the system leading to design enhancement.

We propose to *exploit the redundancy in the system state, which can be considered as a 'nature encoding' for the messages*. A linear system model is adopted, where $\mathbf{x}(t+1) = \mathbf{A}\mathbf{x}(t) + \mathbf{B}\mathbf{u}(t) + \mathbf{n}(t)$ is used to describe the dynamics of system state $\mathbf{x}$ subject to the control $\mathbf{u}(t)$ and noise $\mathbf{n}(t)$. We observed that the system state is similar to the convolutional codes except that the 'encoding' of the system state is in the real field instead of the Galois field. Hence, the message actually has been channel coded by the nature although no explicit or little explicit channel coding is used at the transmitter.

1.3 Contributions

The contribution of this dissertation work can be summarized as follows:

Firstly, we propose to *exploit the redundancy in the system state, which can be considered as a 'nature encoding' for the messages*. We use both schemes of Kalman filtering and Pearl's Belief Propagation (BP) for the soft decoding, combined with the soft demodulation to improve the reliability of demodulation and decoding. A practical dynamic system for electric generator dynamic system is used for numerical simulation, which demonstrates the performance gain of incorporating the inherent redundancy in the 'nature encoding'. The procedure is illustrated in Figure 1.2. Note that such a scheme is similar to the *Turbo processing techniques* like Turbo decoding (Berrou et al., 1993), Turbo multiuser detection (Alexander et al., 1999) and Turbo equalization (Tüchler et al., 2002) in wireless communication systems. However, the 'nature encoding' is analog and implicit, thus resulting in a different processing procedure.

Firstly, for systems with or without explicit channel coding, a decoding procedures based on Pearl's Belief Propagation (BP), in a similar manner to Turbo processing in traditional data communication systems, is proposed. Numerical simulations have demonstrated the validity of the schemes, using a linear model of electric generator

dynamic system. One disadvantage of this proposed scheme is that there is error propagation at low SNR for uncoded system.

Secondly, we propose a quickest detection based error propagation detection scheme to detect error propagation online. Then we combine this proposed error propagation detection scheme with the proposed BP based channel decoding and state estimation algorithm. The numerical results show that error propagation is eliminated and consistent performance gain is observed in the proposed BP based channel decoding and state estimation with protection of error propagation detection.

Finally, we propose to use MSE-based transfer chart to evaluate the performance of BP based channel decoding and state estimation. We focus on two models, BP based **sequential** and **iterative** channel decoding and state estimation. The first model is used to evaluate the performance of sequential channel decoding and state estimation over time slots; and the second model is used to evaluate the performance of iterative channel decoding and state estimation over two time slots. The numerical results show that MSE-based transfer chart can provide much insight about the performance of the proposed BP based channel decoding and state estimation algorithm.

1.4 Dissertation Outline

The remainder of this dissertation is organized as follows. Literatures on the topics listed above are surveyed in next chapter, chapter 2. Chapter 3,4 and 5 report main work of this dissertation: a) chapter 3 presents the proposed BP based channel decoding and state estimation procedure; b) chapter 4 shows the proposed error propagation detection scheme and how to utilize it eliminate error propagation of the proposed BP based channel decoding and state estimation scheme; c) chapter 5 demonstrates the proposed MSE-based transfer chart performance evaluation framework and how to use it to evaluate the performance of proposed channel decoding and system state estimation procedure. We conclude this dissertation, and then outline future work in chapter 6.

Chapter 2

Literature Review

In this chapter we briefly review the existing works that are relevant to the topics in this dissertation. Discussions include state estimation in NCS, evaluation for the relationship between the operation of network and quality of control system, channel coding and decoding and its performance evaluation in communication system.

2.1 State Estimation in NCS

The task of state estimation is to estimate system state at the remote controller side by using information transmitted from plant over lossy network, which may corrupt, delay, or drop transmitted information. The commonly used framework for state estimation is shown in Figure 2.1. The output signals are measured by sensors at given time, optionally processed by local processor, sent via digital network, recovered by estimator at the remote controller side. Note that local processor at the plant side is optional, and it requires extra computation capability at the plant side.

For the framework without local processor at the plant side, the measurement of system observation is transmitted over the network. However, data may be corrupted, delayed or dropped while being trasmitted over network. In most works, it is assumed that erroneous packets are discarded at the estimator side. Therefore, estimator receives only correctly received packets, and is impacted by packet dropout

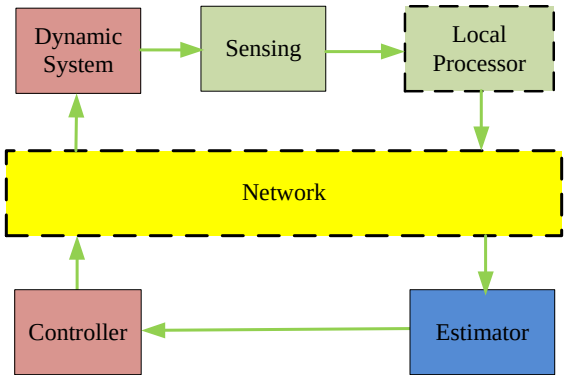

Figure 2.1: State estimaton framework in NCS.

and packet transmission delay. The case with measurement transmission delay was considered by (Alexander, 1991), (Larsen et al., 1998), (Nilsson et al., 1998), and (Matveev and Savkin, 2003). Matveev and Savkin (2003) studied the case with multiple sensors which independently transmit measurements to the estimator with random delay. The case with packet dropout was discussed by (Nahi, 1969), (Sinopoli et al., 2004), (Liu and Goldsmith, 2004), (Imer et al., 2006), in which the system state can be estimated by using time-varying Kalman filter (TVTF). Sinopoli et al. (2004) studied the performance of TVTF when the packet dropout pattern is an i.i.d Bernoulli process. Liu and Goldsmith (2004) extended the results to the case with partial observation loss, in which measurements of output signals are split into two parts which are encoded separately, transmitted and dropped independently over two wireless channels. One concern for TVTF is its complexity since matrices computation has to be conducted online even for time invariant system. In order to avoid this difficulty, Smith and Seiler (2003) proposed to pre-compute a finite set of parameters which can be selected online according to the packet dropout history in the last few time steps. Instead of linear optimal estimator, Ma et al. (2011) designed the optimal estimator for the case with Bernoulli distribution of packet dropout. The case with both packet dropout and delay was addressed by Schenato (2008) in which the minimum error covariance estimator was derived. The case with packet dropout,

delay and measurement loss was addressd by Moayedi et al. (2010) in a probabilistic manner.

All of the above mentioned works assume that measurement transmitted over network is either accurately received or dropped. However, data corruption in wireless communication happens a lot due to channel fading, interference. As pointed out by Mostofi and Murray (2009c) some real-time application is more sensitive to packet drop than data transmission error. Therefore, the stability of these applications can be improved by accepting erroneous packets instead of discarding them. However, keeping packets with transmission error increases communication noise. Mostofi and Murray (2009c) (Mostofi and Murray, 2009b)(Mostofi and Murray, 2009a) discussed the impact of keeping erroneous packets on estimation and identified the conditions to keep or drop packets. Another issue, called unknown packet arrival issue, is observed by Ma et al. (2009)(Ma et al., 2010)(Ma et al., 2012) while utilizing cognitive radio as communication medium for WNCS. Cognitive radio is an intelligent communication, in which secondary user keeps monitoring primary user's spectrum usage in order to look for spectrum holes. When primary user does not use the spectrum, then secondary user can use the spectrum hole to transmit data; however, secondary user cannot transmit when all spectrum is being used by primary users. Ma et al. (2009) discussed the challenge of integrating cogntive raido into WNCS. Since the trasmission of secondary user is impacted by spectrum usage of primary user; therefore, the transmission of measurement from sensor is intermittent; in addition, the estimator may not know if packet including measurement is trasmitted or not in current time slot, which is called unknown packet arrival issue. Therefore, estimator has to decide if the received signal contains trasmitted data from sensor or just noise. Ma et al. (2009)(Ma et al., 2010)(Ma et al., 2012) designed the estimation algorithm which takes into account this unknown packet arrival issue introduced by cognitive radio.

The framework with local estimation was studied by Xy and Hespanha (2005), Gupta et al. (2009), and Xu and Hespanha (2004). In this framework, the sensor can also preprocess the measurements to obtain estimates of output signal; then the

estimate of output signals instead of raw measurement is sent to remote estimator. The main advantage of this solution is that every successfully received message at the remote estimator includes all relevant information that can be extracted from all previous raw measurements. Therefore, this framework is more robust to packet drop than the framework without local estimation. Gupta et al. (2009) derived the optimal estimation framework which can handle any packet-dropping process. In addition, when network condition is good sensor can choose to not send estimates to remote estimator to reduce traffic while estimation performance is not degraded. Following this perspective many works have been conducted to explore the balance between communication and estimation performance (Xu and Hespanha, 2004)(Xu and Hespanha, 2005) and (Yook et al., 2002).

Another method to improve the performance of estimation is multi-sensor state estimation, in which multiple sensors are used to measure the dynamic system and their measurement results are co-used to estimate system state. As pointed out by Duan et al. (2007), multi-sensor state estimation is potential in improving estimation accuracy, extending observability and coverage, enhancing survivability and reliability. Many estimation fusion technologies including centralized fusion and distributed fusion are proposed to efficiently aggregate measurements from multiple sensors (Chiuso and Schenato, 2008), (Duan and Li, 2011), (Liu et al., 2012).

One more perspective to improve the performance of state estimation is to control the network. For instance, Quevedo et al. (2010) and Quevedo et al. (2013) proposed to dynamically control power and coding scheme at the transmitter in order to maintain channel quality while saving energy. Gupta et al. (2006),Mo et al. (2011),Yang et al. (2013) discussed about the sensor scheduling method in order to solve communication competition among sensors. Many fusion technologies are proposed by (Chiuso and Schenato, 2008), (Duan and Li, 2011), (Liu et al., 2012) to efficiently aggregate measurements from multiple sensors. Bai et al. (2012) proposed the cross-layer adaptive sampling rate and network scheduling. Chamaken and Litz

(2010) used a practical case study to demonstrate the performance improvement and efficiency of jointly designing control and communication system.

2.2 Evaluation for Relationship between the Operation of Network and Quality of Control System

In this section, we briefly introduce the relative works which explore the condition for stability with quantization error, packet drop and packet transmission delay.

2.2.1 Data Rate Therorem

The aim of data rate theorem is to determine how much rate is necessary to construct a stabilizing quantizer/controller pair in order to cope with the challenge of limited bandwidth in NCS. Data rate theorem is analogous to Shannon's source coding theory in communication theory, which aims to determine the lowest data rate above which a give random process can be communicated with arbitrarily small probability of errors (Shannon, 1948)(Cover and Thomas, 1991). However, source coding theory allows the usage of arbitrarily long codes leading to unbounded transmission delay and breakage of causality of the system. Therefore source coding theory is not applicable for control system due to that close-loop feedback control in control system requires that data transmission has to be causal and real-time.

The widely used plant model for the research of data rate theorem is an unstable linear dynamical system. The output signals are measured at fixed sampling interval, quantized, encoded, and sent to decoder at the controller side over a noiseless digital link. One special constraint is that both encoder at the system side and decoder at the controller have only causal knowledge of channel state, i.e., current supported data rate. The simplified case of constant data rate was addressed by Tatikonda and

Mitter (2004) and Nair and Evans (2004). The case with a time-varying independent and identically distributed (i.i.d.) rate process was considered by Martins et al. (2006) and Minero et al. (2009). Since the wireless channel is temporally correlated, the case of Markov rate process which has one state with channel rate 0 and the other state with constant channel rate was studied by You and Xie (2011). Finally, Minero et al. (2013) derived data rate theorem for general case with Markov channel rate process. This result can also be used to derive the data rate theorem for many special test cases, such as constant channel rate, time-varying i.i.d. channel rate process.

2.2.2 Packet Dropout Rate

The task of stability analysis for packet dropout is to find out the critical packet dropout rate above which no control scheme can stabilize the system. In this context, the output signals of the plant are sampled, encoded as a packet, and transmitted over network. Quantization effect is ignored, and a packet carries whole information of sampled output signals. However, packets may be dropped due to transmission error from physical layer especially wireless communication, buffer overflow due to congestion, and long transmission delay.

The case with i.i.d Bernoulli packet dropout pattern were addressed by Sinopoli et al. (2004) and Gupta et al. (2007a). The case with Markov packet drop process including bad state, i.e., over which packet is dropped over network, and good state, i.e., over which packet is successfully delivered, was studied by Gupta et al. (2007b). Note that the results for data rate theorem can also be used to derive the critical packet dropout rate over which system cannot be stabilized by any control scheme. Minero et al. (2009) recovered that packet loss model can be represented by model for data rate theorem, i.e., by letting the rate take value 0 and ∞.

2.2.3 Sampling and Delay

To transmit continuous signal over digital communication network, the transmitter has to sample the continuous signal, and then encode it and send it to receiver over transmission medium. Then the receiver decodes the transmitted signal. In digital control, the interval between two samples at the receiver is equal to the sampling interval. However, in NCS the interval between two samples is impacted by sampling interval, network access time (i.e., the interval between the transmitter receives the data and transmitter starts to transmit over network) and packet transmission time (i.e., the interval between transmitter starts to transmit the data and transmitter finishs transmitting the data). In addition, the network access time and packet transmission time are variable, which are dependent on network traffic condition and channel quality, respectively.

One case is one-channel feedback NCS, in which plant is modeled as a continuous-time linear time-invariant system (LTI). The output signal is sampled and sent over the communication network to the controller. The interval between two receiving sampled output signals at the controller is impacted by sampling interval, network access time, packet transmission time, and packet dropout. Before the arrival of next sampled output signal, the value of last received sampled output signal is held as constant and used to make decision for actions. The case with periodic-sampling and fixed delay was considered by Branicky et al. (2000), and Zhang et al. (2001) concluded the sufficient condition for the stability of LTI NCS by referring to the results for nonlinear hybrid system (Branicky, 1997). Since the delays in most cases are not constant, the case with variable delay has also drawn attentions. Lin et al (Lin et al., 2003)(Lin and Antsaklis, 2004)(Lin and Antsaklis, 2005) addressed one special case of periodic sampling and variable delay, in which computation and transmission time can be ignored, and the main source of delay is network access time. Lin et al. (2003) discretized delay and concluded the condition for stability by using average dwell time results for discrete switched systems (Zhai et al., 2002). The case with

variable sampling interval or variable delay is most chanllenging . Zhang and Branicky (2001) expressed the sufficient conditions for its stability as a a Lyapunov function. However, it is generally not simple to solve this Lyapunov function in order to check if a given interval for sampling and delay is stable or not. They proposed a randomized algorithm to find the largest value of sampling interval for the stability of a special case in which the minimum sampling is 0 and there is no delay.

Another case for stability analysis is model-based networked control system (MB-NCS), which is introduced by Montestruque and Antsaklis (2002a). The main purpose of MB-NCS is to reduce the amount of data exchange in network, by making use of model of the plant at the controller. More specifically, most of time the system is controlled with open-loop mode in which actions are made based on the plant model at the controller. The model of plant at the controller is updated at fixed interval by using close-loop mode. Comparing with one-channel feedback NCS in which last data received from network is held constant, MB-NCS instantaneously updates the state of controller after receiving data from network. Montestruque and Antsaklis (Montestruque and Antsaklis, 2002a)(Montestruque and Antsaklis, 2002b)(Montestruque and Antsaklis, 2003a) first derived the maximum value of periodic sampling interval for which the NCS is still stable; then they considered the case with stochastic sampling interval. The stability condition for i.i.d sampling interval was considered in (Montestruque and Antsaklis, 2003b); then the results was further generalized to Markov sampling intervals in (Montestruque and Antsaklis, 2004).

A general nonlinear case was addressed by Walsh et al. (2002) and Nesic and Teel (2004), where a nonlinear plant and remote controller are impacted by exogenous disturbances. Both control signals and output signals are sampled and transmitted over network. Between sampling times, the data for control signals and output signals are held constant at the actuator and controller, respectively. In addition, it is allowed to transmit a portion of entries of control signals and output signals at given sampling

times. This can be used to capture some network access protocols by which only a part of control signals and output signals can be transmitted in the given time.

2.3 Channel Coding and Decoding

The development of channel coding and decoding has split into two paths. One category is that source coding and decoding are not taken into account while designing channel coding and decoding. This is guided by the separation principle, which states there is no gain from joint data compression and channel transmission. Due to the independence of source many diverse source can share the same coding scheme. Therefore, many coding schemes have been wildly used, such as convolutional code (Elias, 1955), turbo code (Heegard and Wicker, 1999), serially concatenated code (Benedetto et al., 1998) and LDPC code (Gallager, 1963).

However, separation principle holds only when channels are stationary and there is no delay requirement for sources (Vembu et al., 1995). For fixed length blocks, there is redundancy in source no matter if source is encoded or not. Therefore, the redundancy in source drives the development of joint source decoding and channel coding. There are two models to describe the redundancy left in the source. One model is based on the high level information from the source, and is highly dependent on the source (Yin et al., 2002; Mei and Wu, 2006; Pan et al., 2006; Pu et al., 2007; Ramzan et al., 2007). The other model for redundancy from source is Markov source (Garcia-Frias and Villasenor, 1997, 1998, 2001; Garcia-Frias and Zhao, 2001, 2002; Garcia-Frias and Zhong, 2003; Garcia-Frias et al., 2003; Fresia et al., 2010). The advantage of Markov model is that the parameters do not have to be known at the receiver side. Garcia-Frias and Villasenor (1998, 2001) extended the joint source coding and channel decoding for Markov model with unknown parameters. Zhao and Garcia-Frias (2002, 2005) extended it to non-binary source.

2.4 Performance Analysis For Channel Decoding

The purpose of performance analysis for iterative decoding scheme is to find out for a given codec and decoder, for which kind of channel noise power the message-passing decoder can correct the errors or not. Then the results of performance analysis can be used to assist the design of codec and decoder.

Gallager (1963) proposed to use density evolution to track the iterative decoding performance. It is based on the assumption that, for very long codes, the extrinsic LLRs passed between the component decoders are independent and identically distributed. Then, for the iterative decoding performance it is equivalent to track the evolution of extrinsic LLRs probability density functions through iterative decoding process.

ten Brink (1999, 2000, 2001) proposed to use extrinsic information transfer chart (EXIT) to track the iterative decoding performance. Based on the assumption that the distribution of extrinsic log-likelihood ratio (LLR) is Gaussian EXIT tracks mutual information of extrinsic LLRs instead of density evolution. Comparing with density evolution, the computation for EXIT is simplified. In addition, the evolution of mutual information through iterative decoding process can be illustrated in a graph and easy to visualize. EXIT has two properties. One property is that for convergence of iterative decoding, the flipped EXIT curve of the outer decoder should lie below the EXIT curve of the inner coder. The other property is that the area under EXIT curve of outer code relates to the rate of inner coder. Ashikhmin et al. (2004) demonstrated that if the a priori channel is an erasure channel, for any outer code of rate R, the area under the EXIT curve is $1 - R$. To the best knowledge of us, the area property of EXIT has been proved only for erasure priori channel.

Instead of tracking mutual information MSE is proposed to track the iterative decoding performance (Bhattad and Narayanan, 2007). The MSE-based chart analysis method is based on the relationship between mutual information and minimum mean square error (MMSE) in AWGN channel (Guo et al., 2005). Bhattad

and Narayanan (2007) has proven the area property of MSE chart when the priori channel is Gaussian.

The difference of iterative channel decoding and state estimation in our work is that we have a hybrid model. The system state and observation are non-binary source in continuous domain; on the other hand the information transmitted in wireless system is quantized bits. Therefore, the method proposed in (Guo et al., 2005) cannot be used directly. The key challenge is how to handle the message transfer between non-binary source and information bits. The other difference is that the source is correlated over time. The estimation error from previous time slots also affects the performance of estimation in current time slots. Therefore, besides evaluating the performance of iterative channel decoding and state estimation in two time slots, it is also very important to evaluate the performance of state estimation over time.

Another area in wireless communication related to our work is joint source and channel decoding (Yin et al., 2002; Mei and Wu, 2006; Pan et al., 2006; Pu et al., 2007; Ramzan et al., 2007; Garcia-Frias and Villasenor, 1997, 1998, 2001; Garcia-Frias and Zhao, 2001, 2002; Garcia-Frias and Zhong, 2003; Garcia-Frias et al., 2003). The idea of joint source and channel decoding is to utilize redundancy in source to assist channel decoding. Our work can also be considered as one special case of joint source and channel decoding. However, there are two major differences. One difference is that most works focus on binary source and EXIT chart was used for performance analysis (Fresia et al., 2010). Zhao and Garcia-Frias (2002, 2005) considered the case with non-binary source, but the performance analysis was not provided. The other difference is these works considered the joint source and channel decoding over only two time slots. In our work, the dynamic state changes over time. Therefore, the performance of channel decoding and system estimation at the current time slots also impacts its performance in the future. Therefore, we also study the performance of iterative estimation and decoding over time.

Chapter 3

Decoding the 'Nature Encoded' Messages for Wireless Networked Control System

3.1 Introduction

In this chapter, we study *the decoding procedure (including the demodulation procedure) for the messages with no or weak channel coding protection in the context of wireless networked control system (WNCS).* The key point is to *exploit the redundancy in the system state, which can be considered as a 'nature encoding' for the messages.* In this work, a linear system model is adopted, where $\mathbf{x}(t+1) = \mathbf{A}\mathbf{x}(t) + \mathbf{B}\mathbf{u}(t) + \mathbf{n}(t)$ is used to describe the dynamics of system state $\mathbf{x}$ subject to the control $\mathbf{u}(t)$ and noise $\mathbf{n}(t)$. We observe that the system state is similar to the convolutional codes except that the 'encoding' of the system state is in the real field instead of the Galois field. Hence, the message actually has been channel coded by the nature although no explicit or little explicit channel coding is used at the transmitter. We use both schemes of Kalman filtering and Pearl's Belief Propagation (BP) for the soft decoding, combined with the soft demodulation to improve the reliability of demodulation and decoding.

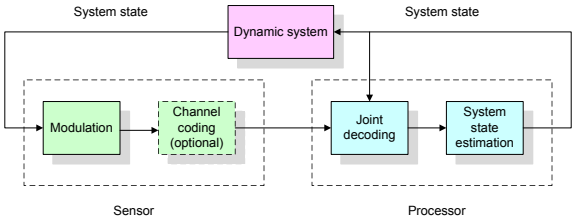

Figure 3.1: An illustration of the communication procedure and dynamic system.

An electric generator dynamic system will be used for numerical simulation, which demonstrates the performance gain of incorporating the inherent redundancy in the 'nature encoding'. The procedure is illustrated in Figure 3.1. Note that such a scheme is similar to the *Turbo processing techniques* like Turbo decoding (Berrou et al., 1993), Turbo multiuser detection (Alexander et al., 1999) and Turbo equalization (Tüchler et al., 2002) in wireless communication systems. However, the 'nature encoding' is analog and implicit, thus resulting in a different processing procedure.

The remainder of this chapter is organized as follows. The system model is introduced in Section 3.2. The decoding procedure is discussed for the schemes of Kalman filtering based heuristic approach and the BP approach in Sections 3.3 and 3.4, respectively. Numerical simulation results are shown in Section 3.5. Finally, the conclusions are drawn in Section 3.6.

3.2 System Model

3.2.1 Linear System

We consider a discrete time linear dynamic system, whose system state evolution is given by

$$\begin{cases} \mathbf{x}(t+1) = \mathbf{A}\mathbf{x}(t) + \mathbf{B}\mathbf{u}(t) + \mathbf{n}(t), \\ \mathbf{y}(t) = \mathbf{C}\mathbf{x}(t) + \mathbf{w}(t) \end{cases}, \tag{3.1}$$

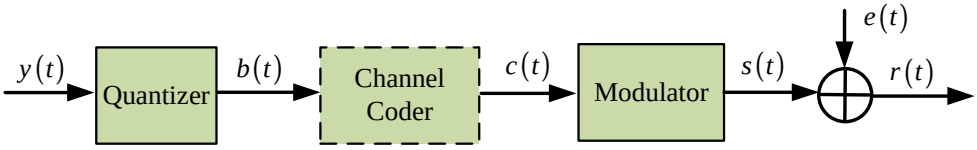

Figure 3.2: Model for communication system.

where $\mathbf{x}(t)$ is the N-dimensional vector of system state at time slot t, $\mathbf{u}(t)$ is the M-dimensional control vector, $\mathbf{y}$ is the K-dimensional observation vector and $\mathbf{n}$ and $\mathbf{w}$ are noise vectors, which are assumed to be Gaussian distributed with zero expectation and covariance matrices $\mathbf{\Sigma}_n$ and $\mathbf{\Sigma}_w$, respectively. For simplicity, in this work we do not consider $\mathbf{u}(t)$.

We assume that the observation vector $\mathbf{y}(t)$ is obtained by a sensor*. The sensor quantizes each dimension of the observation using B bits, thus forming a bit sequence which is given by

$$\mathbf{b}(t) = (b_1(t), b_2(t), ..., b_{KB}(t)) \,. \tag{3.2}$$

3.2.2 Communication System

The framework for communication system is shown in Figure 3.2. Suppose that binary phase shift keying (BPSK) is used for the transmission from the sensor to the controller. The bit sequence is passed through an optional channel encoder, which generates an L-bit sequence $\mathbf{s}(t)$. Finally modulated sequence $\mathbf{s}(t)$ is transmitted. Then, the received signal at the controller is given by

$$\mathbf{r}(t) = \mathbf{s}(t) + \mathbf{e}(t), \tag{3.3}$$

where the additive white Gaussian noise $\mathbf{e}(t)$ has a zero expectation and variance σ_e^2. Note that we ignore the fading and normalize the transmit power to be 1. The

*It is easy to extend to the case of multiple sensors.

algorithm and conclusion in this work can be easily extended to the case with different types of fading.

3.3 Kalman Filtering based Heuristic Approach

In this section, we adopt a heuristic approach, which is based on Kalman filtering, to exploit the redundancy in the system state. We first carry out the Kalman filtering and then apply the prediction to the soft demodulation and soft decoding.

3.3.1 Kalman Filtering

When the observations $\mathbf{y}(t)$ are sent to the controller perfectly, the controller can use the following Kalman filtering to predict the future system state, whose expectation is given by

$$\mathbf{x}(t+1|t) = \mathbf{A}\mathbf{x}(t|t), \tag{3.4}$$

where

$$\mathbf{x}(t|t) = \mathbf{x}(t|t-1) + \mathbf{K}(t)\left(\mathbf{y} - \mathbf{C}\mathbf{x}(t|t-1)\right), \tag{3.5}$$

and

$$\mathbf{K}(t) = \mathbf{\Sigma}(t|t-1)\mathbf{C}^T\left(\mathbf{C}\mathbf{\Sigma}(\mathbf{t}|\mathbf{t}-\mathbf{1})\mathbf{C}^{\mathbf{T}} + \mathbf{\Sigma}_{\mathbf{w}}\right)^{-1}, \tag{3.6}$$

and the covariance matrix given by

$$\mathbf{\Sigma}(\mathbf{t}|\mathbf{t}) = \mathbf{\Sigma}(t|t-1) - \mathbf{K}_t\mathbf{C}\mathbf{\Sigma}(t|t-1), \tag{3.7}$$

where

$$\mathbf{\Sigma(t|t-1)} = \mathbf{A\Sigma(t-1|t-1)A}^T + \mathbf{\Sigma}_n. \tag{3.8}$$

3.3.2 Soft Decoding and Demodulation

Based on the Kalman filtering, the controller can obtain the distribution of the observation, which is Gaussian distributed with the expectation $\mathbf{x}(t|t-1)$ given by Eq. (3.4) and the covariance $\mathbf{\Sigma}(t|t-1)$ given by Eq. (3.8).

Because different dimensions in the observation $\mathbf{y}_t$ are not independent, it is challenging to directly compute the *a priori* probability for each bit, which is given by (suppose that i is used to describe the i-th bit in $\mathbf{b}(t)$)

$$\begin{aligned}
\xi_i(t) &\triangleq P(b_i(t)=1|\mathbf{y}(-\infty:t)) \\
&= \frac{1}{\sqrt{2\pi|\mathbf{\Sigma}(t|t-1)|}} \int I(b_i(t)=1, \mathbf{y}(t)=\mathbf{y}) \\
&\times \exp(-\frac{1}{2}(\mathbf{y}-\mathbf{Cx}(t|t-1))^T \times \mathbf{\Sigma}^{-1}(t|t-1) \\
&\times (\mathbf{y}-\mathbf{Cx}(t|t-1)))d\mathbf{y}.
\end{aligned} \tag{3.9}$$

We propose to use the Monte Carlo simulation to obtain a series of samples of $\{\mathbf{y}_t\}$ based on the prediction of Kalman filtering, then quantize these samples to obtain a series of samples $\mathbf{b}_{t-1}$ and calculate the prior probability $\xi_i(t)$ for $\mathbf{b}_t$. We use $\{\xi_i(t)\}$ as the *a priori* probability of being 1 for demodulating $\mathbf{b}(t)$. Then, the *a posteriori* probability of $b_i(t)$ is given by

$$\begin{aligned}
& P(b_i(t)=1|\mathbf{r}(-\infty:t)) \\
= & \frac{P(r_i(t)|b_i(t)=1)\xi_i(t)}{P(r_i(t)|b_i(t)=1)\xi_i(t) + P(r_i(t)|b_i(t)=0)(1-\xi_i(t))},
\end{aligned} \tag{3.10}$$

$$P(r_i(t)|b_i(t)=1) = \frac{1}{\sqrt{2\pi\sigma_e^2}} \exp\left(-\frac{(r_i(t)-1)^2}{2\sigma_e^2}\right). \tag{3.11}$$

$$P(r_i(t)|b_i(t)=0) = \frac{1}{\sqrt{2\pi\sigma_e^2}} \exp\left(-\frac{(r_i(t)+1)^2}{2\sigma_e^2}\right). \tag{3.12}$$

Note that the Kalman filtering is no longer rigorous in the networked control system due to the quantization error and possible decoding error. The proposed heuristic approach is based on the assumption that the Kalman filtering is very precise. As will be shown in the numerical results, this approach will be seriously affected by the propagation of decoding errors.

3.4 BP based Iterative Decoding

In this section, we consider the iterative decoding using BP with the mechanism of message passing between the system state and received signals. The key observation is that *the entire information passing is similar to a concatenated coding structure*, as illustrated in Figure 3.3. The outer coding is carried out by the dynamic system, where the system state $\mathbf{x}$ is encoded similarly to a convolutional code and the observation $\mathbf{y}$ is linearly encoded by the observation matrix $\mathbf{C}$ and the system state $\mathbf{x}$. The inner code is the explicit encoding of the observation vector. Hence, we can adopt the iterative decoding approach in Turbo codes or LDPC codes (Richardson and Urbanke, 2001). In a sharp contrast, the proposed Kalman filtering based heuristic approach has only one round.

McEliece et al. (1998) has shown that many iterative decoding algorithm, such as Turbo decoding can be considered as the application of Pearl's BP algorithm (Pearl, 1988). In this section, we first illustrate the principle of Pearl's BP through an example and then explain how to apply Pearl's BP into our dynamic state system.

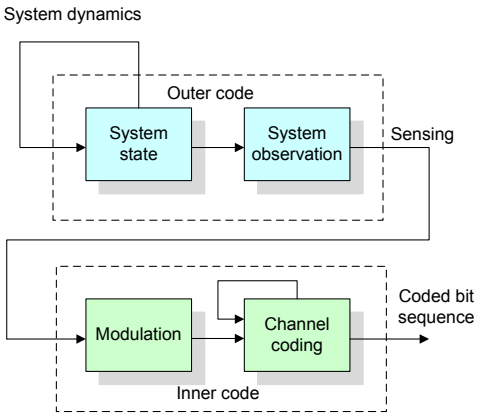

Figure 3.3: An illustration of the coding structure.

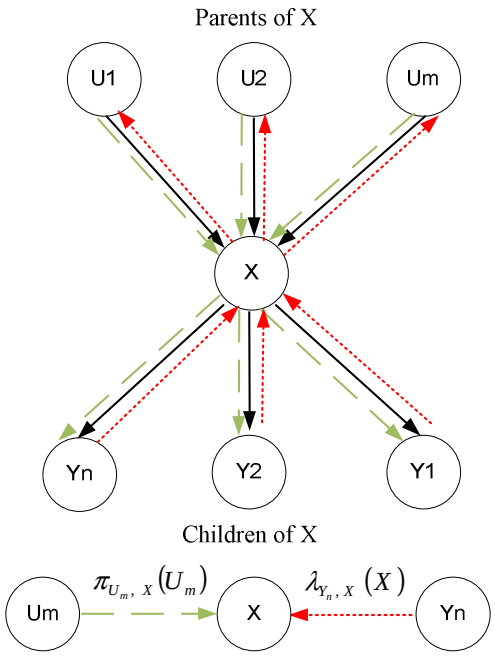

Figure 3.4: Message Passing of BP.

3.4.1 Introduction of Pearl's BP

As shown in Figure 3.4, random variable X has parents $U_1, U_2, \cdots, U_M$ and children $Y_1, Y_2, \cdots, Y_N$. The message passing of Pearl's BP is indicated by green arrows and red arrows in the figure. Green arrows transmit π-message which is sent from parent to its children. For instance, the message passing from U_m to X is $\pi_{U_m,X}(U_m)$, which is the prior information of U_m conditioned on all the information U_m has received. Red arrows transmit λ-message which is from children to its parent. For instance, the message passing from Y_n to X is $\lambda_{Y_n,X}(X)$, which is the likelihood of X based on the information Y_n has received. After X receives all π-message $\pi_{U_m,X}(U_m)$ from its parents $U_1, U_2, \cdots, U_M$ and all λ-message $\lambda_{Y_n,X}(X)$, X from its children $Y_1, Y_2, \cdots, Y_N$, X updates its belief information $BEL_X(\mathbf{x})$ and transmits λ-messages $\lambda_{X,U_m}(U_m)$ to its parents and π-message $\pi_{X,Y_n}(\mathbf{x})$ to its children. The expressions of the quantities are given by

$$\pi_X(\mathbf{x}) = \sum_{\mathbf{U}} p(\mathbf{x}|\mathbf{U}) \prod_{m=1}^{M} \pi_{U_m,X}(U_m) \tag{3.13}$$

$$\gamma_X(\mathbf{U}) = \sum_{\mathbf{x}} \prod_{n=1}^{N} \lambda_{Y_n,X}(\mathbf{x}) p(\mathbf{x}|\mathbf{U}) \tag{3.14}$$

$$BEL_X(\mathbf{x}) = \alpha \times \prod_{n=1}^{N} \lambda_{Y_n,X}(\mathbf{x}) \times \pi_X(\mathbf{x}) \tag{3.15}$$

$$\lambda_{X,U_m}(U_m) = \sum_{\mathbf{U},\neq U_m} \gamma_X(\mathbf{U}) \times \prod_{j\neq m} \pi_{U_j,X}(U_j) \tag{3.16}$$

$$\pi_{X,Y_n}(\mathbf{x}) = \pi_X(\mathbf{x}) \times \prod_{i\neq n} \lambda_{Y_i,X}(\mathbf{x}) \tag{3.17}$$

where $\mathbf{U} = (U_1, U_2, \cdots, U_M)$ and $\mathbf{Y} = (Y_1, Y_2, \cdots, U_N)$

In the initialization procedure of Pearl's BP, some initial values are needed for the running of Pearl's BP. The initial values are defined as

$$\lambda_{X,U}(\mathbf{u}) = \begin{cases} p(\mathbf{x}_0|\mathbf{u}), & X \text{is evidence}, \mathbf{x} = \mathbf{x}_0 \\ 1, & X \text{is not evidence} \end{cases}, \tag{3.18}$$

and

$$\pi_{X,Y}(\mathbf{x}) = \begin{cases} \delta(\mathbf{x}, \mathbf{x}_0), & X \text{is evidence}, \mathbf{x} = \mathbf{x}_0 \\ p(\mathbf{x}), & X \text{ is source, not evidence} \end{cases} . \tag{3.19}$$

3.4.2 Application of Pearl's BP in NCS

The Bayesian network structure of the control system and communication system in the NCS is shown for three time slots in Figure 3.5. In the Bayesian network, the system state $\mathbf{x}_t$ is dependent on the previous system state $\mathbf{x}_{t-1}$ and the control action $\mathbf{u}_t$; the observation $\mathbf{y}_t$ is dependent on the system state $\mathbf{x}_t$; the uncoded bits $\mathbf{b}_t$ are dependent on the observation vector $\mathbf{y}_t$; the received signal $\mathbf{r}_t$ is dependent on the uncoded bits $\mathbf{b}_t$. Here we omit the coded bits $\mathbf{s}_t$ as the relationship between the uncoded bits $\mathbf{b}_t$ and the coded bits $\mathbf{s}_t$ is deterministic. Figure 3.5 shows the Bayesian Network structure for the dynamic system with three observations: $\mathbf{x}_{t-2}$, $\mathbf{x}_{t-1}$ and $\mathbf{x}_t$.

Based on the Bayesian network structure, the iterative decoding procedure can be derived. Figure 3.5 shows the message passing in the dynamic system. $\mathbf{x}_{t-2}$ summarizes all the information obtained from previous time slots and transmits π-message $\pi_{\mathbf{x}_{t-2},\mathbf{x}_{t-1}}(\mathbf{x}_{t-2})$ to $\mathbf{x}_{t-1}$. The BP procedure can be implemented in synchronous or asynchronous manners. As the decoding process has a large overhead, we implement asynchronous Pearl's BP. The updating order and message passing in one iteration is as follows: step 1): $\mathbf{x}_{t-1} \rightarrow \mathbf{y}_{t-1}$; step 2): $\mathbf{y}_{t-1} \rightarrow \mathbf{b}_{t-1}$; step 3): $\mathbf{b}_{t-1} \rightarrow \mathbf{y}_{t-1}$; step 4): $\mathbf{y}_{t-1} \rightarrow \mathbf{x}_{t-1}$; step 5): $\mathbf{x}_{t-1} \rightarrow \mathbf{x}_t$; step 6): $\mathbf{x}_t \rightarrow \mathbf{y}_t$; step 7): $\mathbf{y}_t \rightarrow \mathbf{b}_t$; step 8): $\mathbf{b}_t \rightarrow \mathbf{y}_t$; step 9): $\mathbf{y}_t \rightarrow \mathbf{x}_t$; step 10): $\mathbf{x}_t \rightarrow \mathbf{x}_{t-1}$; step 11): $\mathbf{x}_{t-1}$ updates information. The detailed mathematical derivation for each step is shown in Appendix A.1 and the messaging passing between $\mathbf{y}(t)$ and $\mathbf{b}(t)$ is shown in next subsection.

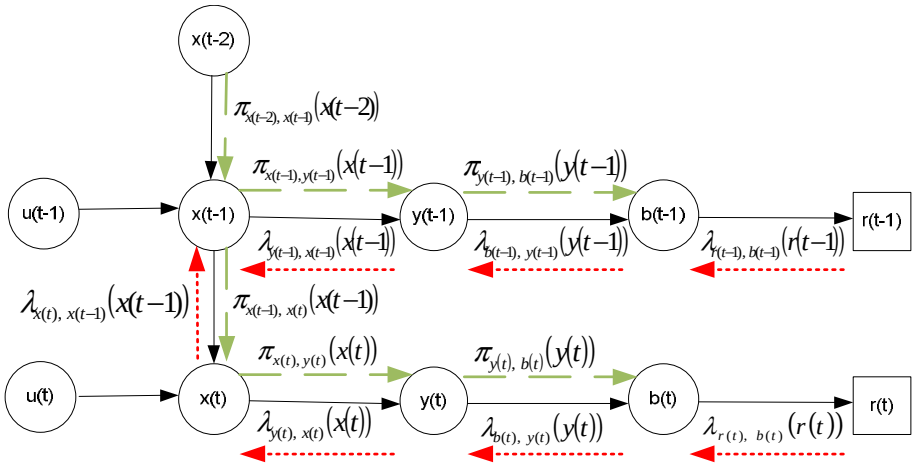

Figure 3.5: Bayesian network structure and message passing for the dynamic system.

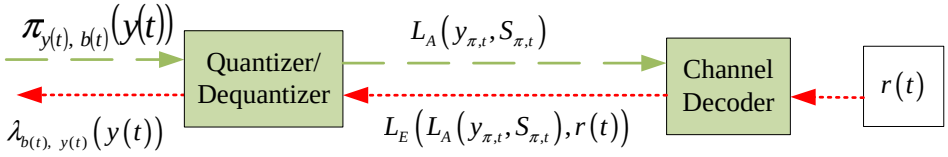

Figure 3.6: Message passing between $\mathbf{y}_t$ and $\mathbf{b}_t$

3.4.3 Computation of message $\lambda_{\mathbf{b}_t,\mathbf{y}_t}(\mathbf{y}_t)$ sent from $\mathbf{b}_t$ to $\mathbf{y}_t$

Figure 3.6 illustrates the message passing scheme between $\mathbf{y}_t$ and $\mathbf{b}_t$. The message from $\mathbf{y}_t$ to $\mathbf{b}_t$ is $\pi_{\mathbf{y}_t,\mathbf{b}_t}(\mathbf{y}_t)$; and the message from $\mathbf{b}_t$ to $\mathbf{y}_t$ is $\lambda_{\mathbf{b}_t,\mathbf{y}_t}(\mathbf{y}_t)$. In this subsection, we will show how to compute $\lambda_{\mathbf{b}_t,\mathbf{y}_t}(\mathbf{y}_t)$ based on $\pi_{\mathbf{y}_t,\mathbf{b}_t}(\mathbf{y}_t)$ and received signals $\mathbf{r}(t)$. As shown in Figure 3.6, we can divide the computation process into three sub-steps:

1. Compute priori information $\mathbf{L}_A(\mathbf{y}_{\pi,t}, S_{\pi,t})$ for $\mathbf{b}_t$ based on $\pi_{\mathbf{y}_t,\mathbf{b}_t}(\mathbf{y}_t)$ and quantization scheme. $\mathbf{L}_A(\mathbf{y}_{\pi,t}, S_{\pi,t})$ is denoted as the priori LLR of $\mathbf{b}_t$ from $\pi_{\mathbf{y}_t,\mathbf{b}_t}(\mathbf{y}_t)$ and its ith value means priori information for b_i which is equal to

$$L_{A,b_i}(\mathbf{y}_{\pi,t}, \mathbf{S}_{\pi,t}) = \log \frac{P\left(b_i(t) = 1 | \mathbf{y}(t) \in \mathcal{N}(\mathbf{y}_t, \mathbf{y}_{\pi,t}, \mathbf{S}_{\pi,t})\right)}{P\left(b_i(t) = 0 | \mathbf{y}(t) \in \mathcal{N}(\mathbf{y}_t, \mathbf{y}_{\pi,t}, \mathbf{S}_{\pi,t})\right)} \tag{3.20}$$

where $P\left(b_i(t)=1|\mathbf{y}(t)\in\mathcal{N}(\mathbf{y}_t,\mathbf{y}_{\pi,t},\mathbf{S}_{\pi,t})\right)$ and $P\left(b_i(t)=0|\mathbf{y}(t)\in\mathcal{N}(\mathbf{y}_t,\mathbf{y}_{\pi,t},\mathbf{S}_{\pi,t})\right)$ can be computed according to the method described in subsection 3.3.2.

2. Soft decoding and demodulation

   We compute $\mathbf{L}_E(\mathbf{L}_A(\mathbf{y}_{\pi,t},S_{\pi,t}),\mathbf{r}(t))$ using soft dedomulation in uncoded case and soft decoding in coded case.

   (a) Soft demodulation for uncoded system

$$\begin{aligned} L(b_i|\mathbf{r}(t)) &= \log\frac{P(b_i=1|\mathbf{r}(t))}{P(b_i=0|\mathbf{r}(t))} \\ &= \log\frac{P(b_i=1|r_i(t))}{P(b_i=0|r_i(t))} \\ &= L_{A,b_i}(\mathbf{y}_{\pi,t},\mathbf{S}_{\pi,t})+L_c*r_i \end{aligned} \tag{3.21}$$

   where σ_0^2 is the power of channel noise, L_c is the channel reliability value, which equals to $\frac{2}{\sigma^2}$.

   As shown in 3.21, the output of soft demodulation includes two parts: the prior information $L_{A,b_i}(\mathbf{y}_{\pi,t},\mathbf{S}_{\pi,t})$ and L_c*r_i. The new information which can be fed back from $\mathbf{b}_t$ to $\mathbf{y}_t$ is L_c*r_i, i.e,

$$\mathbf{L}_{E,b_i}(\mathbf{L}_A(\mathbf{y}_{\pi,t},S_{\pi,t}),\mathbf{r}(t))=L_c*r_i \tag{3.22}$$

   As L_c*r_k is a constant, the information sent from $\mathbf{b}_t$ to $\mathbf{y}_t$ keeps constant in different iteration, which means it's not necessary to run BP many times. In addition, since L_c*r_i is independent of $\mathbf{L}_A(\mathbf{y}_{\pi,t},S_{\pi,t})$, the priori information provided by $\pi_{\mathbf{y}_t,\mathbf{b}_t}(\mathbf{y}_t)$ cannot be utilized.

   (b) Soft decoding for coded system

   In this work we use convolutional code and Log-Map decoding algorithm. The input for the decoding algorithm is the received signal $\mathbf{r}_t$ and prior probability $L(b_k)$, the output of soft decoding can be written as Berrou

et al. (1993):

$$\begin{aligned} L(b_k|\mathbf{r}_t) &= \log \frac{P(b_k=1|\mathbf{r}_t)}{P(b_k=0|\mathbf{r}_t} \\ &= L_{A,b_i}(\mathbf{y}_{\pi,t}, \mathbf{S}_{\pi,t}) + L_c r_{ks} + L_e(b_k) \end{aligned} \tag{3.23}$$

Therefore, the information which needs to be fed from $\mathbf{b}_t$ to $\mathbf{y}_t$ is $L_c r_{ks} + L_e(b_k)$, i.e.,

$$\mathbf{L}_{E,b_i}(\mathbf{L}_A(\mathbf{y}_{\pi,t}, S_{\pi,t}), \mathbf{r}(t)) = L_c r_i(t) + L_e(b_i) \tag{3.24}$$

3. Compute $\lambda_{\mathbf{b}_t,\mathbf{y}_t}(\mathbf{y}_t)$ from $\mathbf{L}_E(\mathbf{L}_A(\mathbf{y}_{\pi,t}, S_{\pi,t}), \mathbf{r}(t))$

   Based on $\mathbf{L}_E(\mathbf{L}_A(\mathbf{y}_{\pi,t}, S_{\pi,t}), \mathbf{r}(t))$, $\mathbf{b}(t)$ can be estimated as (Bhattad and Narayanan, 2007):

$$\tilde{\mathbf{b}}_i(t) = \frac{1}{2}\tanh\left(\frac{1}{2}\mathbf{L}_{E,b_i}\left(\mathbf{L}_A(\mathbf{y}_{\pi,t}, \mathbf{S}_{\pi,t}), \mathbf{r}(t)\right)\right) + \frac{1}{2} \tag{3.25}$$

   and MMSE in estimating $\mathbf{b}_i(t)$ is given by

$$\begin{aligned} &mmse\left(\mathbf{b}_i(t)|\mathbf{L}_A(\mathbf{y}_{\pi,t}, \mathbf{S}_{\pi,t}), \mathbf{r}(t)\right) \\ &= \frac{1}{4} - \frac{1}{4}\tanh^2\left(\frac{1}{2}\mathbf{L}_{E,b_i}\left(\mathbf{L}_A(\mathbf{y}_{\pi,t}, \mathbf{S}_{\pi,t}), \mathbf{r}(t)\right)\right) \end{aligned} \tag{3.26}$$

   Then, $\mathbf{y}(t)$ can be estimated:

$$\tilde{y}_k(t) = \sum_{i=1}^{B} Q_I^{i-1}\tilde{\mathbf{b}}_{(k-1)B+i}(t) - \frac{Q_{max} - Q_{min}}{2} \tag{3.27}$$

and MMSE in estimating $\mathbf{y}(t)$ is given by:

$$\begin{aligned} & mmse\left(y_k(t)|\mathbf{L}_A(\mathbf{y}_{\pi,t},\mathbf{S}_{\pi,t}),\mathbf{r}(t)\right) \\ = & \sum_{i=1}^{B} Q_I^{2(i-1)} mmse\left(\mathbf{b}'_{(k-1)B+i}(t)|\mathbf{L}_A(\mathbf{y}_{\pi,t},\mathbf{S}_{\pi,t}),\mathbf{r}(t)\right) \end{aligned} \tag{3.28}$$

where $[Q_{min}, Q_{max}]$ is the range for quantization, Q_I is the quantization interval, which is given by:

$$Q_I = \frac{Q_{max} - Q_{min}}{2^B - 1} \tag{3.29}$$

We assume that the distribution of estimated $\mathbf{y}(t)$ is Gaussian, i.e.,

$$\lambda_{\mathbf{b}_t,\mathbf{y}_t}(\mathbf{y}_t) \;=\; \mathcal{N}(\mathbf{y}_t, \mathbf{y}_{\lambda,t}, S_{\lambda,t}) \tag{3.30}$$

where $\mathbf{y}_{\lambda,t}$ is the mean which is equal to

$$\mathbf{y}_{\lambda,t} = [\tilde{y}_1(t), \cdots, \tilde{y}_K(t)] \tag{3.31}$$

and $S_{\lambda,t}$ is the covariance matrix which is diagonal and its kth element is equal to

$$\mathbf{S}_{\lambda,t}^{k,k} = mmse\left(y_k(t)|\mathbf{L}_A(\mathbf{y}_{\pi,t},\mathbf{S}_{\pi,t}),\mathbf{r}(t)\right) \tag{3.32}$$

3.5 Numerical Simulations

In this section, we use numerical simulations to demonstrate the algorithms proposed in this chapter.

We consider an electric generator dynamic system in which the system state is a 7-dimensional vector. The system is in the continuous time. The system dynamics

is described by a differential equation $\dot{\mathbf{x}}(t) = \mathbf{A}'\mathbf{x}(t)$, where the matrix $\mathbf{A}'$ is given by (3.20) (Example 12.9 in (Machowski et al., 2008)). The physical meanings of the system states are given in Table 3.1. For simplicity, we assume that the system is unregulated, i.e., $\mathbf{B} = 0$, and the sensor can sense the system state directly, i.e., $\mathbf{C} = \mathbf{I}$. We approximate the continuous time system using the discrete time system with a small step size δt. Therefore, the matrix $\mathbf{A}$ in the discrete time system is given by $\mathbf{A} = \mathbf{I} + \delta t \mathbf{A}'$.

Table 3.1: Physical Meaning of System States

x_1,x_2	rotor swings
x_3	excitation circuit
x_4	damping circuit in the d-axis and excitation circuit
x_5	damping circuit in the q-axis
x_6	voltage controller and excitation circuit
x_7	voltage controller

We run the simulations using Matlab to compare the performances of Kalman filtering and Pearl's BP based algorithms for systems with and without channel coding. The baseline approach is the separated Kalman filtering and decoding process. In the following, these three algorithms are referred as 'KF Prior', 'BP' and 'KF', respectively. The performance metrics are the mean square error (MSE) of each sample and the average bit error rate (BER). Each simulation runs 1000 times slots. The configuration for both systems are as follows: for the dynamic system of power system described in (3.1): $\delta t = 0.01$, $\mathbf{\Sigma}_n = 0.05$, $\mathbf{\Sigma}_w = 0.05$. Each dimension of the observation $\mathbf{y}_t$ is quantized with 16 bits, and the dynamic range for quantization is $[-200, 200]$. A 1/2 rate Recursive Systematic Convolutional (RSC) code is used as the channel coding scheme; and the code generator is $g = [1, 1, 1]$. The decoding algorithm is Log-Map algorithm.

$$\mathbf{A}' = \begin{pmatrix} 0 & 1 & 0 & 0 & 0 & 0 & 0 \\ -20.316 & 0 & 0 & -25.048 & -1.411 & 0 & 0 \\ -0.061 & 0 & -0.773 & -0.083 & 0.018 & 15.06 & 30.12 \\ -0.213 & 0 & 7.050 & -5.026 & 0.063 & 0 & 0 \\ -2.654 & 0 & 0 & -1.463 & -12.958 & 0 & 0 \\ 0 & 0 & 0 & 0 & 0 & 0 & 1 \\ -0.008 & 0 & 0 & -0.565 & 0.971 & -3.33 & -33.33 \end{pmatrix} \tag{3.20}$$

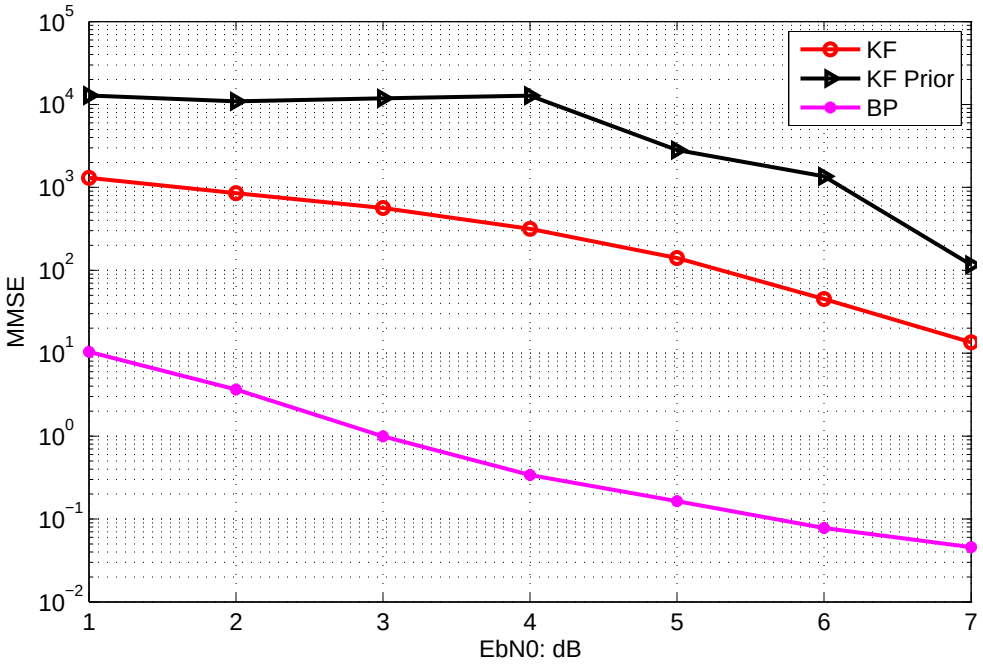

Figure 3.7: Mean Square Error comparison for system without channel coding

3.5.1 Uncoded Case

Figures 3.7 and 3.8 show the simulation results for the uncoded case with different E_b/N_0. The performance of 'BP' is the best; however, the performance of 'KF Priori' is worse than 'KF'. The reason for the bad performance of 'KF Prior' is:

1. The MSE of the estimate of $\mathbf{y}(t)$ is not transferred to estimator, then, the statistics of communication noise is unknown to estimator. However, both estimator and channel decoder are not aware that the estimated performance

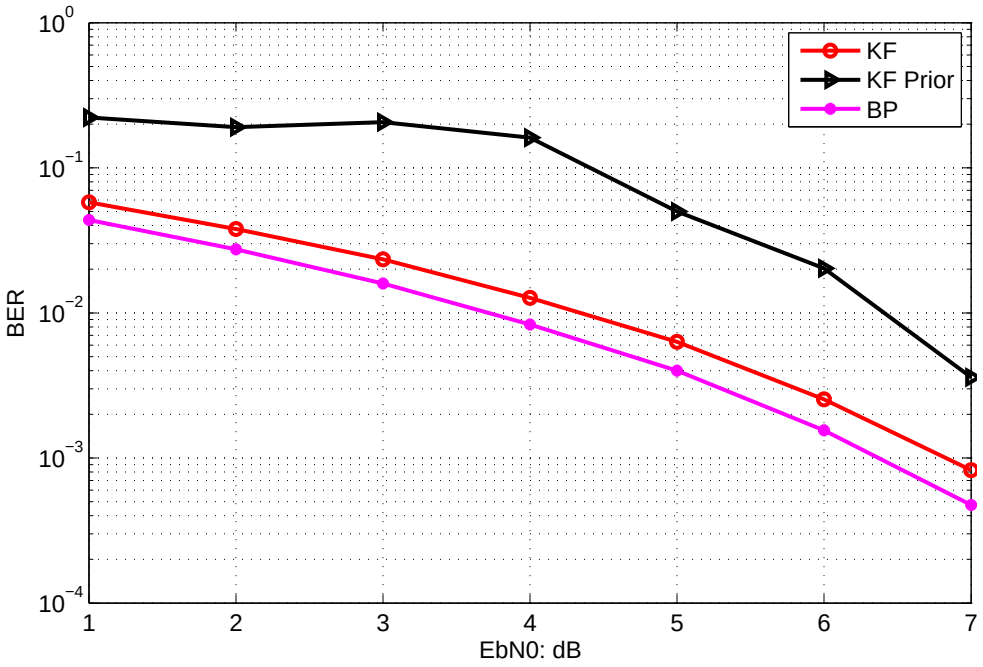

Figure 3.8: Bit Error Rate comparison for system without channel coding

of estimator is better than its actual performance, then, the prediction from estimator has higher weights in channel demodulation than the expected weights;

2. the prediction of system observation is used twice including the update step of Kalman Filter and prediction assisted channel demodulation, which accelarates error propagation.

Note that in uncoded case, the redundancy of system dynamics cannot improve the performance of 'BP' due to that the extrinsic information transferred from channel demodulator to estimator is independent of the prediction of $\mathbf{y}(t)$. The performance gain of 'BP' comes from the feedback of MSE of the estimate of $\mathbf{y}(t)$ which makes estimator has correct statistics about its estimation.

Note that the results are different from that in our conference paper (Gong et al., 2011). In our conference paper, the simulation results show that there is performance gain from system dynamics assisted channel decoding in both 'BP' and 'KF Prior', and there is also error propagation for both approaches. The cause is that we used

different initial simulation condition. In our conference paper, at time slot 1 estimator has perfect information of system state. Therefore, on one hand the estimator has good prediction of system state which can help improve the performance of channel decoding at high SNR; on the other hand, the estimator still thinks that it has good prediction although its performance is degraded by communication noise especially at low SNR leading to error propagation. In this dissertation, at time slot 1 estimator has no priori information of system state from previous time slot. Therefore, for 'KF Prior' there is no performance gain from system dynamics assisted channel decoding. As the weight of prediction from estimator is much lower than that in our conference paper, error propagation is not seen in 'BP'.

3.5.2 Coded Case

Figures 3.9 and 3.10 show the simulation results for the channel coded case with different E_b/N_0. As shown in the figures, the performance of 'BP' is always the best. The performance of system dynamics assisted channel decoding is also seen in 'KF prior' when E_b/N_0 is equal to 4dB and 5dB. However, there is error propagation for 'KF prior' when E_b/N_0 is lower than 4dB. The cause is similar as that for uncoded case.

3.6 Conclusions

In this chapter, we have proposed to use Kalman Filter based and Pearl's BP based decoding procedure (including the demodulation procedure) to exploit the redundancy, i.e., the nature encoding in the system state for the system with no or weak channel coding protection in the context of WNCS. The numerical simulation results have shown that, for coded case there is performance gain from system dynamics assisted channel decoding. In addition, for estimator keeping erroneous

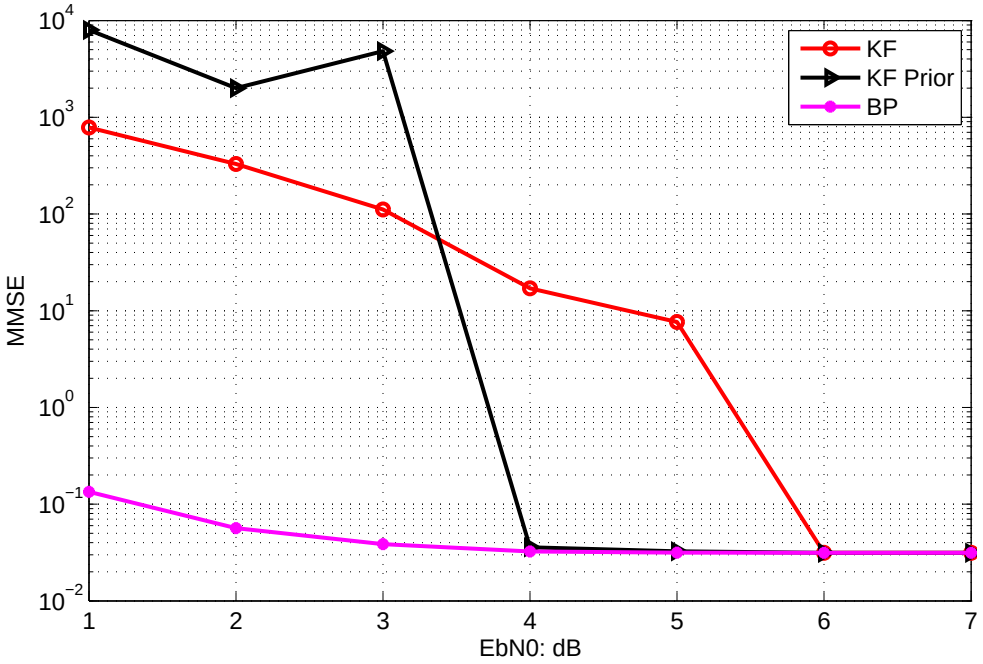

Figure 3.9: Mean Square Error comparison for system with channel coding

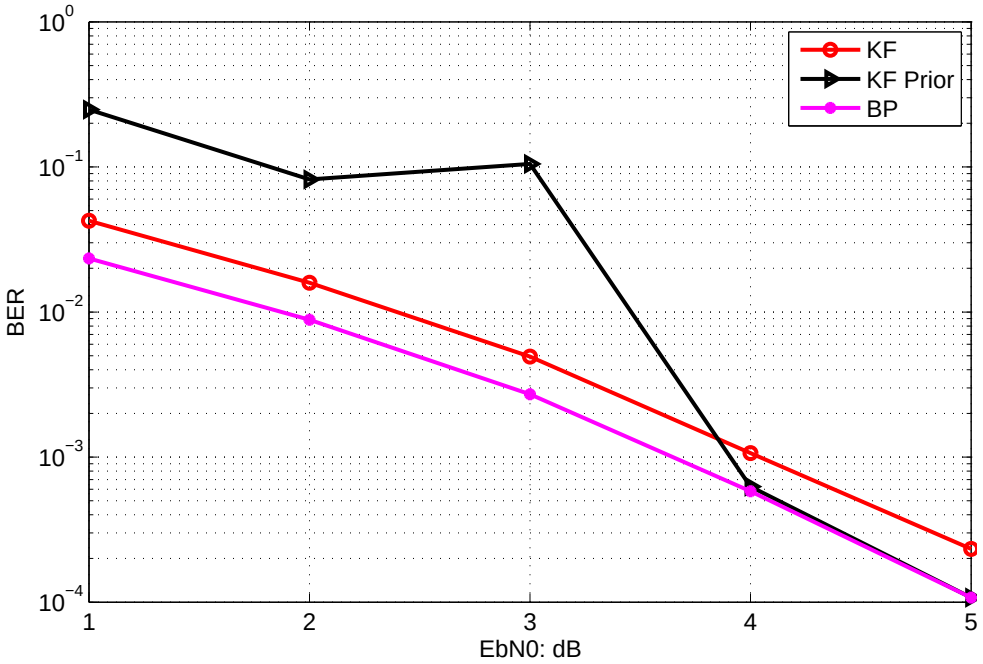

Figure 3.10: Bit Error Rate comparison for system with channel coding

packets the performance can be improved by transferring the statistics of the estimate of system observation to estimator.

Chapter 4

Quickest Detection Based Error Propagation Detection and Its Application for the Protection of System Dynamics Assisted Channel Decoding

4.1 Introduction

Because of low installation and reconfiguration cost wireless communication has been widely applied in networked control system (NCS). NCS is a control system which uses multi-purpose shared network as communication medium to connect spatially distributed components of control system including sensors, actuator, controller. The integration of wireless communication in NCS is challenging due to channel unreliability such as fading, shadowing, interference, mobility and receiver thermal noise leading to packet corruption, packet dropout and packet transmission delay.

In chapter 3 we proposed to utilize time-domain redundancy of system dynamics to assist channel decoding and designed a belief propagation (BP) based channel decoding and state estimation algorithm. The effectiveness of this proposed channel decoding and state estimation algorithm is verified by numerical results. However, in chapter 3, the simulation results especially Kalman Filtering based herustic approach show error propagation at low SNR. Note that the error propagation for BP based channel decoding and state estimation is also observed in our conference paper with different initial simulation condition (Gong et al., 2011). In order to guarantee the reliability of NCS, it is necessary to detect and eliminate error propagation from decoding procedure. In this chapter, at first we show the root cause for error propagation. Then, quickest detection based algorithm is proposed to detect error propagation. We also apply this proposed error propagation detection algorithm into system dynamics assisted channel decoding and state estimation algorithm. The error porpagation detection algorithm is running at the same time with the system dynamics assisted channel decoding and state estimation. Once propagation of errors is detected, then system dynamics assisted channel decoding and state estimation module is reset to eliminate propagation error.

The organization of this chapter is as follows. In section 4.2 the system model, communication model and BP based channel decoding and state estimation algorithm are briefly introduced. Section 4.3 analyzes the root cause for error propagation. Then, quickest detection based error propagation detection algorithm is proposed in section 4.4. Section 4.5 shows how to integrate quickest detection based propagation error detection algorithm into the framework of system dynamics assisted channel decoding and state estimation. The simulation results are demonstrated in section 4.6. Section 4.7 concludes the work in this chapter.

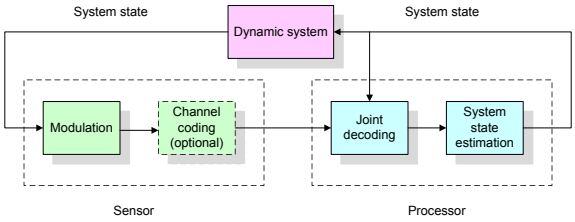

Figure 4.1: An illustration of the communication and dynamic system.

4.2 System Model

In the previous chapter, we proposed a BP based channel decoding and state estimation algorithm. As shown in Figure 4.1, BP based decoding and estimation algorithm works as following: the prediction of system observation $\hat{\mathbf{y}}(t)$ from previous time slot is used to assist channel decoding; then, the soft output of channel decoding is utilized to estimate current system observation $\mathbf{y}(t)$ and system state $\mathbf{x}(t)$.

In this section, the linear system, communication model and BP based iterative channel decoding and state estimation algorithm will be briefly described.

4.2.1 Linear System

We consider a discrete time linear dynamic system, whose system state evolution is given by

$$\begin{cases} \mathbf{x}(t+1) = \mathbf{A}\mathbf{x}(t) + \mathbf{B}\mathbf{u}(t) + \mathbf{n}(t), \\ \mathbf{y}(t) = \mathbf{C}\mathbf{x}(t) + \mathbf{w}(t) \end{cases}, \tag{4.1}$$

where $\mathbf{x}(t)$ is the N-dimensional vector of system state at time slot t, $\mathbf{u}(t)$ is the M-dimensional control vector, $\mathbf{y}$ is the K-dimensional observation vector and $\mathbf{n}$ and $\mathbf{w}$ are noise vectors, which are assumed to be Gaussian distributed with zero expectation and covariance matrices $\mathbf{\Sigma}_n$ and $\mathbf{\Sigma}_w$, respectively. For simplicity, in this work we do not consider $\mathbf{u}(t)$.

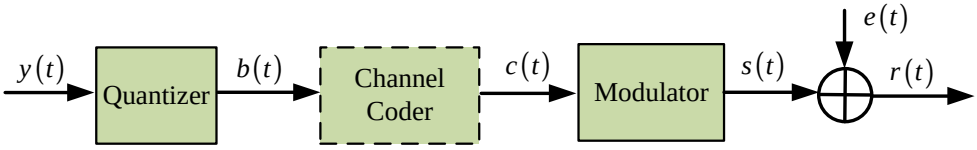

Figure 4.2: Model for communication system.

We assume that the observation vector $\mathbf{y}(t)$ is obtained by a sensor*. The sensor quantizes each dimension of the observation using B bits, thus forming a bit sequence which is given by

$$\mathbf{b}(t) = (b_1(t), b_2(t), ..., b_{KB}(t)) \,. \tag{4.2}$$

4.2.2 Communication System

The framework for communication system is shown in Figure 4.2. Suppose that binary phase shift keying (BPSK) is used for the transmission from the sensor to the controller. The bit sequence is passed through an optional channel encoder, which generates an L-bit sequence $\mathbf{c}(t)$. Finally modulated sequence $\mathbf{s}(t)$ is transmitted. Then, the received signal at the controller is given by

$$\mathbf{r}(t) = \mathbf{s}(t) + \mathbf{e}(t), \tag{4.3}$$

where the additive white Gaussian noise $\mathbf{e}(t)$ has a zero expectation and variance σ_e^2. Note that we ignore the fading and normalize the transmit power to be 1. The algorithm and conclusion in this paper can be easily extended to the case with different types of fading.

4.2.3 Pearl's BP based Iterative Decoding

The Bayesian network structure of the control system and communication system in WNCS is shown for three time slots in Figure 4.3. In the Bayesian network, the

*It is easy to extend to the case of multiple sensors.

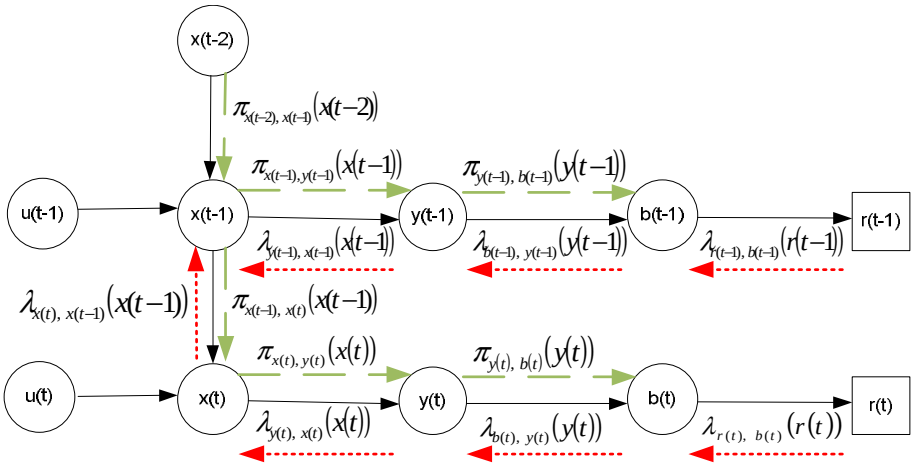

Figure 4.3: Bayesian network structure and message passing for the dynamic system.

system state $\mathbf{x}_t$ is dependent on the previous system state $\mathbf{x}_{t-1}$ and the control action $\mathbf{u}_t$; the observation $\mathbf{y}_t$ is dependent on the system state $\mathbf{x}_t$; the uncoded bits $\mathbf{b}_t$ are dependent on the observation vector $\mathbf{y}_t$; the received signal $\mathbf{r}_t$ is dependent on the uncoded bits $\mathbf{b}_t$. Here we omit the coded bits $\mathbf{s}_t$ as the relationship between the uncoded bits $\mathbf{b}_t$ and the coded bits $\mathbf{s}_t$ is deterministic. Figure 5.6 shows the Bayesian Network structure for the dynamic system with three observations: $\mathbf{x}_{t-2}$, $\mathbf{x}_{t-1}$ and $\mathbf{x}_t$.

Based on the Bayesian network structure, the iterative decoding procedure can be derived. Figure 4.3 shows the message passing in the dynamic system. $\mathbf{x}_{t-2}$ summarizes all the information obtained from previous time slots and transmits π-message $\pi_{\mathbf{x}_{t-2},\mathbf{x}_{t-1}}(\mathbf{x}_{t-2})$ to $\mathbf{x}_{t-1}$. The BP procedure can be implemented in synchronous or asynchronous manners. As the decoding process has a large overhead, we implement asynchronous Pearl's BP. The updating order and message passing in one iteration is as follows: step 1): $\mathbf{x}_{t-1} \rightarrow \mathbf{y}_{t-1}$; step 2): $\mathbf{y}_{t-1} \rightarrow \mathbf{b}_{t-1}$; step 3): $\mathbf{b}_{t-1} \rightarrow \mathbf{y}_{t-1}$; step 4): $\mathbf{y}_{t-1} \rightarrow \mathbf{x}_{t-1}$; step 5): $\mathbf{x}_{t-1} \rightarrow \mathbf{x}_t$; step 6): $\mathbf{x}_t \rightarrow \mathbf{y}_t$; step 7): $\mathbf{y}_t \rightarrow \mathbf{b}_t$; step 8): $\mathbf{b}_t \rightarrow \mathbf{y}_t$; step 9): $\mathbf{y}_t \rightarrow \mathbf{x}_t$; step 10): $\mathbf{x}_t \rightarrow \mathbf{x}_{t-1}$; step 11): $\mathbf{x}_{t-1}$ updates information.Please refer to chapter 3 for detailed mathematical derivation for each step.

4.3 Cause For Error Propagation

As observed in the simulation results of system dynamics based channel decoding and state estimation algorithm, there exists error propagation at low SNR. In this section we will use a simplified example to illustrate the cause of error propagation, which is estimation error of MSE of system observation prediction. In this section we assume that system observation $\mathbf{y}(t)$ has just one dimension and the distribution of $\mathbf{y}(t)$ is standard Gaussian.

In previous chapter, in BP based channel decoding and state estimation algorithm, message $\pi_{\mathbf{y}_t,\mathbf{b}_t}(\mathbf{y}_t)$ is passed from $\mathbf{y}_t$ to $\mathbf{b}_t$ to assist channel decoding. In other words, $\pi_{\mathbf{y}_t,\mathbf{b}_t}(\mathbf{y}_t)$ and received signals $\mathbf{r}(t)$ are used to jointly estimate $\mathbf{y}_t$. However, the distribution of $\pi_{\mathbf{y}_t,\mathbf{b}_t}(\mathbf{y}_t)$ is assumed to be Gaussian with mean $\mathbf{y}_{\pi,t}$ and covariance matrix $S_{\pi,t}$. The Gaussian assumption does not hold all the time; in addition, $\mathbf{y}_{\pi,t}$ and $S_{\pi,t}$ are estimated value. We evaluate the impact of error of estimated $S_{\pi,t}$ on the estimation of system state and observation. Since there is no analytical expression for the conversion of $\pi_{\mathbf{y}_t,\mathbf{b}_t}(\mathbf{y}_t)$ to the priori information of $\mathbf{b}(t)$, the evaluation is done in continous domain.

Figure 4.4 shows the ideal model for joint estimation. $r_c^s(t)$ is the estimated $y(t)$ based received signals $\mathbf{r}(t)$, and $r_p^s(t)$ is the predicted $y(t)$ based on $\pi_{\mathbf{y}_t,\mathbf{b}_t}(\mathbf{y}_t)$. The detailed procedure to estimate $r_c^s(t)$ from received signals $\mathbf{r}(t)$ will be provided in the next section. In this section, we model $r_c^s(t)$ as

$$r_c^s(t) = y(t) + \sigma_c N_c(t) \tag{4.4}$$

in which σ_c^2 is the MSE of $r_c^s(t)$ and $N_c(t)$ is standard Gaussian noise. The prediction of $y(t)$, i.e, $r_p^s(t)$, based on $\pi_{\mathbf{y}_t,\mathbf{b}_t}(\mathbf{y}_t)$ is modeled as

$$r_p^s(t) = y(t) + \sigma_p N_p(t) \tag{4.5}$$

in which σ_p^2 is the MSE of $r_p^s(t)$ and $N_p(t)$ is standard Gaussian noise.

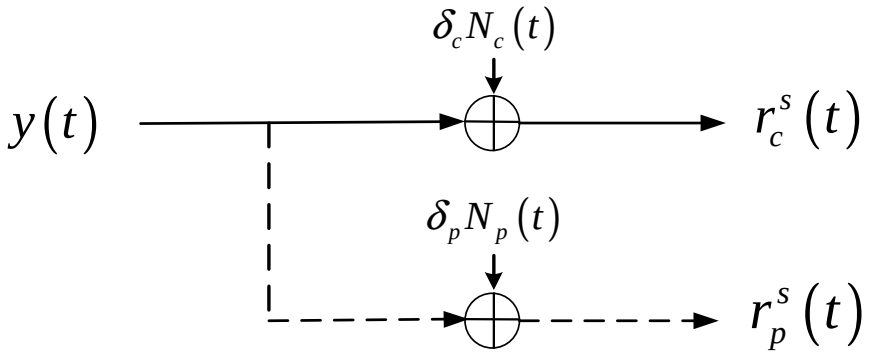

Figure 4.4: Model for estimation from received signal and prediction with known σ_c^2 and σ_p^2

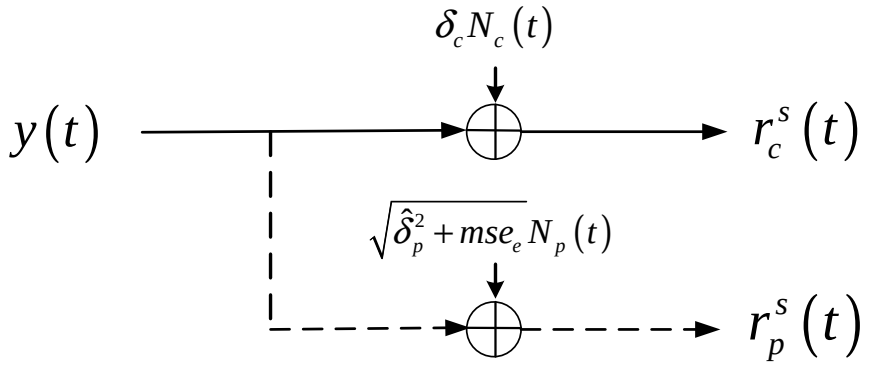

Figure 4.5: Model for estimation from received signal from channel and prediction with known σ_c^2 and estimated $\hat{\sigma}_p^2$

Then the ideal joint estimation of $\hat{y}(t)$ is:

$$\begin{aligned} \hat{y}(t) &= E[y(t)|r_c^s(t), r_p^s(t), \sigma_c^2, \sigma_p^2] \\ &= \frac{\frac{1}{\sigma_c^2}}{1 + \frac{1}{\sigma_c^2} + \frac{1}{\sigma_p^2}} r_c^s(t) + \frac{\frac{1}{\sigma_p^2}}{1 + \frac{1}{\sigma_c^2} + \frac{1}{\sigma_p^2}} r_p^s(t) \end{aligned} \tag{4.6}$$

$$mse(y(t)) = E[(y(t) - \hat{y}_t)^2] = \frac{1}{1 + \frac{1}{\sigma_c^2} + \frac{1}{\sigma_p^2}} \tag{4.7}$$

In the above ideal model, we assume that σ_p and σ_c are known. However, σ_p and σ_c are estimated values. When channel noise power σ_e^2 is known, then the estimation of σ_c is correct. But σ_p depends on estimation over all previous time slots. It is more likely that σ_p deviates from its real value. Therefore, there exists error for estimation of σ_p^2. We model the estimation error as mse_e:

$$mse_e = \sigma_p^2 - \hat{\sigma}_p^2 \tag{4.8}$$

As both σ_p^2 and $\hat{\sigma}_p^2$ are positive values. The range for mse_e is $[\hat{\sigma}_p^2, +\infty]$. Figure 4.5 shows the model of observation with estimation error. The joint estimation is:

$$\begin{aligned} \hat{y}_e(t) &= E[y(t)|r_c^s(t), r_p^s(t), \sigma_c^2, \hat{\sigma}_p^2] \\ &= \frac{\frac{1}{\sigma_c^2}}{1+\frac{1}{\sigma_c^2}+\frac{1}{\hat{\sigma}_p^2}} r_c^s(t) + \frac{\frac{1}{\hat{\sigma}_p^2}}{1+\frac{1}{\sigma_c^2}+\frac{1}{\hat{\sigma}_p^2}} r_p^s(t) \end{aligned} \tag{4.9}$$

and MSE is:

$$\text{mse}_e(y(t)) = \frac{1}{1+\frac{1}{\sigma_c^2}+\frac{1}{\hat{\sigma}_p^2}} + \frac{\frac{\text{mse}_e}{\hat{\sigma}_p^4}}{\left(1+\frac{1}{\sigma_c^2}+\frac{1}{\hat{\sigma}_p^2}\right)^2} \tag{4.10}$$

Besides joint estimation, we can also estimate $y(t)$ based on received channel signal:

$$\hat{y}_c(t) = \frac{\frac{1}{\sigma_c^2}}{1+\frac{1}{\sigma_c^2}} r_c^s(t) \tag{4.11}$$

and MSE is:

$$mse_c(y(t)) = \frac{1}{1+\frac{1}{\sigma_c^2}} \tag{4.12}$$

As shown in Figure 4.6, when mse_e is small, joint estimation is better than estimation only from channel observation. However, when mse_e becomes larger, then

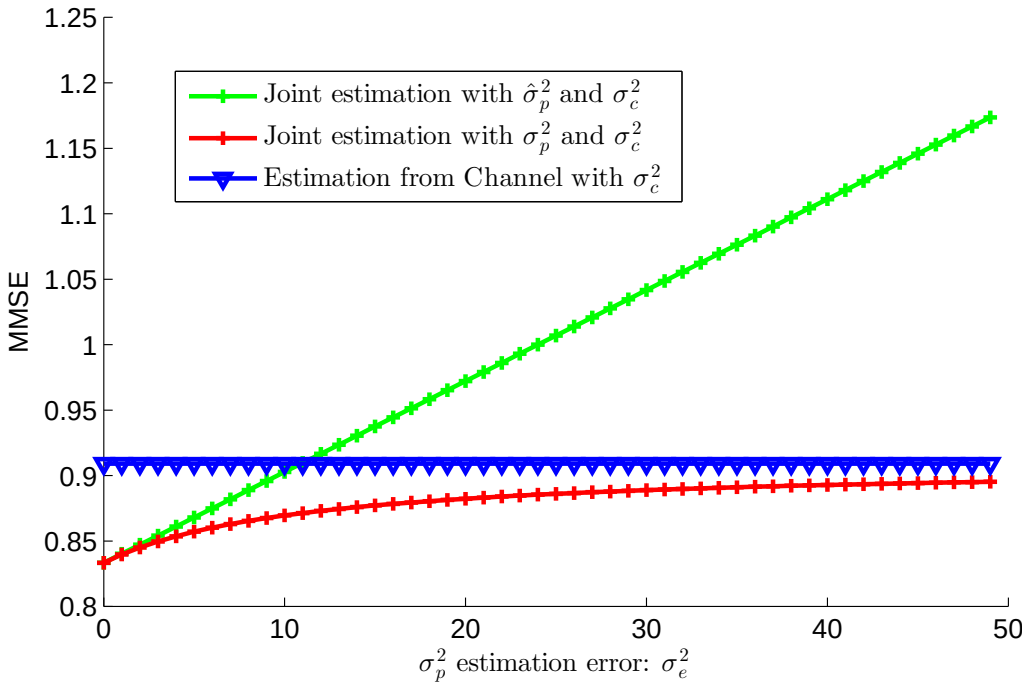

Figure 4.6: MMSE for joint estimation from prediction and estimation from received signal with different σ_e^2: $\hat{\sigma}_p^2 = 10$, $\sigma_c^2 = 10\ \sigma_c^2$ and estimated $\hat{\sigma}_p^2$

the joint estimation from channel observation and prediction is worse than that based only on channel observation. In other words, error propagation happens when mse_e is larger than one threshold.

4.4 Quickest Detection Based Error Propagation Detection

In previous section, we have illustrated that the error of estimated $S_{\pi,t}$ leads to error propagation. Therefore, we can use the estimated MSE of predicted system observations $\mathbf{r}_p^s(t)$ to construct a hypothesis for the detection of error propagation.

$$H0 \quad : \quad \mathbf{r}_p^s(t) = \mathbf{y}(t) + \left(\hat{\mathbf{\Sigma}}_p(t)\right)^{\frac{1}{2}} \mathbf{N}_p(t) \tag{4.13}$$

$$H1 \quad : \quad \mathbf{r}_p^s(t) = \mathbf{y}(t) + \left(\hat{\mathbf{\Sigma}}_p(t) + \mathbf{\Sigma}_e(t)\right)^{\frac{1}{2}} \mathbf{N}_p(t) \tag{4.14}$$

where $\mathbf{r}_p^s(t)$ is the prediction of $\mathbf{y}(t)$ based on information prior to current time slot t, $\hat{\mathbf{\Sigma}}_p(t)$ is the estimation of mean squre error $\mathbf{\Sigma}_p(t)$:

$$\mathbf{\Sigma}_p(t) = E[(\mathbf{y}(t) - \mathbf{r}_p^s(t))(\mathbf{y}(t) - \mathbf{r}_p^s(t))^T] \tag{4.15}$$

$\mathbf{\Sigma}_e$ is the estimation error of $\mathbf{\Sigma}_p(t)$:

$$\mathbf{\Sigma}_e = \mathbf{\Sigma}_p(t) - \hat{\mathbf{\Sigma}}_p(t) \tag{4.16}$$

and $\mathbf{N}_p(t)$ is standard Gaussian vector. H0 refers to the hypothesis in which error propagation does not happen. Therefore, $\hat{\mathbf{\Sigma}}(t)$ is equal to $\mathbf{\Sigma}(t)$. H1 refers to the hypothesis in which error propagation happens and $\mathbf{\Sigma}_e(t)$ is a semi-positive matrix. For simplicity, we assume that $\mathbf{\Sigma}_e(t)$ is an unknown constant diagonal matrix. Note that we will use $\mathbf{\Sigma}_e$ instead of using $\mathbf{\Sigma}_e(t)$ in the remaining of this work. However, we cannot directly detect error propagation from this hypothesis due to that $\mathbf{y}(t)$ is unknown. As mentioned in the previous section, when channel noise power σ_e^2 is known, system observation $\mathbf{y}(t)$ can be estimated received channel signals $\mathbf{r}(t)$.

$$\mathbf{r}_c^s(t) = \mathbf{y}(t) + \left(\hat{\mathbf{\Sigma}}_c(t)\right)^{\frac{1}{2}} \mathbf{N}_c(t) \tag{4.17}$$

$$\tag{4.18}$$

where $\mathbf{r}_c^s(t)$ is the estimation of $\mathbf{y}(t)$ from channel observation and the kth element of $\mathbf{r}_c^s(t)$ is:

$$r_{c,k}^s(t) = \sum_{i=0}^{i=B-1} \hat{s}_{kB+i}(t) Q_I^i, k = 0, \cdots, K-1 \tag{4.19}$$

where $\hat{b}_{kB+i}(t)$ is the estimation of ith modulated bit of quantized $y_k(t)$, $s_{kB+i}(t)$, based on channel observation $r_{kB+i}(t)$ and is equal to:

$$\begin{aligned} \hat{s}_{kB+i}(t) &= P(S_{kB+i}(t) = 1 | r_{kB+i}(t)) - P(s_{kB+1}(t) = -1 | r_{kB+i}(t)) \\ &= \tan\left(\frac{r_{kB+i}(t)}{(\sigma_c^b)^2}\right) \end{aligned} \tag{4.20}$$

and Q_I is the base of quantization and B is the number of quantization bits. $\hat{\mathbf{\Sigma}}_c(t)$ is the MSE of estimated $\mathbf{y}(t)$ from channel observation, which is a diagonal matrix and the kth diagonal element of $\hat{\mathbf{\Sigma}}_c(t)$ is:

$$\hat{\mathbf{\Sigma}}_{c,k}(t) = \sum_{i=0}^{i=B-1} \text{mse}_{kB+i}(t) Q_I^{2i} \tag{4.21}$$

where $\text{mse}_{kB+i}(t)$ is the mse of the estimated $s_{kB+i}(t)$ from channel only:

$$\text{mse}_{kB+i}(t) = E[(\hat{b}_{kB+i}(t) - b_{kB+i}(t))^2] = 1 - \tan^2\left(\frac{r_{kB+i}(t)}{(\sigma_c^b)^2}\right) \tag{4.22}$$

Then, we use $\mathbf{r}_c^s(t)$ as reference for the above hypothesis detection. Note that the way to obtain $\mathbf{r}_c^s(t)$ works for uncoded systrem and the system systematic coding case. For coding case, if the coding scheme is not systematic, then more complicated procedures are needed to obtain estimated $\mathbf{r}_c^s(t)$.

Deduct $\mathbf{r}_c^s(t)$ from $\mathbf{r}_p^s(t)$, then the hypothesis is:

$$\begin{aligned} H_0 &: \mathbf{d}(t) = \left(\hat{\mathbf{\Sigma}}_p(t)\right)^{\frac{1}{2}} \mathbf{N}_p(t) - \left(\hat{\mathbf{\Sigma}}_c(t)\right)^{\frac{1}{2}} \mathbf{N}_c(t) \\ H_1 &: \mathbf{d}(t) = \left(\hat{\mathbf{\Sigma}}_p(t) + \mathbf{\Sigma}_e\right)^{\frac{1}{2}} \mathbf{N}_p(t) - \left(\hat{\mathbf{\Sigma}}_c(t)\right)^{\frac{1}{2}} \mathbf{N}_c(t) \end{aligned} \tag{4.23}$$

where

$$\mathbf{d}(t) = \mathbf{r}_p^s(t) - \mathbf{r}_c^s(t) \tag{4.24}$$

We re-write above hypothesis equation as:

$$\begin{aligned} H_0 &: \mathbf{d}(t) = (\mathbf{\Sigma}_0(t))^{\frac{1}{2}} \mathbf{N}_0(t) \\ H_1 &: \mathbf{d}(t) = (\mathbf{\Sigma}_0(t) + \mathbf{\Sigma}_e)^{\frac{1}{2}} \mathbf{N}_1(t) \end{aligned} \tag{4.25}$$

where

$$\mathbf{\Sigma}_0(t) = \hat{\mathbf{\Sigma}}_p(t) + \hat{\mathbf{\Sigma}}_c(t) \tag{4.26}$$

$\mathbf{N}_0(t)$ and $\mathbf{N}_1(t)$ are K-dimension standard Gaussian variables. From the above equations, when error propagation happens at the unknown time instant t_0, the distribution of $\mathbf{d}(t)$ is changed from $\mathbf{\Sigma_0}(t)$ to $\mathbf{\Sigma_0}(t) + \mathbf{\Sigma}_e$, where $\mathbf{\Sigma}_e$ is unknown. In this paper, we adopt CUSUM algorithm to estimate unknown parameters t_0 and $\mathbf{\Sigma}_e$. Based on CUSUM method we construct the log-likelihood ratio for the observations $\mathbf{d}(t)$ from time j up to k, which is equal to:

$$S_j^k(\mathbf{\Sigma}_e) = \sum_{t=j}^{k} l_\theta(t) = \sum_{t=1}^{k} \frac{P_{\mathbf{\Sigma}_0(t)}(\mathbf{d}(t))}{P_{\mathbf{\Sigma}_0(t)+\mathbf{\Sigma}_e}(\mathbf{d}(t))} \tag{4.27}$$

where:

$$P_{\mathbf{\Sigma}_0(t)}(\mathbf{d}(t)) = \frac{1}{(2\pi|\mathbf{\Sigma}_0(t)|)^{\frac{K}{2}}} \mathbf{d}^T(t) \mathbf{\Sigma}_0^{-1}(t) \mathbf{d}^T(t) \tag{4.28}$$

and

$$P_{\mathbf{\Sigma}_0(t)+\mathbf{\Sigma}_e}(\mathbf{d}(t)) = \frac{1}{(2\pi|\mathbf{\Sigma}_0(t) + \mathbf{\Sigma}_e|)^{\frac{K}{2}}} \mathbf{d}^T(t) (\mathbf{\Sigma}_0(t) + \mathbf{\Sigma}_e)^{-1} \mathbf{d}^T(t) \tag{4.29}$$

The statistical metric is the maximum likelihood estimation of $\mathbf{\Sigma}_e$, which results in the decision function given by

$$g_k = \max_{1 \le j \le k} \sup_{\mathbf{\Sigma}_e \in \Theta} S_j^k(\mathbf{\Sigma}_e) \tag{4.30}$$

where Θ is the region of $\mathbf{\Sigma}_e$. Then the decision rule is

$$\begin{cases} H_0 \text{ is selected; if } g_k < h \\ H_1 \text{ is selected; if } g_k \ge h \end{cases} \tag{4.31}$$

where h is the pre-determined threshold. The alarm time for error propagation is obtained by the following stopping rule:

$$t_0 = min\{k : g_k \ge h\} \tag{4.32}$$

Finally, the procedure of CUSUM quickest detection based error propagation detection algorithm is shown in Procedure 1.

Procedure 1 Procedure for CUSUM quickest detection based propagation error detection algorithm

1: **for** each time slot t, $t = 1, 2, ...,$ **do**
2: Current observation prediction $\mathbf{r}_p^s(t)$ and $\hat{\mathbf{\Sigma}}_p(t)$ are obtained from time slot $t-1$;
3: Estimation from channel received signals $\mathbf{r}_c^s(t)$ and $\hat{\mathbf{\Sigma}}_c(t)$ are obtained via equation 4.17;
4: Obtain $\mathbf{d}(t)$ via equation 4.24 ;
5: Calculate detection metric g_k from equation 4.30;
6: Make decision based on rule defined in equation 4.31 ;
7: **if** Propagaton error is deteced **then**
8: calculate time slot of error propagation $t_0(t)$ from equation 4.32.
9: **end if**
10: **end for**

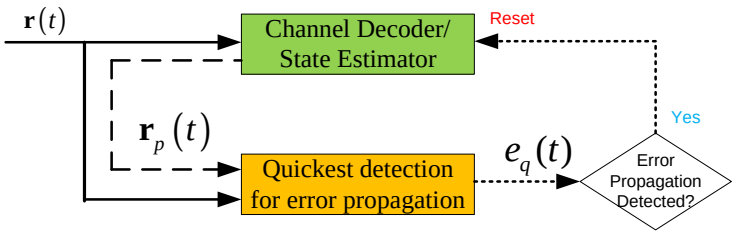

Figure 4.7: BP based channel decoding and system estimation with protection of error propagation detection

4.5 System Dynamics Assisted Channel Decoding and State Estimation with Protection of Error Propagation Detection

In this section, we demonstrate how to utilize the proposed error propagation dedection algorithm to improve performance and robustness of the system dynamics assisted channel decoding and state estimation algorithm. In this scheme, the channel decoding and state estimation module resets and discards any priori information from previous time slots once error propagation is detected. . The framework is shown in Figure 4.7. The received signal $\mathbf{r}(t)$ is input for both modules. $\mathbf{r}_p(t)$ is sent from BP based channel decoding and state estimation module to error propagation detection module. Once error propagation module detects error propagation, it sends a reset signal to BP based channel decoding and state estimation module. Then, BP based channel decoding and state estimation module resets the memory and clear up the error.

4.6 Numerical Simulations

We run the simulations using Matlab to verify the performance of Kalman Filter based heuristic approach and BP based channel decoding and system estimation with protection of error propagation detection. The baseline approach is the separated

Kalman filtering and decoding process. In the following, these three algorithms are referred as 'KF Prior', 'BP' and 'KF', respectively. And the corresponding algorithms with protection of error propagation detection are referred as 'EP based KF Prior' and 'EP based BP', respectively. The performance metrics are the mean square error (MSE) of each sample and the average bit error rate (BER). Each simulation runs 1000 times slots. The configuration for simulation is the same as that in section 3.5. The simulation results for uncoded case and coded case are presented in this section.

4.6.1 Uncoded Case

Figures 4.8 and 4.9 show the simulation results for the uncoded case with different E_b/N_0. The performance of 'EP based BP' is identical with that of 'BP'. The reason why we suggest using error propagation detection scheme for 'BP' is to improve its robustness. The MSE of 'EP based KF Prior' is always lower than 'KF' which means that error propagation of 'KF prior' is eliminated by error propagation detection algorithm. Note that BER of 'EP based KF Prior' is higher than that of 'KF' when E_b/N_0 is less than 4dB. At low E_b/N_0 the mse gain of 'EP based KF Prior' over 'KF' comes from the reset of estimator triggered by error propagation detection scheme instead of system dynamics assisted channel decoding.

4.6.2 Coded Case

Figures 4.10 and 4.11 show the simulation results for the uncoded case with different E_b/N_0. The results are similar as that for uncoded case. The performance of 'EP based BP' is identical with that of 'BP'. The MSE of 'EP based KF Prior' is always lower than 'KF' which means that error propagation of 'KF prior' is eliminated by error propagation detection algorithm. Note that BER of 'EP based KF Prior' is higher than that of 'KF' when E_b/N_0 is lower than 4dB. At low E_b/N_0 the mse gain of 'EP based KF Prior' over 'KF' comes from the reset of estimator triggered by error propagation detection scheme instead of system dynamics assisted channel decoding.

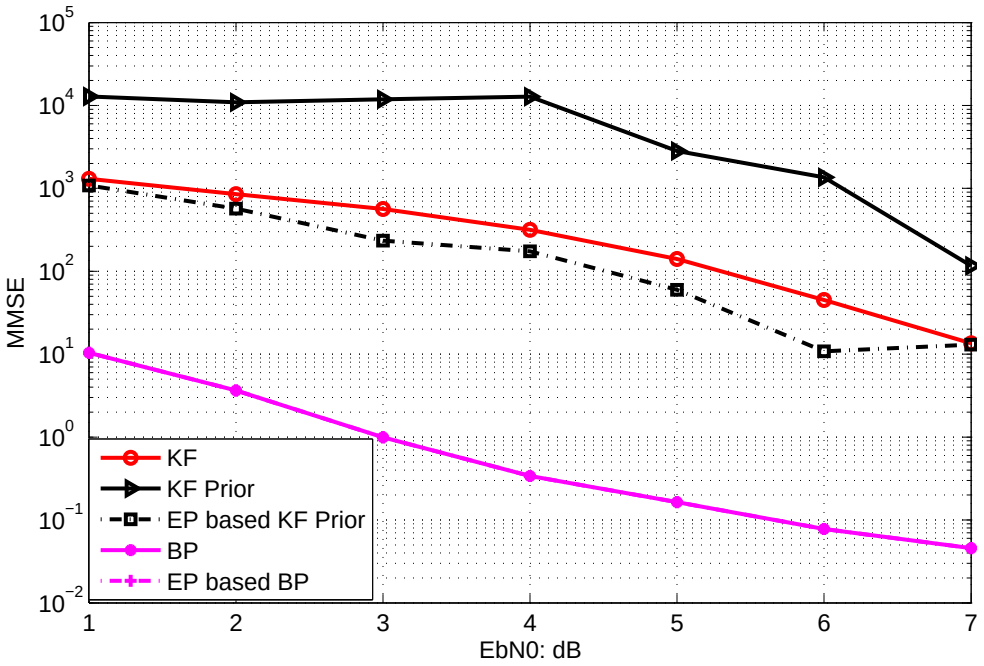

Figure 4.8: Mean Square Error comparison for system without channel coding

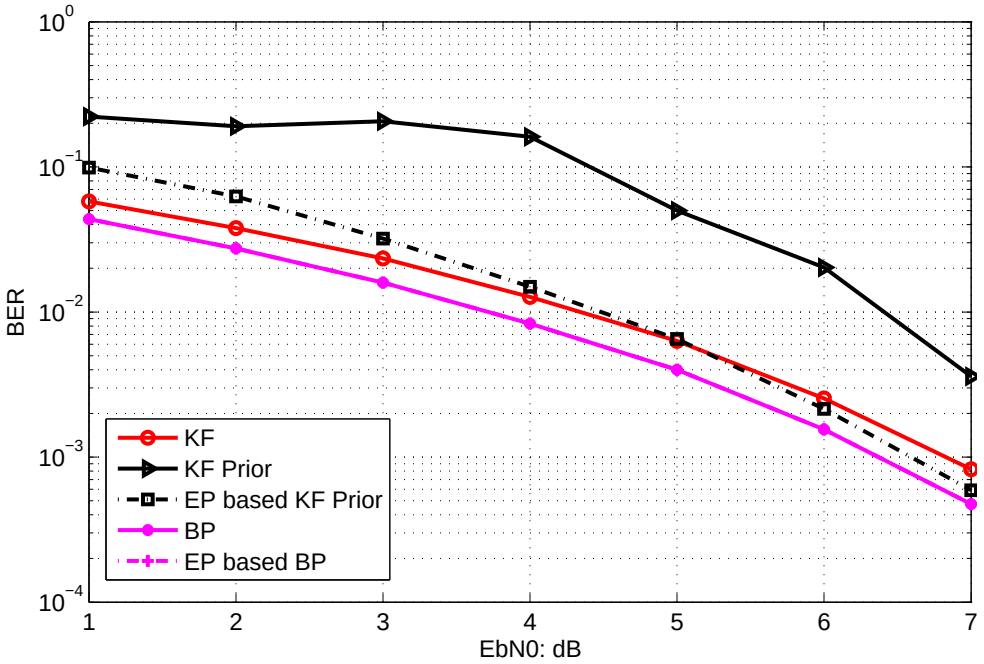

Figure 4.9: Bit Error Rate comparison for system without channel coding

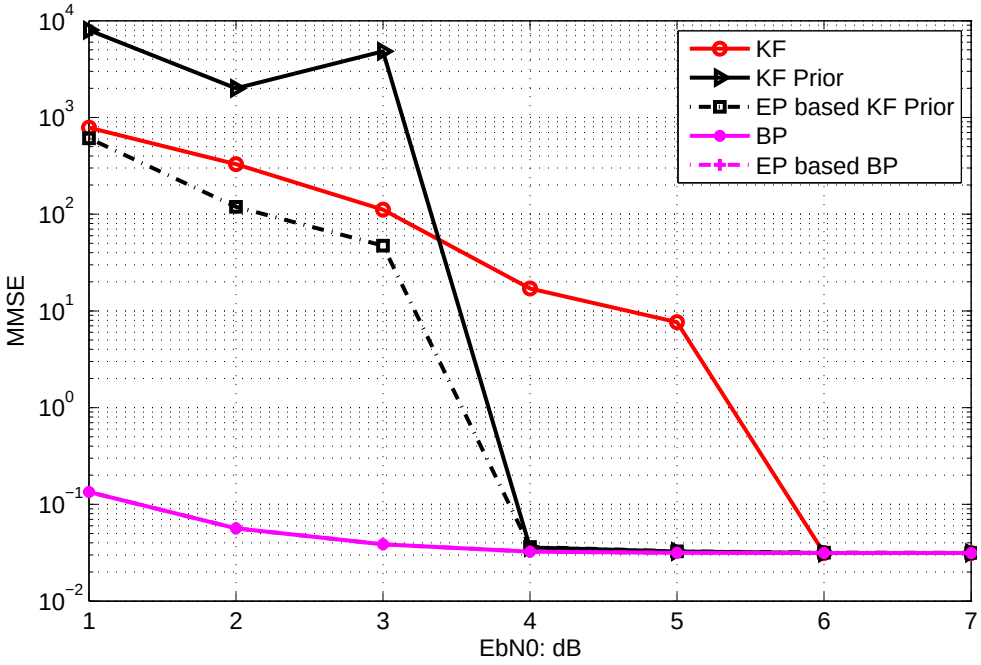

Figure 4.10: Mean Square Error comparison for system with channel coding

When E_b/N_0 is equal to 4 dB and 5dB, BER of 'KF Prior' and 'EP based KF Prior' are lower than that of 'KF', which demonstrates the performance gain of system dynamics assisted channel decoding.

4.7 Conclusions

In this chapter, we have analyzed the cause for error propagation. Based on the analysis result, we propose to use quickest detection to detect error propagation. Then, we propose to utilize the proposed error propagation detection algorithm to protect system dynamics assisted channel decoding and state estimation. The simulation results show that error propagation is eliminated in the new proposed scheme.

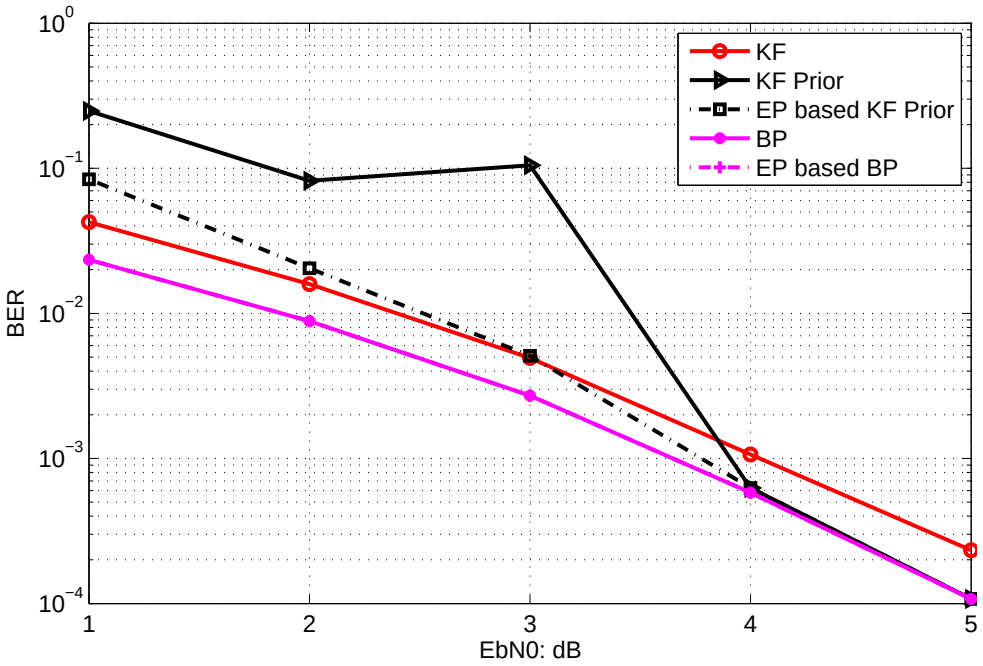

Figure 4.11: Bit Error Rate comparison for system with channel coding

Chapter 5

MSE-based Transfer Chart for Performance Evaluation of Belief Propagation based Sequential and Iterative Channel Decoding and System Estimation

5.1 Introduction

Because of low installation and reconfiguration cost wireless communication has been widely applied in networked control system (NCS). NCS is a control system which uses multi-purpose shared network as communication medium to connect spatially distributed components of control system including sensors, actuator, and controller. The integration of wireless communication in NCS is challenging due to channel unreliability such as fading, shadowing, interference, mobility and receiver thermal noise leading to packet corruption, packet dropout and packet transmission delay.

In chapter 3 we proposed to utilize time-domain redundancy of system state to assist channel decoding and designed a belief propagation (BP) based channel decoding and system state estimation algorithm. And the effectiveness of this proposed iterative channel decoding and system state estimation algorithm is verified by numerical results. In this chapter, we evaluate its performance from the following perspectives:

- How much gain can be obtained from using redundancy of system state in time-domain to assist channel decoding?
- Does iterative channel decoding and system state estimation converge and help improve the performance of channel decoding and system state estimation?
- Does the channel decoding and system state estimation converge over time?

As pointed out in chapter 1 NCS is a hybrid system: non-binary and continuous system state $\mathbf{x}(t)$/observation $\mathbf{y}(t)$ and quantized information bits $\mathbf{b}(t)$ transmitted in wireless communication system. In the iterative channel decoding and system state estimation framework, the priori information transmitted from state estimator to channel decoder is the prediction of $\mathbf{y}(t)$; however, channel decoding requires the prior information of each quantized bit of $\mathbf{y}(t)$. The output of channel decoder is the extrinsic information of each quantized bit; however, the state estimator requires estimates of $\mathbf{y}(t)$ from channel decoder. The challenge for performance analysis is how to handle the information exchange between channel decoder which processes information of quantized bits and state estimator which handles information of continuous variables. We proposed to use MSE-based chart to analyze the performance of BP based channel decoding and system state estimation. The information transferred from non-binary source to channel decoding is the priori mutual information of transmitted information bits. We used the MSE-based analysis framework proposed in (Bhattad and Narayanan, 2007) to evaluate the performance of channel decoding. Then the MSE of decoded information bits is converted to MSE of system observation estimation.

We proposed two models to evaluate the performance of BP based iterative channel decoding and system state estimation. The first model can be used to check the following points:

1. Does the iterative channel decoding and estimation converge?
2. How many iterations are sufficient?
3. How much gain can be obtained from redundancy of source?

The second model can be used to evaluate the performance of system state estimation over time.

The remainder of this chapter is organized as following. Next section, section 5.2 surveys the literature of iterative decoding performance analysis method. Section 5.3 briefly introduce about EXIT and MSE transfer chart for the performance evaluation of iterative channel decoding. Section 5.4 describes the message passing models for analysis. Section 5.5 presents the message transfer framework between system observation and channel decoder. Section 5.6 describes the MSE-base transfer chart, and section 5.7 presents how to use the MSE-based transfer chart to evaluate BP based sequential and iterative channel decoding and state estimation. Section 5.8 concludes this chapter.

5.2 Literature Review

In the area of wireless communication, the purpose of performance analysis for iterative decoding scheme is to find out that, for a given codec and decoder and a given channel noise power, the message-passing iterative decoder can correct the errors or not. Then the results of performance analysis can be used to assist the design of codec and decoder. Gallager (1963) proposed to use density evolution to track the iterative decoding performance. It is based on the assumption that, for very long codes, the extrinsic log likelihood ratios (LLRs) passed between the component decoders are

independent and identically distributed. Then, for the iterative decoding performance it is equivalent to track the evolution of extrinsic LLRs probability density function (pdf) through iterative decoding process. The probability of decoding error tends to zero if extrinsic LLRs goes to either $+\infty$ or $-\infty$.

ten Brink (1999, 2000, 2001) proposed to use extrinsic information transfer chart (EXIT) to track the iterative decoding performance. Based on the assumption that the distribution of extrinsic LLR is Gaussian EXIT tracks mutual information of extrinsic LLRs instead of pdf. Comparing with density evolution, the computation for EXIT is simplified. In addition, the evolution of mutual information through iterative decoding process can be illustrated in a graph and easy to visualize. EXIT has two properties. One property is about the necessary condition for the convergence of iterative decoding: the flipped EXIT curve of the outer decoder should lie below the EXIT curve of the inner coder. The other property is that the area under EXIT curve of outer code relates to the rate of inner coder. Ashikhmin et al. (2004) demonstrated that if the a priori channel is an erasure channel, for any outer code of rate R, the area under the EXIT curve is $1 - R$. To the best knowledge of us, the area property of EXIT has been proved only for erasure priori channel.

Another alternative for density evolution is MSE chart. Instead of tracking mutual information MSE is proposed to track the iterative decoding performance (Bhattad and Narayanan, 2007). The MSE chart analysis method is based on the relationship between mutual information and minimum mean square error (MMSE) in AWGN channel (Guo et al., 2005). Bhattad and Narayanan (2007) has proven the area property of MSE chart when the priori channel is Gaussian.

In this chapter, we also used MSE chart to analyze the performance of iterative channel decoding and state estimation. Comparing with (Guo et al., 2005) the difference in this dissertation work is that we have a hybrid model. The system state and observation are non-binary source in continuous domain; on the other hand the information transmitted in wireless system is quantized bits. Therefore, the method proposed in (Guo et al., 2005) cannot be used directly. The challenge is how to

handle the message transfer between non-binary source and information bits. The other difference is that the source is correlated over time. The estimation error from previous time slots also affects the performance of estimation in current time slot. Therefore, besides evaluating the performance of iterative channel decoding and state estimation in two time slots, it is also very important to evaluate the performance of state estimation over time.

Another area in wireless communication related to our work is joint source and channel decoding (Yin et al., 2002; Mei and Wu, 2006; Pan et al., 2006; Pu et al., 2007; Ramzan et al., 2007; Garcia-Frias and Villasenor, 1997, 1998, 2001; Garcia-Frias and Zhao, 2001, 2002; Garcia-Frias and Zhong, 2003; Garcia-Frias et al., 2003). The idea of joint source and channel decoding is to utilize redundancy in source to assist channel decoding. Our work can also be considered as one special case of joint source and channel decoding. However, there are two major differences. One difference is that most works focus on binary source and EXIT chart was used for performance analysis (Fresia et al., 2010). Zhao and Garcia-Frias (2002, 2005) considered the case with non-binary source, but the performance analysis was not provided. The other difference is these works considered the joint source and channel decoding over only two time slots. In our work, the dynamic state changes over time. Therefore, the performance of channel decoding and system estimation at the current time slots also impacts its performance in the future. Therefore, we also study the performance of iterative estimation and decoding over time.

In NCS area studying the impact of the communication on estimation and control has received considerable attentions. The impact of quantization on stability of estimation and control system has been studied extensively (Nair and Evans, 2004),(Tatikonda and Mitter, 2004),(Cover and Thomas, 1991), (Minero et al., 2009), (You and Xie, 2011) and (Minero et al., 2013). However, the analysis in these works is based on the assumption that the transmission over networking is loss-less. Most works considering the impact of communication on estimation and control generally assume that all erroneous packets are dropped by the estimator. Therefore, these

works studies only the impact of packet drop or packet delay on the stability and performance of estimation and control (Sinopoli et al., 2004), (Imer et al., 2006), (Schenato et al., 2007), (Schenato, 2008). It was proposed by Mostofi and Murray (2009c) keep some erroneous packets can improve stability and performance for real-time control application.Mostofi and Murray (2009c). Mostofi and Murray (2009b) considered the communication noise resulted from accepting corrupted received samples and reformulated the Kalman filter based estimation problem. The criteria to keep or drop erroneous packets were set in this work. However, it is based on the assumption that the knowledge about the statistics of communication noise is available. Although the statistics of communication noise for uncoded case was computed by Mostofi and Murray (2004), it is difficult to compute the statistics of communication noise for coded case. In our work, we considered the case in which all erroneous packets are accepted, which is reasonable as we can estimate the statistics of communication noise. Since we utilize the redundancy of system state over time and use the estimates from previous time slot to assist channel decoding at the current time slot, the statistics of communication noise not only depends on wireless channel but also on the estimate from previous time slot. In our work, we also estimate the statistics of communication noise online.

5.3 Preliminaries: EXIT Chart and MSE Chart for Iterative Decoding of Serially Concatenated Coding Scheme

In this section, we review the concept of EXIT-chart and MSE-chart by the iterative decoding of a serially concatenated coding scheme. In subsection 5.3.1 we use an example to demonstrate serially concatenated coding scheme and its iterative decoding process. Then, in subsection 5.3.2 we review about how to use EXIT chart and MSE chart to analyze the performance of iterative decoding.

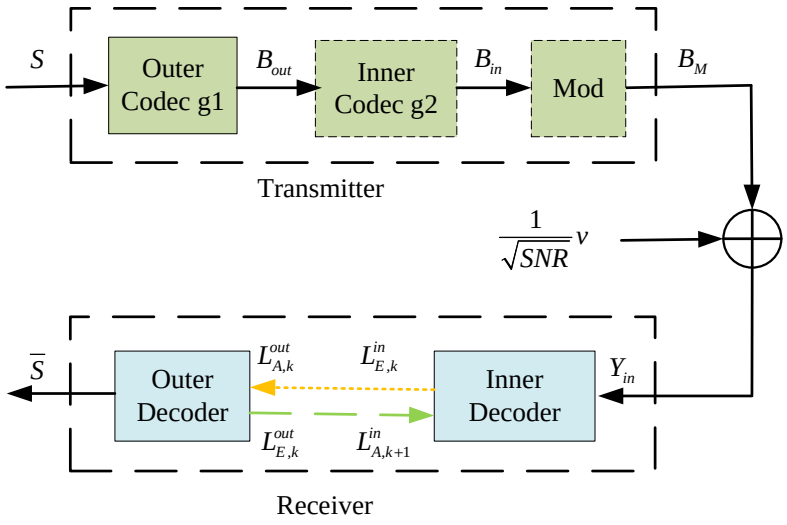

Figure 5.1: A demo of concatenated encode and iterative decoding.

5.3.1 A Serially Concatenated Coding Scheme and Corresponding Iterative Decoding Algorithm

Figure 5.1 shows one simple serial concatenated coding scheme and its corresponding iterative decoding scheme. The binary source $\mathbf{S}$ is a vector with length L_s, i.e., $\mathbf{S} = [S_1, \cdots, S_{L_s}]$. $\mathbf{S}$ is encoded by outer channel encoder, which is a systematic convolutional encoder with generator g_{out}, and the output is $\mathbf{B}_{out}$, which is a vector with length L_{out}. Then, $\mathbf{B}_{out}$ is encoded by innner channel encoder, which is also a systematic convolutional encoder with generator g_{in}, and the output is $\mathbf{B}_{in}$, a vector with length L_{in}. Then $\mathbf{B}_{in}$ is modulated and the output is $\mathbf{B}_m$, i.e., $B_{m,i} = 2B_{in,i} - 1, i = 1, \cdots, L_{in}$, and sent over a AWGN channel:

$$Y_{in,i} = B_{m,i} + \frac{1}{\sqrt{SNR}} v_i, i = 1, \cdots, L_{in} \tag{5.1}$$

where SNR is the signal power to noise power ratio, v_i is a zero mean and unit variance Gaussian noise.

At the receiver, decoding is done iteratively between inner decoder and outer decoder as shown in Figure 5.1. The inputs for inner channel decoder are received

signal $\mathbf{Y}_{in}$ and a priori information from outer decoder, i.e., $\mathbf{L}_A^{in,k} = L_E^{out,k-1}$, where $L_E^{out,k}$ is the extrinsic information of outer decoder from kth decoding round, and the output is $\mathbf{L}_E^{in,k}$, i.e.,

$$\mathbf{L}_{E,i}^{in,k} = LLR(S_i|\mathbf{Y}_{in}, \mathbf{L}_{A,\ i}^{in,k}, g_{in}), i = 1, \cdots, L_s \tag{5.2}$$

where $\mathbf{L}_{A,\ i}^{in,k}$ means the priori information from $\mathbf{L}_{A,\ i}^{in,k}$ for all $\mathbf{S}$ except S_i. The input for outer channel decoder is a priori information from inner decoder, i.e., $\mathbf{L}_A^{out,k} = \mathbf{L}_E^{in,k}$ and the output is $L_E^{out,k}$,i.e.,

$$\mathbf{L}_{E,i}^{out,k} = LLR(S_i|\mathbf{L}_{A,\ i}^{out,k}, g_{out}), i = 1, \cdots, L_s \tag{5.3}$$

where $\mathbf{L}_{A,\ i}^{out,k}$ means the priori information from $\mathbf{L}_{A,\ i}^{out,k}$ for all $\mathbf{S}$ except S_i.

5.3.2 EXIT Chart and MSE Chart

The iterative decoding scheme can be analyzed by tracking density evolution over iterations which is proposed by Gallager (1963). Density evolution is based on the assumption that, for very long codes, the extrinsic LLRs passed between the decoders are i.i.d. Then, for the iterative decoding performance it is equivalent to track the evolution of extrinsic LLRs pdf through iterative decoding process. If extrinsic LLRs goes to either $+\infty$ or $-\infty$, then the probability of decoding error tends to zero. However, density evolution is complex as it requires to obtain pdf of extrinsic LLRs for each iteration; in addition, density evolution does not provide much insight about the operations of iterative decoding. In order to overcome the drawbacks of density evolution, many transfer chart based analysis frameworks have been proposed, such as EXIT chart by ten Brink (1999, 2000, 2001), MSE chart by Guo et al. (2005). The idea of these transfer chart based analysis frameworks is to approximate the pdf of extrinsic LLRs exchanged between inner decoder and outer decoder by a parameter,

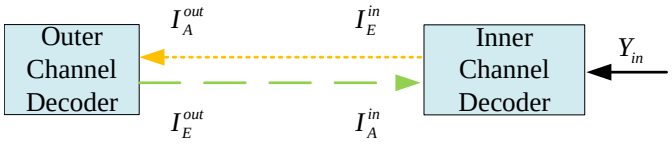

Figure 5.2: EXIT chart model for concatenated encode and iterative decoding.

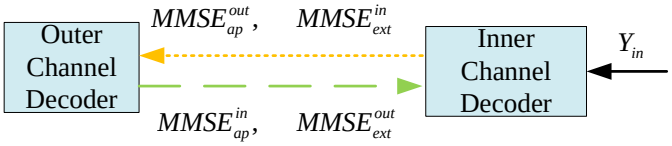

Figure 5.3: MSE-based transfer chart model for concatenated encode and iterative decoding.

i.e.,

$$F(\mathbf{S}, \mathbf{L}) = \frac{1}{L_s} \sum_{i=1}^{L_s} F(S_i, L_i), i = 1, \cdots, L_s \tag{5.4}$$

The measure used by EXIT chart is mutual information, i.e., $I(\mathbf{S}, \mathbf{L})$, which is based on the observation that the pdf of extrinsic LLRs can be approximated by a Gaussian distribution (ten Brink, 1999, 2000, 2001). The measure used by MSE Chart is:

$$F(\mathbf{S}, \mathbf{L}) = E[\tanh^2(L/2)] \tag{5.5}$$

where $E[\tanh^2(L/2)]$ is related to MMSE estimate of X based on observation Y (Guo et al., 2005),i.e.,

$$\begin{aligned} mmse(X|Y) = E[(X - \hat{X})^2] = 1 - E[\tanh^2(L/2)], \\ \hat{X} = E[X|Y] = \tanh(L/2), \\ L = LLR(X|Y) = \log\left(\frac{P(X=1,Y)}{P(X=-1,Y)}\right) \end{aligned} \tag{5.6}$$

The EXIT chart and MSE chart based decoding framework for serially concatenated coding scheme are shown in Figure 5.2 and Figure 5.3, respectively.

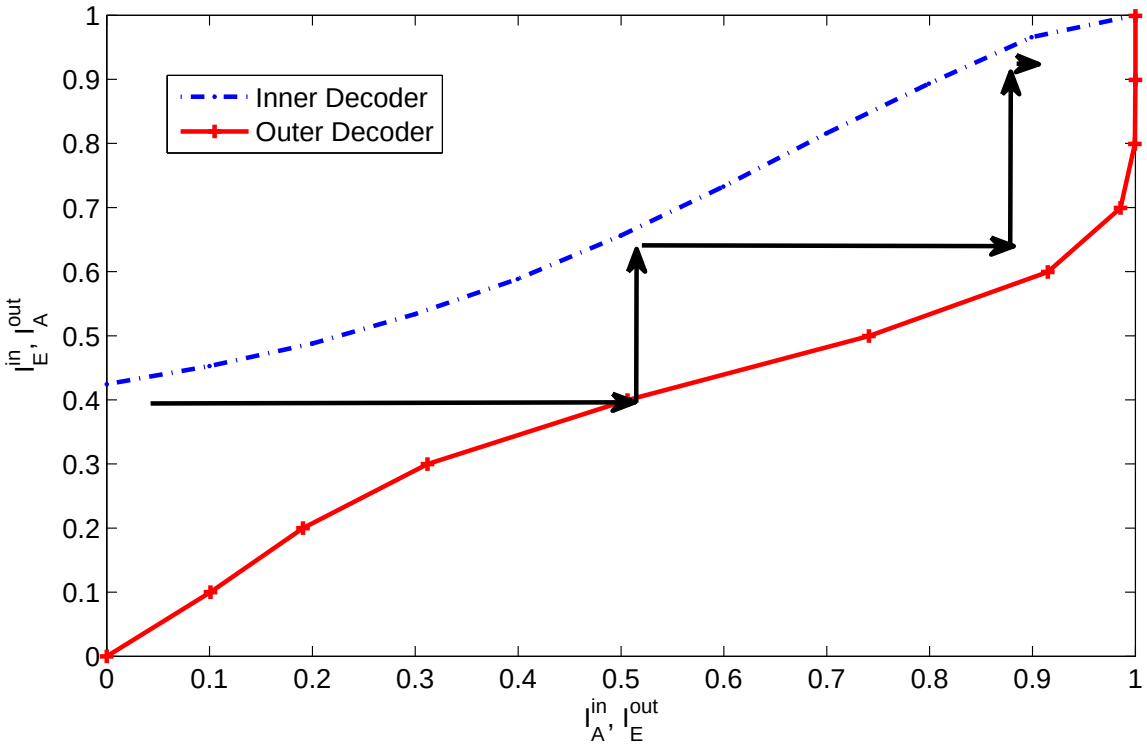

Figure 5.4: An example of EXIT chart for concatenated encode and iterative decoding, $g_{out} = g_{in} = [1, 1, 0, 1; 1, 0, 0, 1]$, $SNR = -2dB$

The transfer chart includes two transfer curves, one curve is the measure for the priori information of inner decoder, i.e., $F_A^{in}(\mathbf{S}, \mathbf{L})$, versus the measure for the extrinsic information of inner decoder, i.e., $F_E^{in}(\mathbf{S}, \mathbf{L})$; the other curve is the measure for the extrinsic information of out decoder, i.e., $F_E^{out}(\mathbf{S}, \mathbf{L})$, versus the measure for the extrinsic information of inner decoder, i.e., $F_A^{out}(\mathbf{S}, \mathbf{L})$. The EXIT chart and MSE chart for serially concatenated coding scheme are shown in Figure 5.4 and Figure 5.5, respectively. The predicted decoding path is also shown in these two figures. The iterative decoding converges if the transfer curve for inner decoder lies above the flipped transfer curve of outer decoder.

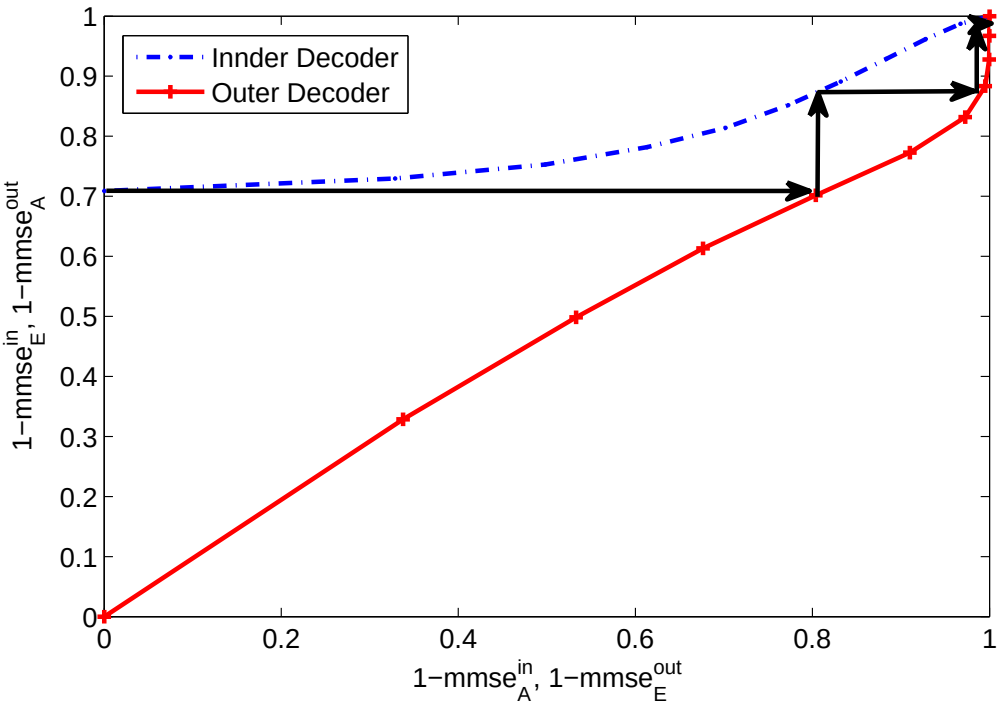

Figure 5.5: An example of MSE-based transfer chart for concatenated encode and iterative decoding, $g_{out} = g_{in} = [1, 1, 0, 1; 1, 0, 0, 1]$, $SNR = -2dB$

5.4 System Model

5.4.1 Linear System

We consider a discrete time linear dynamic system, whose state evolution is given by

$$\begin{cases} \mathbf{x}(t+1) = \mathbf{A}\mathbf{x}(t) + \mathbf{B}\mathbf{u}(t) + \mathbf{n}(t), \\ \mathbf{y}(t) = \mathbf{C}\mathbf{x}(t) + \mathbf{w}(t) \end{cases}, \tag{5.7}$$

where $\mathbf{x}(t)$ is the N-dimensional vector of system state at time slot t, $\mathbf{u}(t)$ is the M-dimensional control vector, $\mathbf{y}$ is the K-dimensional observation vector and $\mathbf{n}$ and $\mathbf{w}$ are noise vectors, which are assumed to be Gaussian distributed with zero expectation and covariance matrices $\mathbf{\Sigma}_n$ and $\mathbf{\Sigma}_w$, respectively. For simplicity, in this proposal we do not consider $\mathbf{u}(t)$.

We assume that the observation vector $\mathbf{y}(t)$ is obtained by a sensor*. The sensor quantizes each dimension of the observation using B bits, thus forming a bit sequence which is given by

$$\mathbf{b}(t) = (b_1(t), b_2(t), ..., b_{KB}(t)) . \tag{5.8}$$

5.4.2 Communication System

Suppose that binary phase shift keying (BPSK) is used for the transmission from the sensor to the controller. The bit sequence is passed through an optional channel encoder, which generates an L-bit sequence $\mathbf{s}(t)$.Finally modulated sequence $\mathbf{s}(t)$ is transmitted. Then, the received signal at the controller is given by

$$\mathbf{r}(t) = \mathbf{s}(t) + \mathbf{e}(t), \tag{5.9}$$

*It is easy to extend to the case of multiple sensors.

where the additive white Gaussian noise $\mathbf{e}(t)$ has a zero expectation and variance σ_e^2. Note that we ignore the fading and normalize the transmit power to be 1. The algorithm and conclusion in this work can be easily extended to the case with different types of fading.

5.4.3 Pearl's BP based Iterative Decoding

The Bayesian network structure of the control system and communication system in WNCS is shown for three time slots in Figure 5.6. In the Bayesian network, the system state $\mathbf{x}_t$ is dependent on the previous system state $\mathbf{x}_{t-1}$ and the control action $\mathbf{u}_t$; the observation $\mathbf{y}_t$ is dependent on the system state $\mathbf{x}_t$; the uncoded bits $\mathbf{b}_t$ are dependent on the observation vector $\mathbf{y}_t$; the received signal $\mathbf{r}_t$ is dependent on the uncoded bits $\mathbf{b}_t$. Here we omit the coded bits $\mathbf{s}_t$ as the relationship between the uncoded bits $\mathbf{b}_t$ and the coded bits $\mathbf{s}_t$ is deterministic. Figure 5.6 shows the Bayesian Network structure for the dynamic system with three observations: $\mathbf{x}_{t-2}$, $\mathbf{x}_{t-1}$ and $\mathbf{x}_t$.

Based on the Bayesian network structure, the iterative decoding procedure can be derived. Figure 5.6 shows the message passing in the dynamic system. $\mathbf{x}_{t-2}$ summarizes all the information obtained from previous time slots and transmits π-message $\pi_{\mathbf{x}_{t-2},\mathbf{x}_{t-1}}(\mathbf{x}_{t-2})$ to $\mathbf{x}_{t-1}$. The BP procedure can be implemented in synchronous or asynchronous manners. As the decoding process has a large overhead, we implement asynchronous Pearl's BP. The updating order and message passing in one iteration is as follows: step 1): $\mathbf{x}_{t-1} \rightarrow \mathbf{y}_{t-1}$; step 2): $\mathbf{y}_{t-1} \rightarrow \mathbf{b}_{t-1}$; step 3): $\mathbf{b}_{t-1} \rightarrow \mathbf{y}_{t-1}$; step 4): $\mathbf{y}_{t-1} \rightarrow \mathbf{x}_{t-1}$; step 5): $\mathbf{x}_{t-1} \rightarrow \mathbf{x}_t$; step 6): $\mathbf{x}_t \rightarrow \mathbf{y}_t$; step 7): $\mathbf{y}_t \rightarrow \mathbf{b}_t$; step 8): $\mathbf{b}_t \rightarrow \mathbf{y}_t$; step 9): $\mathbf{y}_t \rightarrow \mathbf{x}_t$; step 10): $\mathbf{x}_t \rightarrow \mathbf{x}_{t-1}$; step 11): $\mathbf{x}_{t-1}$ updates information. Please refer to chapter 3 for detailed mathematical derivation for each step.

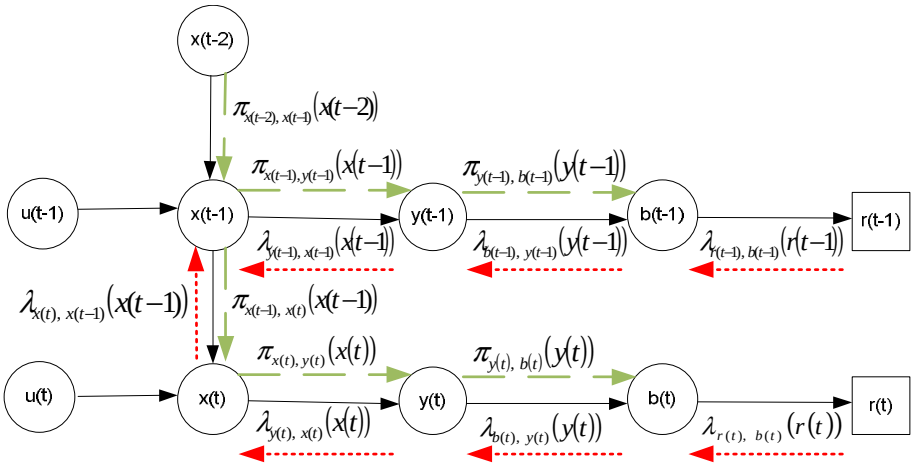

Figure 5.6: Bayesian network structure and message passing for the dynamic system.

5.4.4 Models for Belief Propagation Based Channel Decoding and State Estimation

In this chapter, we use the following two models to evaluate BP based channel decoding and state estimation:

1. BP based sequential channel decoding and state estimation

   We use it to evaluate the performance of channel decoding and state estimation over time. In addition, it can also be used to evaluate how much gain can be obtained by utilizing priori information from previous time slot to assist channel decoding and state estimation at current time slot.

2. BP based iterative channel decoding and state estimation

   We use it to evaluate the performance of iterative channel decoding and state estimation over two time slots from the following points:

   (a) Does the iterative channel decoding and estimation converge?

   (b) How many iterations are sufficient?

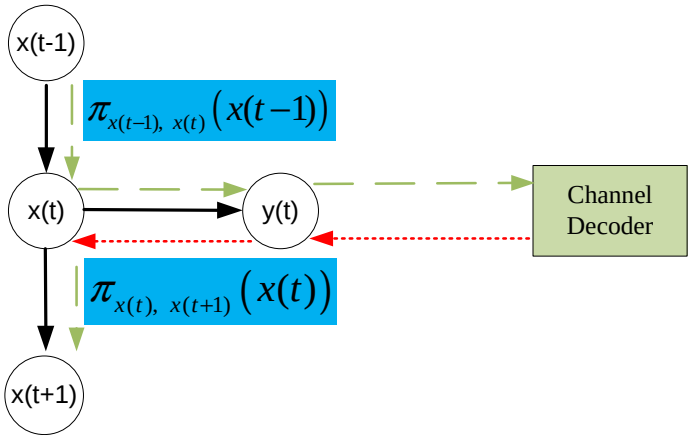

Figure 5.7: Sequential channel decoding and state estimation framework

Model for BP Based Sequential Channel Decoding and State Estimation

We use the framework as shown in Figure 5.7 to evaluate sequential channel decoding and state estimation over time slots. The priori information from time slot $t-1$, i.e., $\pi_{x_{t-1},x(t)}(x_{t-1})$, is used to assist channel decoding and state estimation at time slot t. Note that $\pi_{x(t-1),x(t)}(x(t-1))$ is used to model the estimate of $x(t-1)$, and we assume that it has Guassian distribution with mean $\mathbf{x}_{\pi_x,t-1}$ and covariance matrix $P_{\pi_x,t-1}$, i.e. $\mathcal{N}(\mathbf{x}_{t-1}, \mathbf{x}_{\pi_x,t-1}, P_{\pi_x,t-1})$. The first goal is to evaluate how much gain can be obtained by utilizing $\pi_{x_{t-1},x(t)}(x_{t-1})$ to assist channel decoding and state estimation at time slot t; the second goal is to evaluate the performance of state estimation over time, i.e., the evolution of $P_{\pi_x,t-1}$ as shown in Figure 5.8.

The message passing in this framework is as below:

1. $\mathbf{x(t-1)} \rightarrow \mathbf{x(t)}$, we have

$$\pi_{\mathbf{x}_{t-1},\mathbf{x}_t}(\mathbf{x}_{t-1}) \quad = \quad \mathcal{N}(\mathbf{x}_{t-1}, \mathbf{x}_{\pi_x,t-1}, P_{\pi_x,t-1}), \tag{5.10}$$

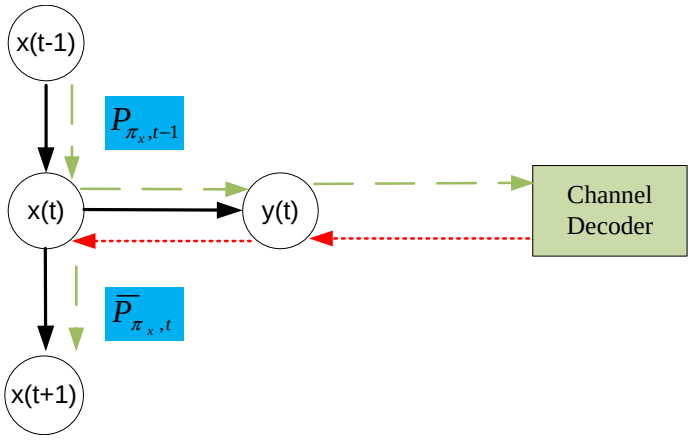

Figure 5.8: Measure for evaluation of sequential channel decoding and state estimation

2. $\mathbf{x(t)} \rightarrow \mathbf{y(t)}$, we have

$$\begin{aligned} \pi_{\mathbf{x}_t,\mathbf{y}_t}(\mathbf{x}_t) &= \mathcal{N}(\mathbf{x}_t, \mathbf{x}_{\pi_y,t}, P_{\pi_y,t}) \\ \text{where} & \\ \mathbf{x}_{\pi_y,t} &= A\mathbf{x}_{\pi_x,t-1} + B\mathbf{u}_{t-1} \\ P_{\pi_y,t} &= A \times P_{\pi_x,t-1} \times A^T + \Sigma_p \end{aligned} \tag{5.11}$$

3. $\mathbf{y(t)} \rightarrow \mathbf{b(t)}$,we have

$$\begin{aligned} \pi_{\mathbf{y}_t,\mathbf{b}_t}(\mathbf{y}_t) &= \mathcal{N}(\mathbf{y}_t, \mathbf{y}_{\pi,t}, S_{\pi,t}) \\ \text{where} & \\ \mathbf{y}_{\pi,t} &= C \times \mathbf{x}_{\pi_y,t} \\ S_{\pi,t} &= C \times P_{\pi_y,t} \times C^T + \Sigma_o \end{aligned} \tag{5.12}$$

4. $\mathbf{b(t)} \rightarrow \mathbf{y(t)}$:

$$\lambda_{\mathbf{b}_t,\mathbf{y}_t}(\mathbf{y}_t) = \mathcal{N}(\mathbf{y}_t, \mathbf{y}_{\lambda,t}, S_{\lambda,t}) \tag{5.13}$$

The detailed derivation of $\mathbf{y}_{\lambda,t}$ and $S_{\lambda,t}$ is provided in section 5.5.

5. $\mathbf{y(t)} \rightarrow \mathbf{x(t)}$, we have

$$\begin{aligned} \lambda_{\mathbf{y}_t,\mathbf{x}_t}(\mathbf{x}_t) &= \mathcal{N}(\mathbf{x}_t, \mathbf{x}_{\lambda_y,t}, P_{\lambda_y,t}) \\ \text{where} & \\ \mathbf{x}_{\lambda_y,t} &= C^{-1} \times \mathbf{y}_{\lambda,t}, \\ P_{\lambda_y,t} &= C^{-1}(S_{\lambda,t} + \Sigma_o) \times (C^{-1})^T. \end{aligned} \tag{5.14}$$

6. $\mathbf{x(t)} \rightarrow \mathbf{x(t+1)}$: we have

$$\pi_{\mathbf{x}_t,\mathbf{x}_{t+1}}(\mathbf{x}_t) = \mathcal{N}(\mathbf{x}_t, \mathbf{x}_{\pi_x,t}, P_{\pi_x,t}), \tag{5.15}$$

where the variance is given by

$$P_{\pi_x,t} = (P_{l,t}^{-1} + P_{\lambda,t}^{-1})^{-1}, \tag{5.16}$$

and the expectation is given by

$$\mathbf{x}_{\pi_x,t} = P_{\pi_x,t} \times (P_{l,t}^{-1} \times \mathbf{x}_{l,t} + P_{\lambda,t}^{-1}\mathbf{x}_{\lambda,t}).$$

where

$$\begin{aligned} \mathbf{x}_{l,t} &= A\mathbf{x}_{\pi_x,t-1} + B\mathbf{u}_{t-1} \\ P_{l,t} &= A \times P_{\pi_x,t-1} \times A^T + \Sigma_p \end{aligned} \tag{5.17}$$

Model for BP Based Iterative Channel Decoding and State Estimation Between Two Time Slots

Figure 5.9 illustrates the model used to evaluate BP based iterative channel decoding and state estimation between two time slots. The inputs for this model include

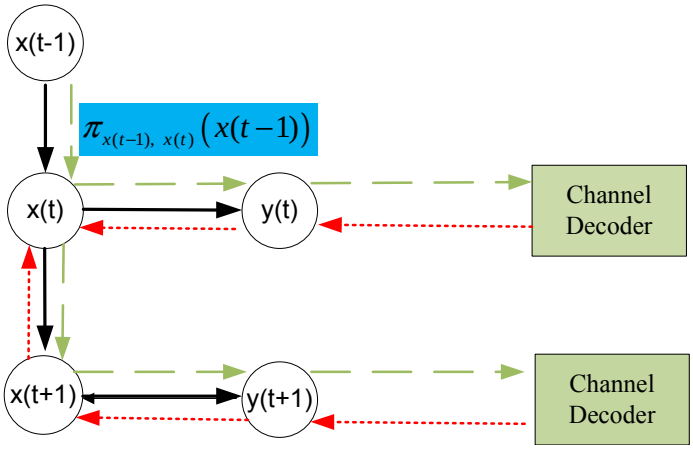

Figure 5.9: Model for iterative message passing

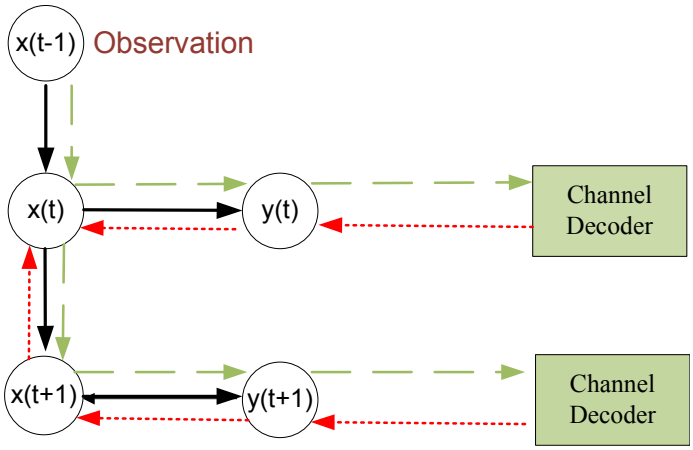

Figure 5.10: Model for iterative message passing with known $\mathbf{x}(t-1)$

received signals in two time slots, i.e., $\mathbf{r}(t)$ and $\mathbf{r}(t+1)$ and the priori information from time slot $t-1$, i.e., $\pi_{x(t-1),x(t)}(x(t-1))$.

The goal is to evaluate the performance of iterative channel decoding and state estimation for different sample of $\pi_{x(t-1),x(t)}(x(t-1))$. Note when $\pi_{x(t-1),x(t)}(x(t-1))$ is equal to $0\mathbf{I}$, then $\mathbf{x}(t-1)$ is a determined state observation. Therefore, this reference model can be converted to the model shown in Figure 5.10 by setting $\pi_{x(t-1),x(t)}(x(t-1))$ as $0\mathbf{I}$. If $\pi_{x(t-1),x(t)}(x(t-1))$ is set as $+\infty\mathbf{I}$, $\mathbf{x(t-1)}$ is unknown. Then the reference model is transformed to the model shown in Figure 5.11.

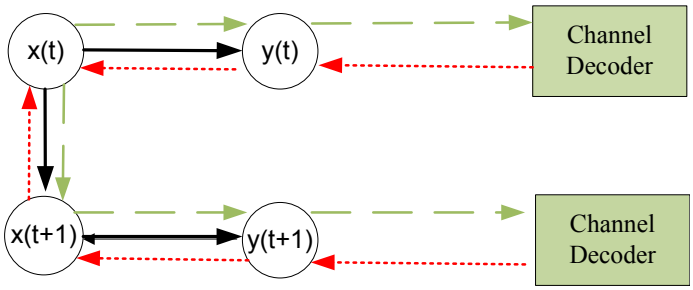

Figure 5.11: Model for iterative message passing without priori information from $\mathbf{x}(t-1)$

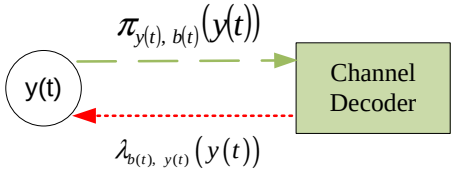

Figure 5.12: Information exchange between channel decoder and state estimator

5.5 Evaluation for the Information Exchange Between Channel Decoder and State Estimator

The most challenging part for the evaluation of BP based channel decoding and state estimation is the information transfer between state estimator and channel decoder. As shown in Figure 5.12, the information sent from state estimator to channel decoder is $\pi_{\mathbf{y}_t,\mathbf{b}_t}(\mathbf{y}_t)$ which is assumed to have Guassian distribution with mean $\mathbf{y}_{\pi,t}$ and covariance matrix $S_{\pi,t}$, i.e., $\mathcal{N}(\mathbf{y}_t, \mathbf{y}_{\pi,t}, S_{\pi,t})$; and the information transferred from channel decoder to state estimator is $\lambda_{\mathbf{b}_t,\mathbf{y}_t}(\mathbf{y}_t)$ which is assumed to have Guassian distribution with mean $\mathbf{y}_{\lambda,t}$ and covariance matrix $\mathbf{y}_{\lambda,t}$, i.e., $\mathcal{N}(\mathbf{y}_t, \mathbf{y}_{\lambda,t}, S_{\lambda,t})$. $S_{\lambda,t}$ is related to $\mathbf{y}_{\pi,t}$, $S_{\pi,t}$, and channel noise. The goal of this section is to compute the average $S_{\lambda,t}$, i.e., $\bar{S}_{\lambda,t}$, corresponding to $S_{\pi,t}$ as shown in Figure 5.13.

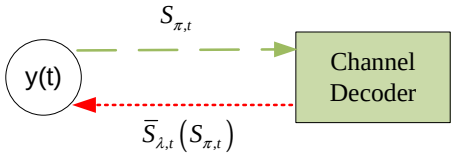

Figure 5.13: Measure for information exchange between channel decoder and state estimator

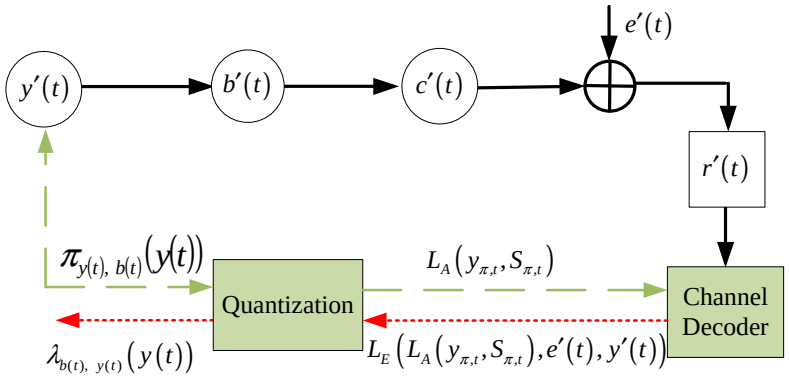

Figure 5.14: Model for $\mathbf{S}_{\lambda,t}$ based on sample $\mathbf{y}_{\pi,t}$, $\mathbf{S}_{\pi,t}$, $\mathbf{y}'(t)$ and $\mathbf{e}'(t)$

5.5.1 Quantizing the Information Exchange Between Channel Decoder and State Estimator

The relationship between $S_{\lambda,t}$ and $\mathbf{y}_{\pi,t}$, $S_{\pi,t}$, and channel noise is shown in Figure 5.14.

We assume that the priori information from $\mathbf{y}(t)$ to $\mathbf{b}(t)$, i.e., $\pi_{\mathbf{y}_t,\mathbf{b}_t}(\mathbf{y}_t)$, is a Gaussian vector with mean $\mathbf{y}_{\pi,t}$ and covariance $\mathbf{S}_{\pi,t}$, i.e.,

$$\pi_{\mathbf{y}_t,\mathbf{b}_t}(\mathbf{y}_t) \;=\; \mathcal{N}(\mathbf{y}_t, \mathbf{y}_{\pi,t}, \mathbf{S}_{\pi,t}) \tag{5.18}$$

Note that the physical meaning of $\pi_{\mathbf{y}_t,\mathbf{b}_t}(\mathbf{y}_t)$ is the prediction of $\mathbf{y}(t)$. Then, $\pi_{\mathbf{y}_t,\mathbf{b}_t}(\mathbf{y}_t)$ is converted to the priori information of each bit based on quantization scheme, i.e., $\mathbf{L}_A(\mathbf{y}_{\pi,t}, \mathbf{S}_{\pi,t})$. It is a $K \times B$-dimension vector and its ith value is

calculated based on quantization scheme:

$$L_{A,i}(\mathbf{y}_{\pi,t}, \mathbf{S}_{\pi,t}) = \log \frac{P\left(b_i(t) = 1 | \mathbf{y}(t) \in \mathcal{N}(\mathbf{y}_t, \mathbf{y}_{\pi,t}, \mathbf{S}_{\pi,t})\right)}{P\left(b_i(t) = 0 | \mathbf{y}(t) \in \mathcal{N}(\mathbf{y}_t, \mathbf{y}_{\pi,t}, \mathbf{S}_{\pi,t})\right)} \tag{5.19}$$

Note that $L_{A,i}(\mathbf{y}_{\pi,t}, \mathbf{S}_{\pi,t})$ is determined by $\pi_{\mathbf{y}_t,\mathbf{b}_t}(\mathbf{y}_t)$ and the quantization scheme.

Observation instance $\mathbf{y}'(t)$ is sampled from $\pi_{\mathbf{y}_t,\mathbf{b}_t}(\mathbf{y}_t)$. Then, $\mathbf{y}'(t)$ is quantized, modulated and transmitted over wireless channel. Denote the corresponding quantized vector, modulated vector, channel noise vector and received vector as $\mathbf{b}'(t)$, $\mathbf{S}'(t)$, $\mathbf{e}'(t)$, $\mathbf{r}'(t)$, respectively.

The inputs for channel decoder is $\mathbf{L}_A(\mathbf{y}_{\pi,t}, \mathbf{S}_{\pi,t})$ and $\mathbf{r}'(t)$. The information fedback from channel decoder to state estimator is extrinsic LLR, which is denoted as $\mathbf{L}'_E\left(\mathbf{L}_A(\mathbf{y}_{\pi,t}, \mathbf{S}_{\pi,t}), \mathbf{y}'(t), \mathbf{e}'(t)\right)$. It is a $K \times B$-dimension vector and its ith value is equal to:

$$\mathbf{L}'_{E,i}\left(\mathbf{L}_A(\mathbf{y}_{\pi,t}, \mathbf{S}_{\pi,t}), \mathbf{y}'(t), \mathbf{e}'(t)\right) = \log \frac{P\left(b_i(t) = 1 | \mathbf{L}_{A,\tilde{i}}(\mathbf{y}_{\pi,t}, \mathbf{S}_{\pi,t}), \mathbf{r}'(t)\right)}{P\left(b_i(t) = 0 | \mathbf{L}_{A,\tilde{i}}(\mathbf{y}_{\pi,t}, \mathbf{S}_{\pi,t}), \mathbf{r}'(t)\right)} \tag{5.20}$$

Note that $\mathbf{L}'_E\left(\mathbf{L}_A(\mathbf{y}_{\pi,t}, \mathbf{S}_{\pi,t}), \mathbf{y}'(t), \mathbf{e}'(t)\right)$ depends on $\mathbf{L}_A(\mathbf{y}_{\pi,t}, \mathbf{S}_{\pi,t})$, $\mathbf{y}'(t)$ and $\mathbf{e}'(t)$.

Based on $\mathbf{L}'_E\left(\mathbf{L}_A(\mathbf{y}_{\pi,t}, \mathbf{S}_{\pi,t}), \mathbf{y}'(t), \mathbf{e}'(t)\right)$, $\mathbf{b}'(t)$ can be estimated as (Bhattad and Narayanan, 2007):

$$\tilde{\mathbf{b}}_i(t) = \frac{1}{2} \tanh\left(\frac{1}{2}\mathbf{L}'_{E,i}\left(\mathbf{L}_A(\mathbf{y}_{\pi,t}, \mathbf{S}_{\pi,t}), \mathbf{y}'(t), \mathbf{e}'(t)\right)\right) + \frac{1}{2} \tag{5.21}$$

and MMSE in estimating $\mathbf{b}'_i(t)$ from $\mathbf{L}'_{E,i}\left(\mathbf{L}_A(\mathbf{y}_{\pi,t}, \mathbf{S}_{\pi,t}), \mathbf{y}'(t), \mathbf{e}'(t)\right)$ is given by

$$\begin{aligned} & mmse\left(\mathbf{b}_i(t) | \mathbf{L}_A(\mathbf{y}_{\pi,t}, \mathbf{S}_{\pi,t}), \mathbf{y}'(t), \mathbf{e}'(t)\right) \\ = & \frac{1}{4} - \frac{1}{4} \tanh^2\left(\frac{1}{2}\mathbf{L}'_{E,i}\left(\mathbf{L}_A(\mathbf{y}_{\pi,t}, \mathbf{S}_{\pi,t}), \mathbf{y}'(t), \mathbf{e}'(t)\right)\right) \end{aligned} \tag{5.22}$$

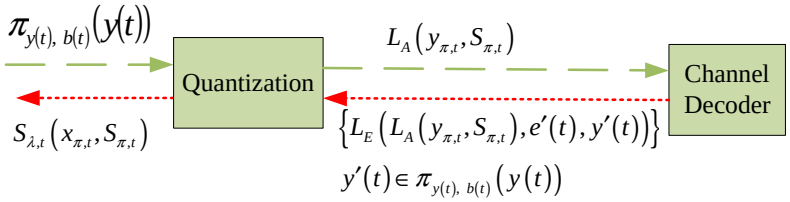

Figure 5.15: Framework for $\mathbf{S}_{\lambda,t}$ averaging over $\mathbf{y}'(t)$ and $\mathbf{e}'(t)$

Then, $\mathbf{y}'(t)$ can be estimated:

$$\tilde{y}_k(t) = \sum_{i=1}^{B} Q_I^{i-1} \tilde{\mathbf{b}}_{(k-1)B+i}(t) - \frac{Q_{max} - Q_{min}}{2} \tag{5.23}$$

and MMSE in estimating $\mathbf{y}'(t)$ is given by:

$$\begin{aligned} &mmse\left(y_k(t) | \mathbf{L}_A(\mathbf{y}_{\pi,t}, \mathbf{S}_{\pi,t}), \mathbf{y}'(t), \mathbf{e}'(t)\right) \\ &= \sum_{i=1}^{B} Q_I^{2(i-1)} mmse\left(\mathbf{b}'_{(k-1)B+i}(t) | \mathbf{L}_A(\mathbf{y}_{\pi,t}, \mathbf{S}_{\pi,t}), \mathbf{y}'(t), \mathbf{e}'(t)\right) \end{aligned} \tag{5.24}$$

where $[Q_{min}, Q_{max}]$ is the range for quantization, Q_I is the quantization interval, which is given by:

$$Q_I = \frac{Q_{max} - Q_{min}}{2^B - 1} \tag{5.25}$$

Then, for a given $\pi_{\mathbf{y}_t, \mathbf{b}_t}(\mathbf{y}_t)$ which has probability distribution $\mathcal{N}(\mathbf{y}_t, \mathbf{y}_{\pi,t}, S_{\pi,t})$, given instance $\mathbf{y}'(t)$ and channel noise vector $\mathbf{e}'(t)$, the backward informatoin from decoder to $\mathbf{y}(t)$, i.e., $\lambda_{\mathbf{b}_t, \mathbf{y}_t}(\mathbf{y}_t)$ is obtained with mean $\mathbf{y}'_{\lambda,t}$ and covariance $\mathbf{S}'_{\lambda,t}\left(\mathbf{L}_A(\mathbf{y}_{\pi,t}, \mathbf{S}_{\pi,t}), \mathbf{y}'(t), \mathbf{e}'(t)\right)$, where

$$\begin{aligned} \mathbf{y}'_{\lambda,t} &= [\tilde{y}_1(t), \cdots, \tilde{y}_K(t)] \\ \mathbf{S}'_{\lambda,t}(k,k) &= mmse\left(y_k(t) | \mathbf{L}'_E\left(\mathbf{L}_A(\mathbf{y}_{\pi,t}, \mathbf{S}_{\pi,t}), \mathbf{y}'(t), \mathbf{e}'(t)\right)\right) \end{aligned} \tag{5.26}$$

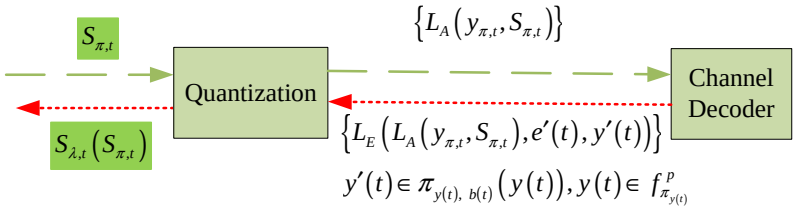

Figure 5.16: Framework for $\mathbf{S}_{\lambda,t}$ averaging over $\mathbf{y}'(t)$, $\mathbf{e}'(t)$ and $\mathbf{y}_{\pi,t}$

Then, for a given $\pi_{\mathbf{y}_t,\mathbf{b}_t}(\mathbf{y}_t)$, extrinsic information transferred from decoder to $\mathbf{y}(t)$ can be computed:

$$\mathbf{S}_{\lambda,t}(\mathbf{y}_{\pi,t}, \mathbf{S}_{\pi,t}) = E_{\mathbf{y}'_t \in \mathcal{U}(\mathbf{R}(\mathbf{y})),\mathbf{e}'(t)}(\mathbf{L}_A(\mathbf{y}_{\pi,t}, \mathbf{S}_{\pi,t}), \mathbf{y}'(t), \mathbf{e}'(t)) \tag{5.27}$$

Denote the probability distribution of $\mathbf{y}_{\pi,t}$ as $f_{\mathbf{y}_{\pi,t}}$. Then, we can obtain average $\mathbf{S}_{\pi,t}$, i.e., $\mathbf{S}_{\lambda,t}(\mathbf{S}_{\pi,t})$ correponding to $\mathbf{S}_{\pi,t}$ by integrating $\mathbf{S}_{\lambda,t}(\mathbf{y}_{\pi,t}, \mathbf{S}_{\pi,t})$ over $\mathbf{y}_{\pi,t}$

$$\begin{aligned} \mathbf{S}_{\lambda,t}(\mathbf{S}_{\pi,t}) &= E_{\mathbf{y}_{\pi,t}}\left(\mathbf{S}_{\lambda,t}(\mathbf{y}_{\pi,t}, \mathbf{S}_{\pi,t})\right) \\ &= E_{\mathbf{y}_{\pi,t}}\left(E_{\mathbf{y}'_t \in \mathcal{U}(\mathbf{R}(\mathbf{y})),\mathbf{e}'(t)}\left(\mathbf{S}'_{\lambda,t}\left(\mathbf{L}_A(\mathbf{y}_{\pi,t}, \mathbf{S}_{\pi,t}), \mathbf{y}'(t), \mathbf{e}'(t)\right)\right)\right) \end{aligned} \tag{5.28}$$

Note that the computation of $\mathbf{S}_{\lambda,t}(\mathbf{S}_{\pi,t})$ requires serially averaging over $\mathbf{y}'(t)$ and $\mathbf{y}_{\pi,t}$. This is because that $\mathbf{y}_{\pi,t}$ not only impacts priori information $\mathbf{L}_A(\mathbf{y}_{\pi,t}, \mathbf{S}_{\pi,t})$, but also defines the set of codewords which are generated by quantizing $\mathbf{y}'(t)$. For performance evaluation it means that the information transfer for the forward process and backward process cannot be considered independently.

5.5.2 Approximation for the Information Exchange Between State Estimator and Channel Decoder

As shown in above subsection, the computation of $\mathbf{S}_{\lambda,t}(\mathbf{S}_{\pi,t})$ prohibits the independent evaluation of the information transfer for **forward process** and **backward process**. **Forward process** generally refers to message passing from a node to its children; and **backward process** generally refers to message passing from a node to its parents.

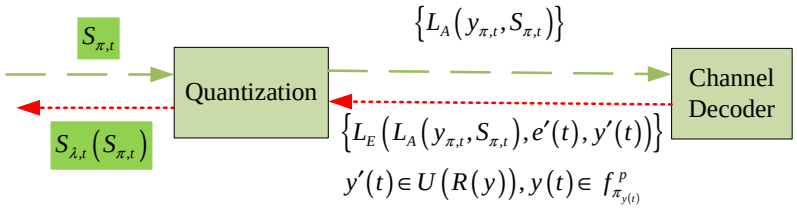

Figure 5.17: Approximate Framework 1 for $\mathbf{S}_{\lambda,t}$ averaging over $\mathbf{y}'(t)$, $\mathbf{e}'(t)$ and $\mathbf{y}_{\pi,t}$

In this subsection, we make approximation for the computation of $\mathbf{S}_{\lambda,t}(\mathbf{S}_{\pi,t})$ so that the **forward process** and **backward process** can be considered separately.

Firstly, we integrate $\mathbf{y}'(t)$ over a uniform distribution instead of over $\mathcal{N}(\mathbf{y}_t, \mathbf{y}_{\pi,t}, \mathbf{S}_{\pi,t})$. Denote the uniform distribution as $\mathcal{U}(\mathbf{R}(\mathbf{y}))$, where $\mathbf{R}(\mathbf{y})$ is the range of $\mathbf{y}$. Then, $\mathbf{y}'(t)$ is independent of $\pi_{\mathbf{y}_t,\mathbf{b}_t}(\mathbf{y}_t)$; and the integration of $\mathbf{y}'(t)$ over $\mathcal{U}(\mathbf{R}(\mathbf{y}))$ is equivalent to the integration of all codewords with equal probability. Then,

$$\begin{aligned}
\mathbf{S}_{\lambda,t}(\mathbf{S}_{\pi,t}) &\simeq E_{\mathbf{y}_{\pi,t}}\left(E_{\mathbf{y}'_t\in\mathcal{U}(\mathbf{R}(\mathbf{y})),\mathbf{e}'(t)}\left(\mathbf{S}'_{\lambda,t}\left(\mathbf{L}_A(\mathbf{y}_{\pi,t},\mathbf{S}_{\pi,t}),\mathbf{y}'(t),\mathbf{e}'(t)\right)\right)\right) \\
&= E_{\mathbf{y}_{\pi,t},\mathbf{y}'_t\in\mathcal{U}(\mathbf{R}(\mathbf{y}),\mathbf{e}'(t)}\left(\mathbf{S}'_{\lambda,t}\left(\mathbf{L}_A(\mathbf{y}_{\pi,t},\mathbf{S}_{\pi,t}),\mathbf{y}'(t),\mathbf{e}'(t)\right)\right) \\
&= E_{\mathbf{L}_A(\mathbf{y}_{\pi,t},\mathbf{S}_{\pi,t}),\mathbf{y}'_t\in\mathcal{U}(\mathbf{R}(\mathbf{y}),\mathbf{e}'(t)}\left(\mathbf{S}'_{\lambda,t}\left(\mathbf{L}_A(\mathbf{y}_{\pi,t},\mathbf{S}_{\pi,t}),\mathbf{y}'(t),\mathbf{e}'(t)\right)\right) \quad (5.29)
\end{aligned}$$

In the final step of Eq. 5.29, the avaraging over $\mathbf{y}_{\pi,t}$ is changed to avaraging over $\mathbf{L}_A(\mathbf{y}_{\pi,t},\mathbf{S}_{\pi,t})$. This is because $\mathbf{y}_{\pi,t}$ impacts only priori information $\mathbf{L}_A(\mathbf{y}_{\pi,t},\mathbf{S}_{\pi,t})$ and the set $\mathbf{L}_A(\mathbf{y}_{\pi,t},\mathbf{S}_{\pi,t})$ includes all information from $\mathbf{y}_{\pi,t}$. The framework equivalent with Eq. 5.29 is shown in Figure 5.17. In this new framework, the computation of $\mathbf{S}_{\lambda,t}(\mathbf{S}_{\pi,t})$ can be divided into three steps:

1. Step 1: compute the distribution of $\mathbf{L}_A(\mathbf{y}_{\pi,t},\mathbf{S}_{\pi,t}$ corresponding to $\mathbf{S}_{\pi,t})$ and $f_{\mathbf{y}_{\pi,t}}$;

2. Step 2: compute the extrinsic information from channel decoder, i.e., the distribution of $\mathbf{L}'_{E,i}\left(\mathbf{L}_A(\mathbf{y}_{\pi,t},\mathbf{S}_{\pi,t}),\mathbf{y}'(t),\mathbf{e}'(t)\right)$;

3. Step 3: compute $\mathbf{S}_{\lambda,t}(\mathbf{S}_{\pi,t})$ from $\mathbf{L}'_{E,i}\left(\mathbf{L}_A(\mathbf{y}_{\pi,t},\mathbf{S}_{\pi,t}),\mathbf{y}'(t),\mathbf{e}'(t)\right)$.

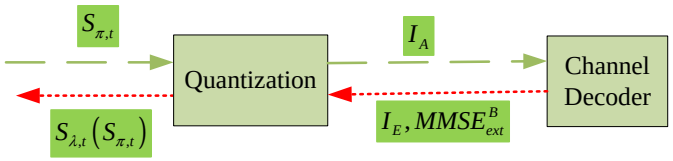

Figure 5.18: Approximate Framework 2 for $\mathbf{S}_{\lambda,t}$ averaging over $\mathbf{y}'(t)$, $\mathbf{e}'(t)$ and $\mathbf{y}_{\pi,t}$

Secondly, we model the distribution of $\mathbf{L}_A(\mathbf{y}_{\pi,t}, \mathbf{S}_{\pi,t})$ and $\mathbf{L}'_{E,i}\left(\mathbf{L}_A(\mathbf{y}_{\pi,t}, \mathbf{S}_{\pi,t}), \mathbf{y}'(t), \mathbf{e}'(t)\right)$ as Gaussian distribution with zero mean. Note that $\mathbf{L}'_{E,i}\left(\mathbf{L}_A(\mathbf{y}_{\pi,t}, \mathbf{S}_{\pi,t}), \mathbf{y}'(t), \mathbf{e}'(t)\right)$ for different bits might have huge difference. This Gaussian model requires a good interleaver which can evenly distribute $\mathbf{L}'_{E,i}\left(\mathbf{L}_A(\mathbf{y}_{\pi,t}, \mathbf{S}_{\pi,t}), \mathbf{y}'(t), \mathbf{e}'(t)\right)$. Since LLR with Guassian distribution can be represented by mutual information or MMSE (Bhattad and Narayanan, 2007), $\mathbf{S}_{\lambda,t}(\mathbf{S}_{\pi,t})$ can be computed in three steps as shown in Figure 5.18:

1. Step 1: compute mutual information I_A of the distribution of $\mathbf{L}_A(\mathbf{y}_{\pi,t}, \mathbf{S}_{\pi,t})$ corresponding to $\mathbf{S}_{\pi,t}$) and $f_{\mathbf{y}_{\pi,t}}$;

2. Step 2: compute the extrinsic information from channel decoder, i.e., mutual information I_E or $MMSE^B_{ext}$ of the distribution of $\mathbf{L}'_{E,i}\left(\mathbf{L}_A(\mathbf{y}_{\pi,t}, \mathbf{S}_{\pi,t}), \mathbf{y}'(t), \mathbf{e}'(t)\right)$;

3. Step 3: compute $\mathbf{S}_{\lambda,t}(\mathbf{S}_{\pi,t})$ from extinsic information from channel decoder I_E or $MMSE^B_{ext}$.

5.6 MSE-based Transfer Chart for Channel Decoding and State Estimation

In the framework of BP based channel decoding and state estimation, the prediction of $\mathbf{y}(t)$, i.e., $\pi_{\mathbf{y}_t,\mathbf{b}_t}(\mathbf{y}_t)$, is utilized to assist channel decoding in order to improve the performanc of channel decoding. However, performance evaluation for this framework is challenging because that the estimated $\mathbf{y}(t)$, i.e., $\lambda_{\mathbf{b}_t,\mathbf{y}_t}(\mathbf{y}_t)$, is correlated with predicted $\mathbf{y}(t)$,i.e., $\pi_{\mathbf{y}_t,\mathbf{b}_t}(\mathbf{y}_t)$. Instead of analytically evaluating the performance of

our proposed estimation scheme, we utilize the MSE-based transfer chart proposed by (Guo et al., 2005) to evaluate its performance. By using MSE-based transfer chart, the performance evaluation can be simplified; in addition, we can get visual insights about the performance of our proposed estimation algorithm. The reason why we select MSE as a measure is that it is aligned with one of the goal of state estimation, i.e., minimizing the mse of estimated $\mathbf{x}(t)$. In this section, we show that how to obtain MSE-based transfer for evaluating BP based sequential channel decoding and state estimation as shown in Figure 5.8, and BP based iterative channel decoding and state estimation as shown in Figure 5.9.

5.6.1 MSE-based Transfer Chart for Sequential Channel Decoding and State Estimation over Time

In this subsection we demonstrate how to get MSE-based transfer for evaluating BP based sequential channel decoding and state estimation as show in Figure 5.8. The corresponding model for **mse** chart of sequential message passing is illusttrated in Figure 5.19; and the MSE-based chart for BP based sequential channel decoding and state estimation is the curve with MMSE_{ap}^{S} versus MMSE_{ext}^{S}. As shown in Figure 5.8, the starting node is $\mathbf{y}(t)$; MMSE_{ap}^{S} is used to represent approximated $S_{\pi,t}$, i.e.,

$$S_{\pi,t} = \text{MMSE}_{ap}^{S}\mathbf{I}_K \tag{5.30}$$

; and the distribution of $\mathbf{y}_{\pi,t}$, i.e., $f_{\mathbf{y}_{\pi,t}}$, is assumed to keep the same in all time slots and all iterations and denoted as $f_{\mathbf{y}_\pi}$. MMSE_{ext}^{S} is used to represent average $S_{\pi,t+1}$ corresponding to $S_{\pi,t}$ equal to $\text{MMSE}_{ap}^{S}\mathbf{I}_K$ and $\mathbf{y}_{\pi,t}$ with distribution $f_{\mathbf{y}_\pi}$. Comparing with the model shown in Figure 5.8, the MSE-based chart has two differences. The starting node for message passing is changed from $\mathbf{x}(t-1)$ to $\mathbf{y}(t)$. The reason for this change is to keep aligns with the structure of MSE-based transfer chart for BP based iterative channel decoding and state estimation. Note that $\mathbf{x}(t-1)$ and $\mathbf{y}(t)$ can

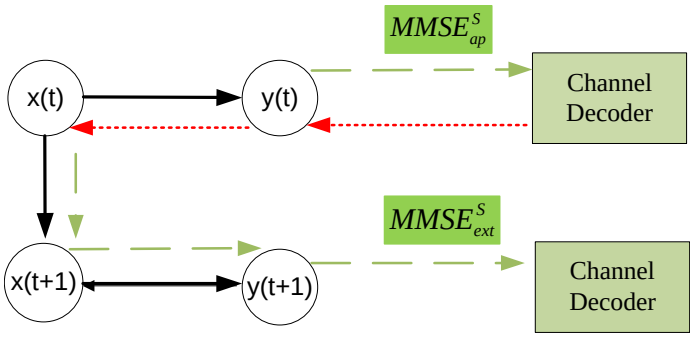

Figure 5.19: MSE-based chart for sequential messaging-passing

provide same amount information for channel decoding. Therefore, these two models are equivalent. The other change is that a scalar measure, MMSE_{ap}^{S} and MMSE_{ext}^{S}, instead of a matrix is used to represent the performance of sequential message passing.

The value of MMSE_{ext}^{S} can be obtained by following the message passing flow in this framework.

1. $\mathbf{y(t)} \rightarrow \mathbf{b(t)}$,we have

   $S_{\pi,t} = \text{MMSE}_{ap}^{S}\mathbf{I}_K$ and the distribution of $\mathbf{y}_{\pi,t}$ is $f_{\mathbf{y}_\pi}$.

2. $\mathbf{b(t)} \rightarrow \mathbf{y(t)}$:

   The detailed derivation of $S_{\lambda,t}$ is provided in section 5.5.

3. $\mathbf{y(t)} \rightarrow \mathbf{x(t)}$, we have

$$P_{\lambda_y,t} = C^{-1}\left(\left(\mathbf{S}_{\lambda,t}^{-1} + \mathbf{S}_{\pi,t}^{-1}\right)^{-1} + \Sigma_w\right) \times (C^{-1})^T. \tag{5.31}$$

   Note that $\mathbf{S}_{\pi,t}$ is used to model the priori information from $\mathbf{x}(t-1)$ to $\mathbf{x}(t)$. Therefore, both $\mathbf{S}_{\pi,t}$ and $\mathbf{S}_{\lambda,t}$ have to be included to calculate the information sent $\mathbf{y}(t)$ to $\mathbf{x}(t)$.

4. $\mathbf{x(t)} \rightarrow \mathbf{x(t+1)}$, we have

$$P_{\pi_x,t} = P_{\lambda_y,t} \tag{5.32}$$

5. $\mathbf{x(t+1)} \rightarrow \mathbf{y(t+1)}$, we have

$$P_{\pi_y,t+1} = A \times P_{\pi_x,t+1} \times A^T + \Sigma_p \tag{5.33}$$

6. $\mathbf{y(t+1)} \rightarrow \mathbf{b(t+1)}$,we have

$$S_{\pi,t+1} = C \times P_{\pi_y,t+1} \times C^T + \Sigma_o \tag{5.34}$$

Note that $S_{\pi,t+1}$ is a matrix, MMSE_{ext}^{S} can be obtained by solving the following equation:

$$I_A(\text{MMSE}_{ext}^{S}\mathbf{I}_K) = I_A(S_{\pi,t+1}) \tag{5.35}$$

The physical meaning of this equation is that MMSE_{ext}^{S} is the value such that $\text{MMSE}_{ext}^{S}\mathbf{I}_K$ can provide the same amount of priori information for channel decoder as $S_{\pi,t+1}$.

5.6.2 MSE-based Transfer Chart for BP Based Iterative Channel Decoding and State Estimation Between Two Time Slots

In this subsection, we illustrate how MSE-based transfer is modeled in order to evaluate BP based iterative channel decoding and state estimation as shown in Figure 5.9. The corresponding model for MSE-based transfer chart is shown in Figure 5.20. It includes two flows of message passing, the flow from $\mathbf{y}(t)$ to $\mathbf{y}(t+1)$ as shown in Figure 5.21 and the flow from $\mathbf{y}(t+1)$ to $\mathbf{y}(t)$ as shown in Figure 5.22.

1. Message passing flow from $\mathbf{y}(t)$ to $\mathbf{y}(t+1)$

The starting node is $\mathbf{y}(t)$; and MMSE_{ap}^{t} is used to represent approximated $S_{\pi,t}$, i.e.,

$$S_{\pi,t} = \text{MMSE}_{ap}^{t}\mathbf{I}_K \tag{5.36}$$

; and the distribution of $\mathbf{y}_{\pi,t}$, i.e., $f_{\mathbf{y}_{\pi,t}}$, is assumed to keep the same in all time slots and all iterations and denoted as $f_{\mathbf{y}_\pi}$. MMSE_{ext}^{t} is used to represent average $S_{\pi,t+1}$ corresponding to $S_{\pi,t}$ equal to $\text{MMSE}_{ap}^{t}\mathbf{I}_K$ and $\mathbf{y}_{\pi,t}$ with distribution $f_{\mathbf{y}_\pi}$.

2. Message passing flow from $\mathbf{y}(t+1)$ to $\mathbf{y}(t)$

   The starting node is $\mathbf{y}(t+1)$; and MMSE_{ap}^{t+1} is used to represent approximated $S_{\pi,t}$, i.e.,

$$S_{\pi,t+1} = \text{MMSE}_{ap}^{t+1}\mathbf{I}_K \tag{5.37}$$

   ; and the distribution of $\mathbf{y}_{\pi,t+1}$, i.e., $f_{\mathbf{y}_{\pi,t+1}}$, is assumed to keep the same in all time slots and all iterations and denoted as $f_{\mathbf{y}_\pi}$. MMSE_{ext}^{t+1} is used to represent average $S_{\pi,t}$ corresponding to $S_{\pi,t}$ equal to $\text{MMSE}_{ap}^{t+1}\mathbf{I}_K$ and $\mathbf{y}_{\pi,t+1}$ with distribution $f_{\mathbf{y}_\pi}$.

Then, we have a curve with MMSE_{ap}^{t} versus MMSE_{ext}^{t} for messaging passing flow from $\mathbf{y}(t)$ to $\mathbf{y}(t+1)$; and flipped curve with MMSE_{ext}^{t+1} versus MMSE_{ap}^{t+1} for messaging passing flow from $\mathbf{y}(t+1)$ to $\mathbf{y}(t)$.

The value of MMSE_{t}^{ext} can be obtained by following the message passing flow in this framework.

1. $\mathbf{y(t)} \rightarrow \mathbf{b(t)}$,we have

   $S_{\pi,t} = \text{MMSE}_{ap}^{t}\mathbf{I}_K$ and the distribution of $\mathbf{y}_{\pi,t}$ is $f_{\mathbf{y}_\pi}$.

2. $\mathbf{b(t)} \rightarrow \mathbf{y(t)}$:

   The detailed derivation of $S_{\lambda,t}$ is provided in section 5.5.

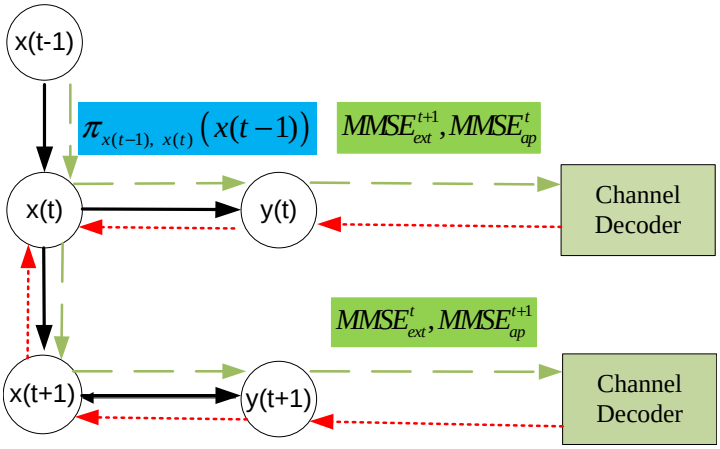

Figure 5.20: Performance analysis framework for iterative message passing

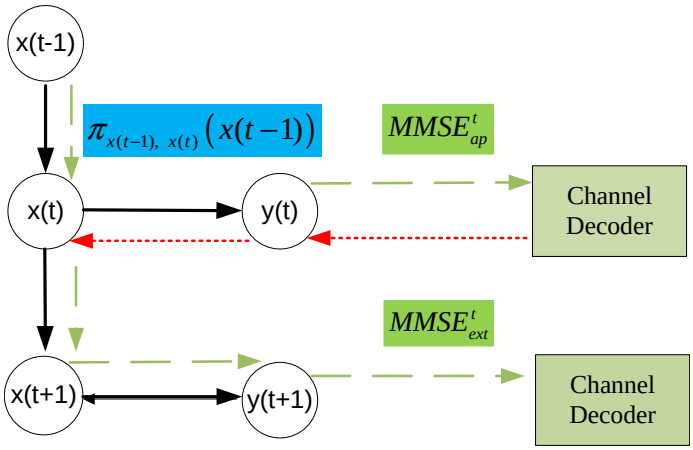

Figure 5.21: Message passing from time slto t to time slot $t+1$

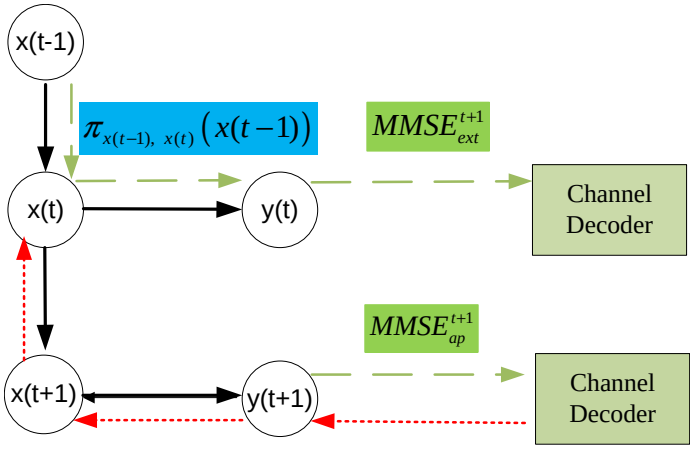

Figure 5.22: Message passing from time slto $t+1$ to time slot t

3. $\mathbf{y(t)} \rightarrow \mathbf{x(t)}$, we have

$$P_{\lambda_y,t} = C^{-1}(S_{\lambda,t} + \Sigma_o) \times (C^{-1})^T. \tag{5.38}$$

4. $\mathbf{x(t)} \rightarrow \mathbf{x(t+1)}$, we have

$$P_{\pi_x,t} = (P_{l,t}^{-1} + P_{\lambda,t}^{-1})^{-1} \tag{5.39}$$

where

$$P_{l,t} = A \times P_{\pi_x,t-1} \times A^T + \Sigma_p \tag{5.40}$$

5. $\mathbf{x(t+1)} \rightarrow \mathbf{y(t+1)}$, we have

$$P_{\pi_y,t+1} = A \times P_{\pi_x,t+1} \times A^T + \Sigma_p \tag{5.41}$$

6. $\mathbf{y(t+1)} \rightarrow \mathbf{b(t+1)}$,we have

$$S_{\pi,t+1} = C \times P_{\pi_y,t+1} \times C^T + \Sigma_o \tag{5.42}$$

Note that $S_{\pi,t+1}$ is a matrix, MMSE_{ext}^t can be obtained by solving the following equation:

$$I_A(\text{MMSE}_{ext}^t \mathbf{I}_K) = I_A(S_{\pi,t+1}) \tag{5.43}$$

The physical meaning of this equation is that MMSE_{ext}^t is the value such that $\text{MMSE}_{ext}^t \mathbf{I}_K$ can provide the same amount of priori information for channel decoder as $S_{\pi,t+1}$.

The value of MMSE_{l+1}^{ext} can be obtained by following the message passing flow in this framework.

1. $\mathbf{y(t+1)} \rightarrow \mathbf{b(t+1)}$,we have

   $S_{\pi,t+1} = \text{MMSE}_{ap}^{t+1}\mathbf{I}_K$ and the distribution of $\mathbf{y}_{\pi,t+1}$ is $f_{\mathbf{y}_\pi}$.

2. $\mathbf{b(t+1)} \rightarrow \mathbf{y(t+1)}$:

   The detailed derivation of $S_{\lambda,t+1}$ is provided in section 5.5.

3. $\mathbf{y(t+1)} \rightarrow \mathbf{x(t+1)}$, we have

$$P_{\lambda_y,t+1} = C^{-1}(S_{\lambda,t+1} + \Sigma_o) \times (C^{-1})^T. \tag{5.44}$$

4. $\mathbf{x(t+1)} \rightarrow \mathbf{x(t)}$, we have

$$P_{\lambda_x,t} = A^{-1}(\Sigma_p + P_{\lambda_y,t+1})(A^{-1})^T \tag{5.45}$$

5. $\mathbf{x(t)} \rightarrow \mathbf{y(t)}$, we have

$$P_{\pi_y,t} = (P_{l,t}^{-1} + P_{\lambda_x,t}^{-1})^{-1} \tag{5.46}$$

   where

$$P_{l,t} = A \times P_{\pi_x,t-1} \times A^T + \Sigma_p \tag{5.47}$$

6. $\mathbf{y(t)} \rightarrow \mathbf{b(t)}$,we have

$$S_{\pi,t} = C \times P_{\pi_y,t} \times C^T + \Sigma_o \tag{5.48}$$

   Note that $S_{\pi,t}$ is a matrix, MMSE_{ext}^{t+1} can be obtained by solving the following equation:

$$I_A(\text{MMSE}_{ext}^{t+1}\mathbf{I}_K) = I_A(S_{\pi,t}) \tag{5.49}$$

The physical meaning of this equation is that MMSE_{ext}^{t+1} is the value such that $\text{MMSE}_{ext}^{t+1}\mathbf{I}_K$ can provide the same amount of priori information for channel decoder as $S_{\pi,t}$.

5.7 Numerical Results

We consider the same electric generator dynamic system used for verification in chapter 3. Each dimension of the observation $\mathbf{y}_t$ is quantized with 14 bits, and the dynamic range for quantization is $[-432, 432]$. A 1/2 rate Recursive Convolutional (RSC) code is used as the channel coding scheme; and the code generator is $g = [1, 1, 1; 1, 0, 1]$. The decoding algorithm is Log-Map algorithm.

The distribution of $\mathbf{y}_{\pi,t}$, i.e., $f_{\mathbf{y}_\pi}$, is Gaussian with zero mean; and the covariance matrix is obtained from the stationary distribution of $\mathbf{y}(t)$,

$$f_{\mathbf{y}_\pi} = \mathcal{N}(\mathbf{y}, \mathbf{0}, \mathbf{\Sigma}_{\mathbf{y}_\pi}) \tag{5.50}$$

where

$$\mathbf{\Sigma}_{\mathbf{y}_\pi} = \begin{pmatrix} 2857 & 0 & 0 & 0 & 0 & 0 & 0 \\ 0 & 6056 & 0 & 0 & 0 & 0 & 0 \\ 0 & 0 & 747 & 0 & 0 & 0 & 0 \\ 0 & 0 & 0 & 1624 & 0 & 0 & 0 \\ 0 & 0 & 0 & 0 & 44 & 0 & 0 \\ 0 & 0 & 0 & 0 & 0 & 10 & 0 \\ 0 & 0 & 0 & 0 & 0 & 0 & 0.79 \end{pmatrix} \tag{5.51}$$

In the model for BP based iterative channel decoding and state estimation, the priori information from $\mathbf{x}(t-1)$ to $\mathbf{x}(t)$ is a Gaussian distribution, i.e.,

$$\pi_{\mathbf{x}_{t-1},\mathbf{x}_t}(\mathbf{x}_{t-1}) \;=\; \mathcal{N}(\mathbf{x}_{t-1}, \mathbf{x}_{\pi_x,t-1}, P_{\pi_x,t-1}) \tag{5.52}$$

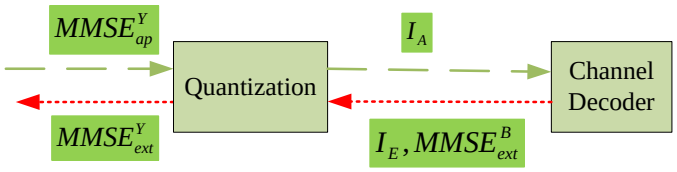

Figure 5.23: Model for message passing between state estimator and channel decoder

where $\mathbf{x}_{\pi_x,t-1} = \mathbf{0}$ and $P_{\pi_x,t-1} = \text{MMSE}^{t-1,x}_{ap}\mathbf{I}_K$.

5.7.1 Information Exchange Between State Estimator and Channel Decoder

In this subsection we will show the performance evaluation results for message passing between state estimator and channel decoder. In addition, we will demonstrate that the gain of using redundancy of system dynamics to assist channel decoding can be obtained by the proposed performance evaluation framework. The model shown in Figure 5.23 is the approximation of the model shown in Figure 5.18 by setting $S_{\pi,t}$ and $S_{\lambda,t}$ as $\text{MMSE}^{Y}_{ap}\mathbf{I}_K$ and $\text{MMSE}^{Y}_{ext}\mathbf{I}_K$, respectively.

Figure 5.24 demonstrates the priori mutual information I_A provided by different MMSE^{Y}_{ap}. There are eight curves in this figure. The curve labeled with Di corresponds to $f_{\mathbf{y}_\pi,i}$ which is a Gaussian distribution with zero mean and variance equal to ith diagonal element of $\mathbf{\Sigma}_{\mathbf{y}_\pi}$. The curve labeled with **mean** correponds to $f_{\mathbf{y}_\pi}$ which is a Gaussian distribution with zero mean and covariance matrix equal to $\mathbf{\Sigma}_{\mathbf{y}_\pi}$. Note that I_A of curve labeled with **mean** is the average I_A of curves labled with $D1, \cdots, D7$. When MMSE^{Y}_{ap} is equal to $1.0e-1$, 1.0, $1.0e+1$, $1.0e+2$, I_A is equal to 0.55, 0.4, 0.25, 0.15, respectively. When MMSE^{Y}_{ap} is equal to $1.0e+5$, the prediction of $\mathbf{y}(t)$ cannot provide any priori information for channel decoder since I_A is equal to 0. Note that although I_A can be as high as 0.8 when MMSE^{Y}_{ap} is equal to $1.0e-3$, it is not achievable as the minimum value of MMSE^{Y}_{ap} is limited by covariance matrix of state dynamics and system observation noise, i.e, $\mathbf{\Sigma}_n$ and $\mathbf{\Sigma}_w$, respectively.

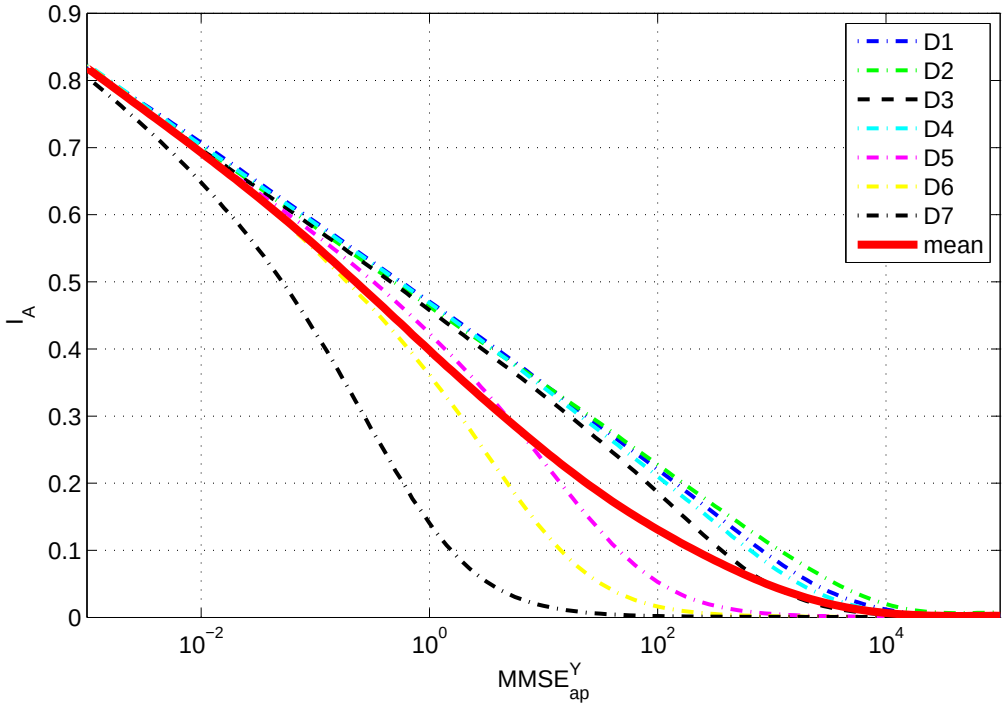

Figure 5.24: Priori mutual information for $\mathbf{b}(t)$ from $\mathbf{y}(t)$ with different MMSE_{ap}^{Y}

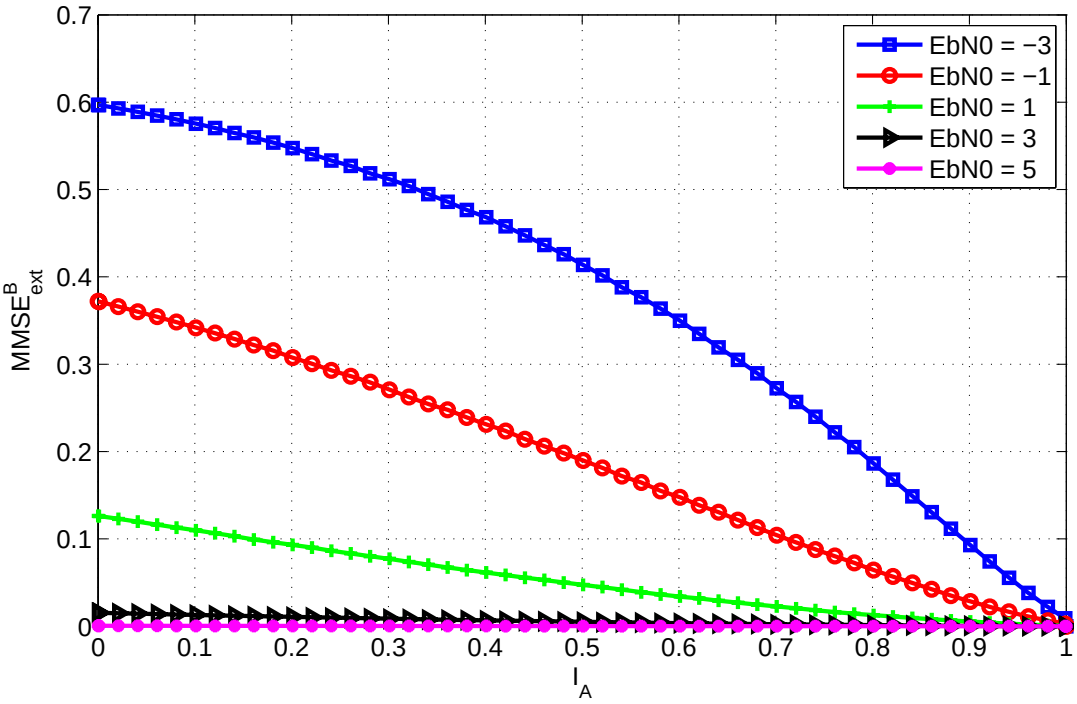

Figure 5.25: MSE curve for channel decoder with different I_A

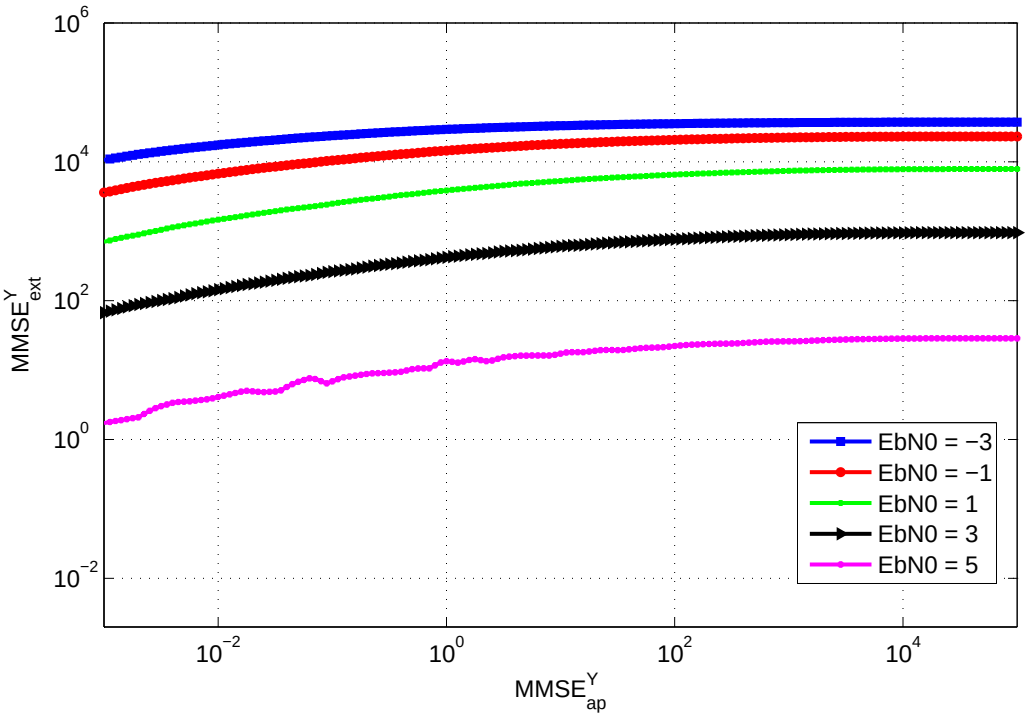

Figure 5.26: MMSE^Y_{ext} with different MMSE^Y_{ap} and E_b/N_0

Figure 5.25 shows the relationship between extrinsic information in terms of MMSE MMSE^B_{ext} and priori information in terms of mutual information I_A. Figure 5.26 illustrates the relationship between MMSE^Y_{ap} and MMSE^Y_{ext}. As shown in Figure 5.24, the prediction of $\mathbf{y}(t)$ cannot provide any priori information for channel decoder when MMSE^Y_{ap} is equal to $1.0e+5$. Therefore, when MMSE^Y_{ap} is equal to $1.0e+5$, the corresponding MMSE^Y_{ext} is based on all information from channel decoder without priori information from MMSE^Y_{ext}. Then, we can set the value of MMSE^Y_{ext} corresponding to MMSE^Y_{ap} equal to $1.0e+5$ as a reference value. For other MMSE^Y_{ap} the gain can be obtained by comparing its MMSE^Y_{ext} with the reference MMSE^Y_{ext}. The gain of MMSE^Y_{ext} with different MMSE^Y_{ap} and E_b/N_0 is shown in Figure 5.27.

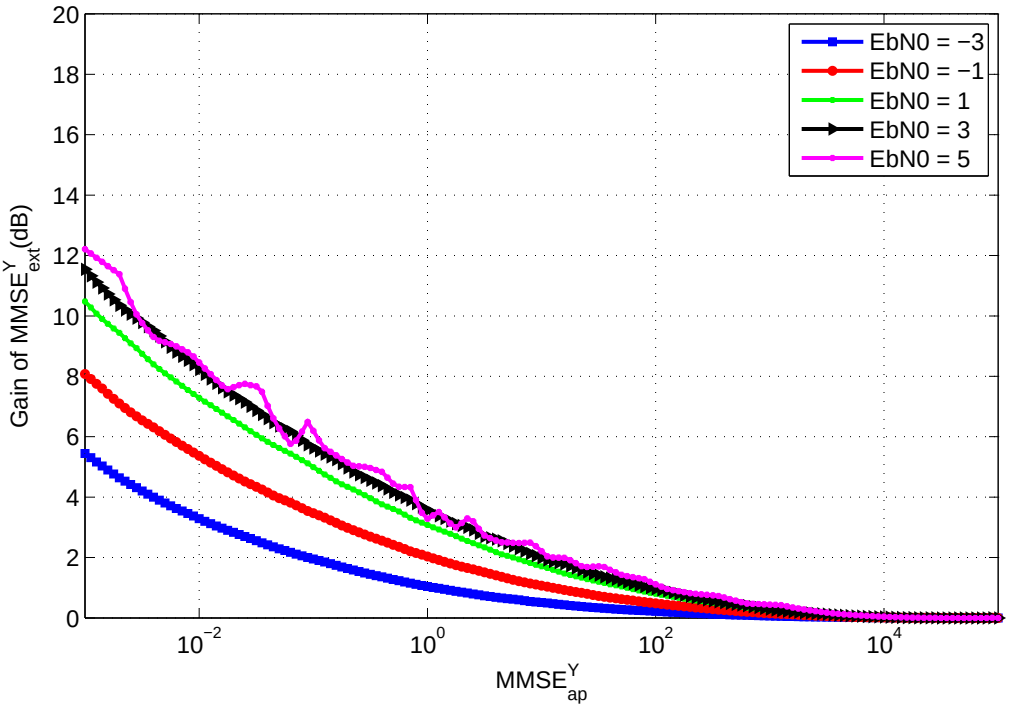

Figure 5.27: Gain of MMSE^Y_{ext} with different MMSE^Y_{ap} and E_b/N_0

5.7.2 Performance Analysis for Sequential Channle Decoding and State Estimation

In this subsection, we will demonstrate how to use the proposed mse-based transfer chart to evaluate the performance of BP based sequential channel decoding and state estimation over time slots under different channel condition, which is modeled by E_b/N_0. Figure 5.28 shows the relationship between MMSE^S_{ap} and MMSE^S_{ext} with different E_b/N_0. In this figure, we have the following observations:

1. When MMSE^S_{ap} is less than 1, the corresponding MMSE^S_{ext} for all E_b/N_0 are equal.

   Note that MMSE^S_{ap} is used to model the amount of priori information from $\mathbf{x}(t-1)$. Therefore, the smaller MMSE^S_{ap} is, the higher the amount of priori information from $\mathbf{x}(t-1)$ is. Although the extrinsic information from channel decoder at time slot t can also contribute to the prediction of $\mathbf{y}(t+1)$, with small

MMSE_{ap}^{S} the priori information from $\mathbf{x}(t-1)$ is dominant in the prediction of $\mathbf{y}(t+1)$. Therefore, the difference of gain from channel decoder with different E_b/N_0 is not seen in MMSE_{ext}^{S}.

2. With large MMSE_{ap}^{S}, the higher E_b/N_0 is, the higher MMSE_{ext}^{S} is. This is because that, with the increase of MMSE_{ap}^{S}, $\mathbf{x}(t-1)$ provides less amount of priori information for the prediction $\mathbf{y}(t)$ and the extrinsic information from channel decoder becomes dominant in the prediction of $\mathbf{y}(t)$. Then, the channel gain with different E_b/N_0 is seen.

3. When MMSE_{ap}^{S} is around $1.0e-2$, there is floor for MMSE_{ext}^{S}.

   It is because, based on information from time slots prior to $t+1$, the prediction of $\mathbf{y}(t)$ cannot be accurate since state dynamics $\mathbf{n}(t)$ and the noise of system observation $\mathbf{w}(t)$ are not predictable. Then, the minimum value of MMSE_{ext}^{S} is limited by the covariance matrix of $\mathbf{n}(t)$ and $\mathbf{w}(t)$, i.e, Σ_n and Σ_w, respectively.

Following the idea of EXIT chart and MSE-based transfer chart for iterative channel decoding, we use MSE-based transfer chart to evaluate the performance of BP based channel decoding and state estimation over time slots. In the MSE-based transfer chart we have two curves. One curve is $\text{MMSE}_{ap}^{S,t}$ versus $\text{MMSE}_{ext}^{S,t}$ which is equivalent with the curve for MMSE_{ap}^{S} versus MMSE_{ext}^{S} in order to represent the relationship between MMSE_{ap}^{S} and MMSE_{ext}^{S} at time slot t. The other curve is $\text{MMSE}_{ext}^{S,t+1}$ versus $\text{MMSE}_{ap}^{S,t+1}$ which is equivalent with flipped curve for MMSE_{ap}^{S} versus MMSE_{ext}^{S} in order to represent the relationship between MMSE_{ap}^{S} and MMSE_{ext}^{S} at time slot $t+1$.

The MSE-based transfer chart for E_b/N_0 equal to 5dB is shown in Figure 5.29. There is one cross point between these two curves, which is the convergence point. The arrows with black color shows the trace of sequential message passing when MMSE_{ap}^{S} is equal to $1.0e-2$ at time slot t. We can see that trace moves toward the convergence point at time slot $t+1$ and $t+2$. The physical meaning is that even if we

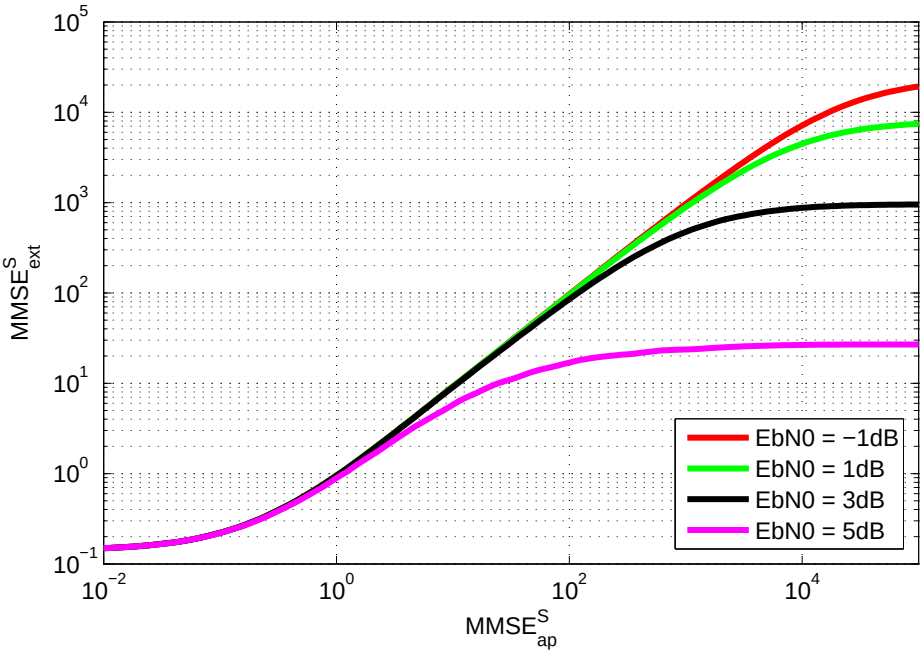

Figure 5.28: Relationship between MMSE^S_{ext} and MMSE^S_{ap} for sequential message passing with different E_b/N_0

have perfect knowledge about $\mathbf{y}(t)$ at time slot t, the performance of state estimation degrades toward the cross point after running a few time slots. The arrows with red color shows the other trace with starting MMSE^S_{ap} equal to $1.0e+5$, at which there is no priori information from prediction of $\mathbf{y}(t)$. We can also see that trace is moving toward the convergence point at time slot $t+1$, $t+2$, $\cdots$. The physical meaning of this trace is that, even if there is no priori information about $\mathbf{y}(t)$ at time slot t, the performance of state estimation would be improved after running a few time slots; finally, its performance is close to the performance of the convergence point.

Figure 5.30 demonstrates the MSE-based transfer chart with E_b/N_0 equal to 3dB. In this figure there is also one cross-point at $\text{MMSE}^{S,t}_{ap}$ equal to $1.0e-0.15$. However, in the rage of $[1.0e-0.15, 1.0e+2]$ the gap between the curve for $\text{MMSE}^{S,t}_{ap}$ versus $\text{MMSE}^{S,t}_{ext}$ and the curve for $\text{MMSE}^{S,t+1}_{ext}$ versus $\text{MMSE}^{S,t+1}_{ap}$ is small. This means that the convergence speed is slow and it would take many time slots to converge to the

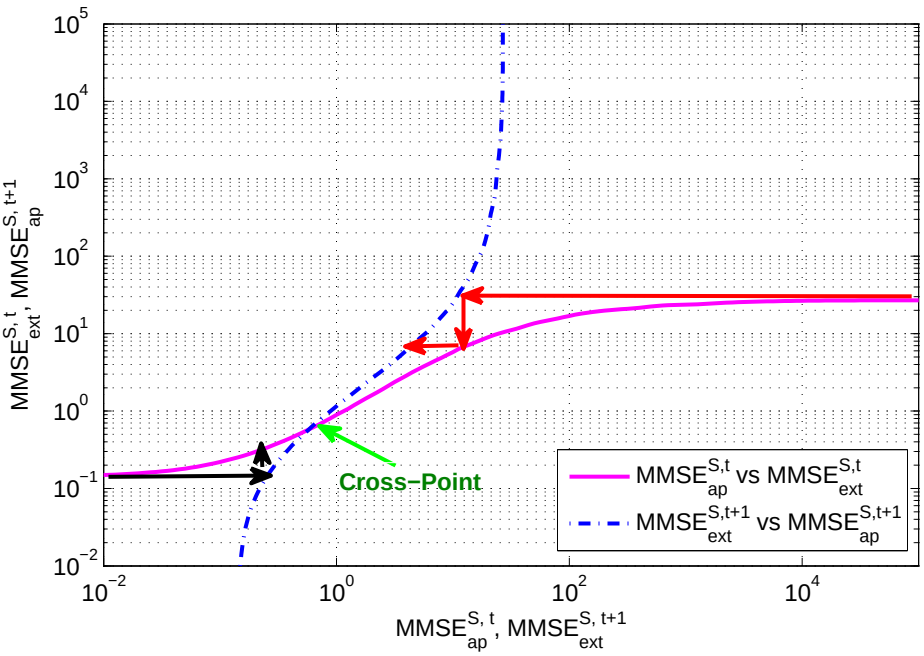

Figure 5.29: MSE transfer chart for sequential channel decoding and state estimation: $E_b/N_0 = 5dB$

convergence point if the estimator has no priori information about $\mathbf{y}(t)$ at time slot t.

Figure 5.31 and Figure 5.32 demonstrates the MSE-based transfer chart with E_b/N_0 equal to 1dB and -1dB, respectively. In these two figures there is also one cross-point at $\text{MMSE}_{ap}^{S,t}$ equal to $1.0e-0.15$. However, after the cross-point the curve for $\text{MMSE}_{ap}^{S,t}$ versus $\text{MMSE}_{ext}^{S,t}$ almost overlaps with the curve for $\text{MMSE}_{ext}^{S,t+1}$ versus $\text{MMSE}_{ap}^{S,t+1}$. Therefore, if the estimator has no priori information about $\mathbf{y}(t)$ at time slot t, then it could either cannot converge to the cross-point and has high MSE or it could take many time slots to converge to the cross-point. Therefore, for E_b/N_0 equals to 1dB and -1dB, the MSE of estimating $\mathbf{x}(t)$ and $\mathbf{y}(t)$ is much higher than that for E_b/N_0 equal to 3dB and 5dB.

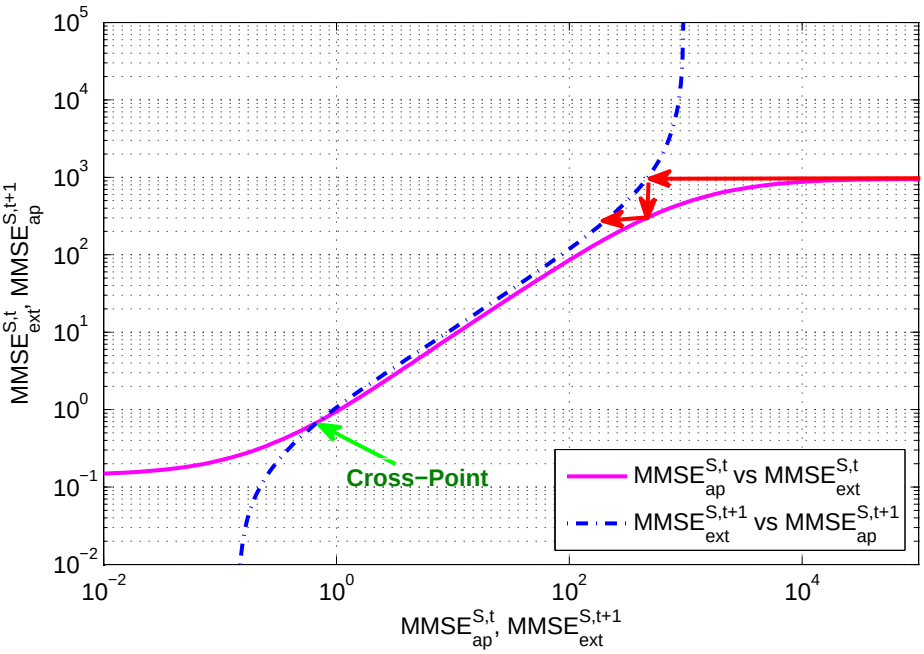

Figure 5.30: MSE transfer chart for sequential channel decoding and state estimation: $E_b/N_0 = 3dB$

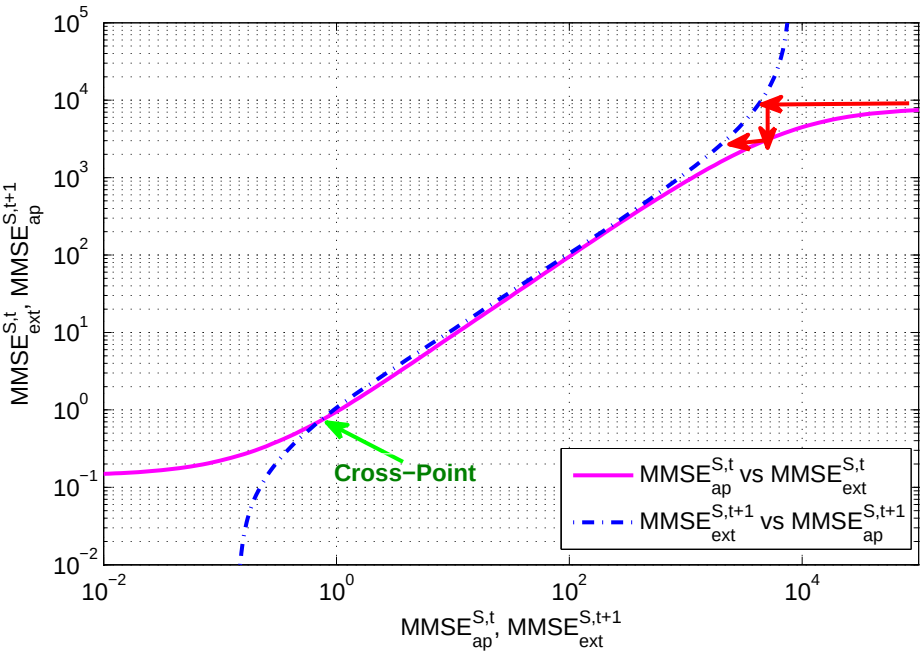

Figure 5.31: MSE transfer chart for sequential channel decoding and state estimation: $E_b/N_0 = 1dB$

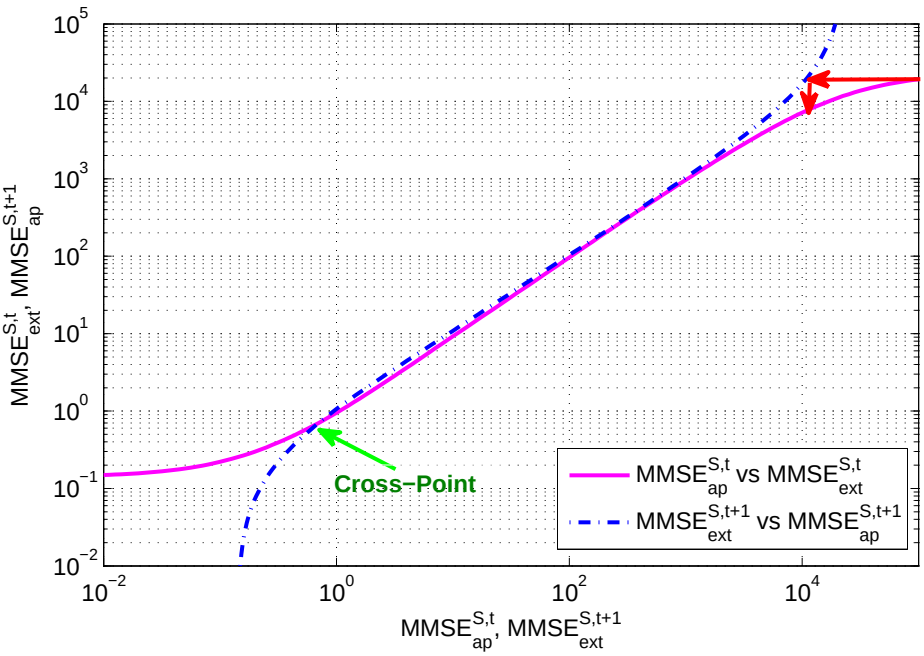

Figure 5.32: MSE transfer chart for sequential channel decoding and state estimation: $E_b/N_0 = -1dB$

5.7.3 Performance Analysis for Iterative Channel Decoding and State Estimation

In this subsection, we show how to use the proposed MSE-based transfer chart to evaluate the performance of BP based iterative channel decoding and state estimation over two time slots. Figure 5.33 shows the relationship between MMSE^t_{ap} and MMSE^t_{ext} with different $\text{MMSE}^{t-1,x}_{ap}$ and $E_b/N_0 = 5dB$. As shown in Figure 5.24 the prediction of $\mathbf{y}(t)$ with MMSE^S_{ap} equal to $1.0e+5$ does not provide any priori information for $\mathbf{b}(t)$. Therefore, when MMSE^t_{ap} is equal to $1.0e+5$, the corresponding MMSE^t_{ext} is contributed by both priori information from $\mathbf{x}(t-1)$ and extrinsic information from channel decoder at time slot t. The gain of MMSE^t_{ext} from MMSE^S_{ap} can be obtained by comparing it with the value of MMSE^t_{ext} corresponding to MMSE^S_{ap} equal to $1.0e+5$. Figure 5.34 shows the gain of MMSE^t_{ext} from MMSE^t_{ap}. From this figure we have the following observation:

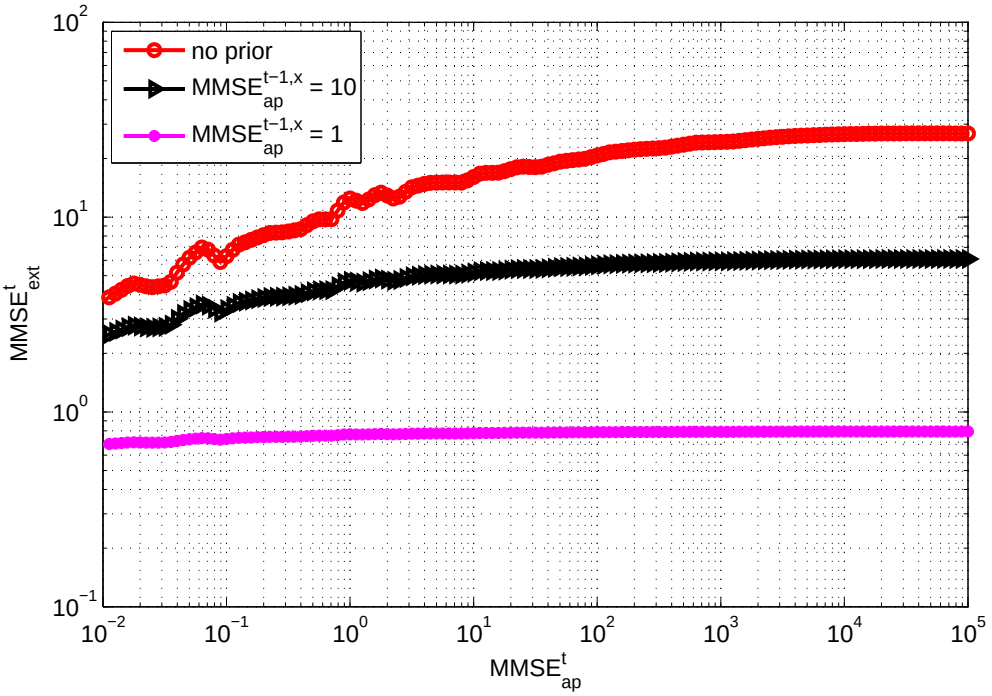

Figure 5.33: MSE curve for MMSE^t_{ap} versus MMSE^t_{ext} with different $\text{MMSE}^{t-1,x}_{ap}$ and $E_b/N_0 = 5dB$

1. With the same $\text{MMSE}^{t-1,x}_{ap}$, the higher MMSE^t_{ap} is, the higher gain of MMSE^t_{ext} can be obtained from MMSE^t_{ap}.

2. The higher the $\text{MMSE}^{t-1,x}_{ap}$ is, the higher gain of MMSE^t_{ext} can be obtained from MMSE^t_{ap}.

   This is because the prediction of $\mathbf{y}(t+1)$ is contributed by both priori information from $\mathbf{x}(t-1)$ and extrinsic information from channel decoder at time slot t. When $\text{MMSE}^{t-1,x}_{ap}$ is small, the information from $\mathbf{x}(t-1)$ is dominant in predicting $\mathbf{y}(t+1)$. Although the prediction of $\mathbf{y}(t)$ can increase the amount of extrinsic information from channel decoder at time slot t, it cannot contribute much to the gain of MMSE^t_{ext} as the priori information from $\mathbf{x}(t-1)$ is dominant.

Figure 5.35 illustrates the relationship between MMSE^{t+1}_{ap} and MMSE^{t+1}_{ext} with different $\text{MMSE}^{t-1,x}_{ap}$ and $E_b/N_0 = 5dB$. Following the idea for the gain of MMSE^t_{ext}

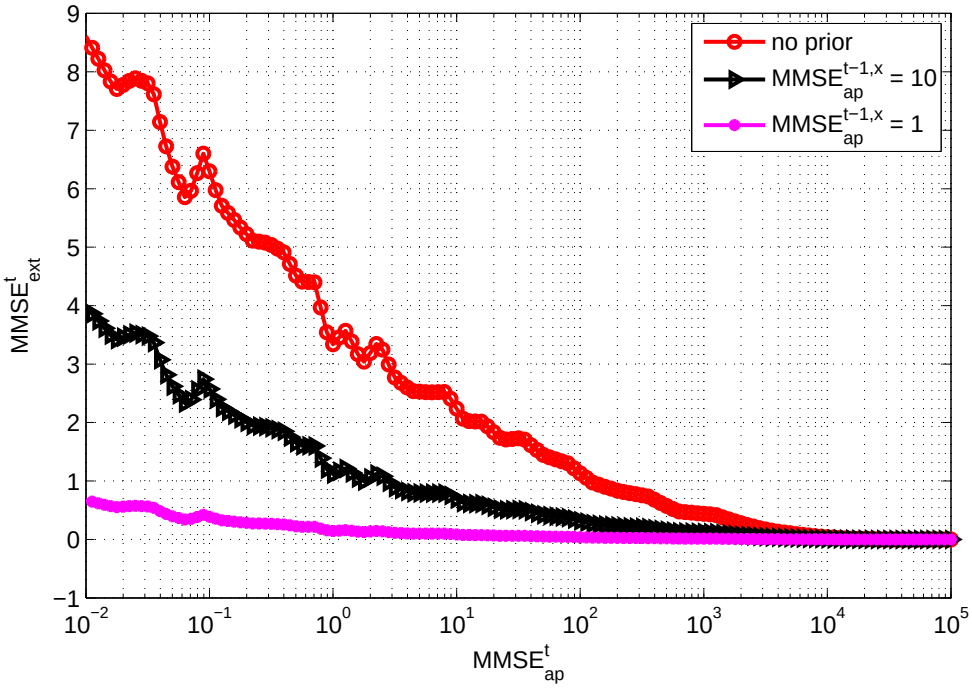

Figure 5.34: Gain of MMSE_{ext}^{t} from MMSE_{ap}^{t} with different $\text{MMSE}_{ap}^{t-1,x}$ and $E_b/N_0 = 5dB$

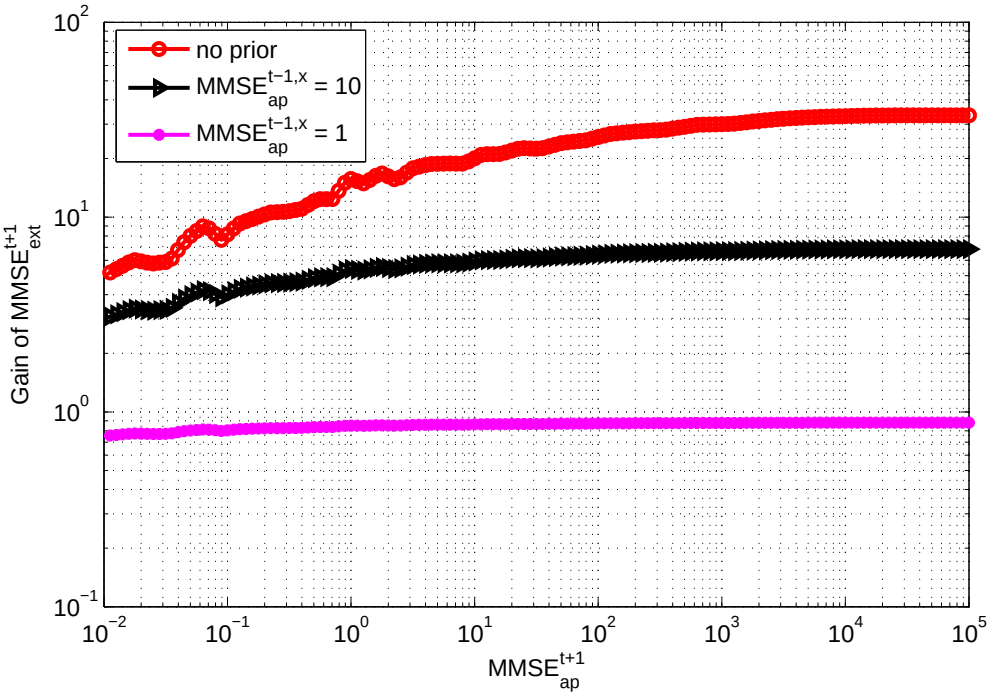

Figure 5.35: MSE curve for MMSE_{ap}^{t+1} versus MMSE_{ext}^{t+1} with different $\text{MMSE}_{ap}^{t-1,x}$ and $E_b/N_0 = 5dB$

from MMSE_{ap}^{t}, the gain of MMSE_{ext}^{t+1} from MMSE_{ap}^{t+1} is obtained and shown in Figure 5.36. We have similar observation as the gain of MMSE_{ext}^{t} from MMSE_{ap}^{t}:

1. With the same $\text{MMSE}_{ap}^{t-1,x}$, the higher MMSE_{ap}^{t+1} is, the higher gain of MMSE_{ext}^{t+1} can be obtained from MMSE_{ap}^{t}.

2. The higher the $\text{MMSE}_{ap}^{t-1,x}$ is, the higher gain of MMSE_{ext}^{t+1} can be obtained from MMSE_{ap}^{t+1}.

We obtain the MSE-based transfer chart for BP based iterative channel decoding and state estimation from the curve for MMSE_{ap}^{t} versus MMSE_{ext}^{t} and the curve for MMSE_{ap}^{t+1} versus MMSE_{ext}^{t+1}. Figure 5.37 demonstrates the MSE-based transfer chart with different $\text{MMSE}_{ap}^{t-1,x}$ and E_b/N_0 equals to 5dB. From this figure, for the case without priori information from $\mathbf{x}(t-1)$ we have the following observation:

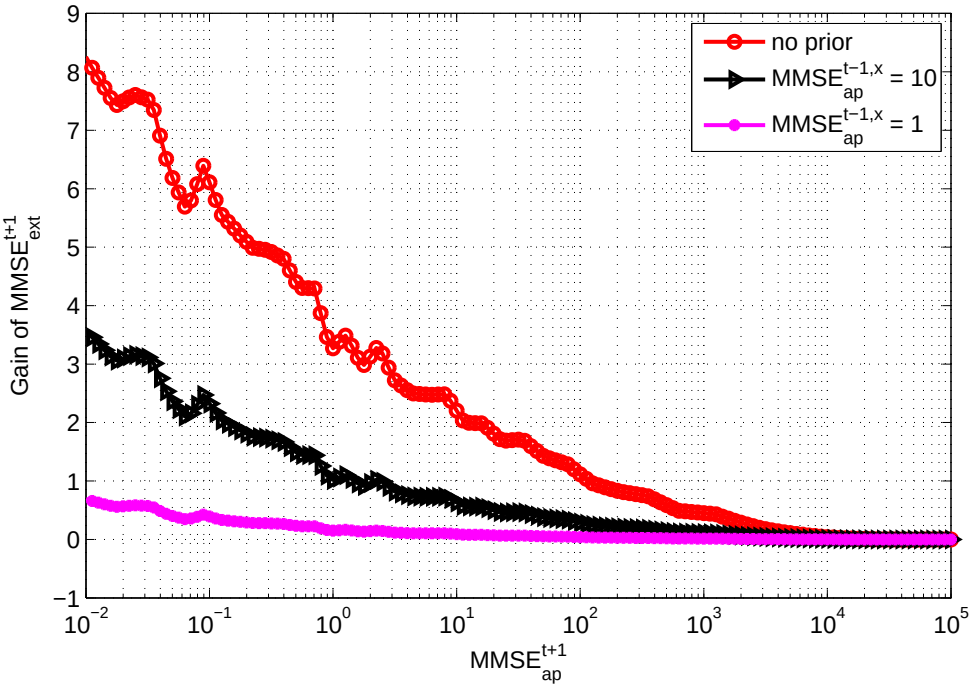

Figure 5.36: Gain of MMSE_{ext}^{t+1} from MMSE_{ap}^{t+1} with different $\text{MMSE}_{ap}^{t-1,x}$ and $E_b/N_0 = 5dB$

1. BP based iterative channel decoding can decrease MMSE_{ext}^{t} and help improve the estimation of $\mathbf{x}(t+1)$.

   The cross-point between the curve for MMSE_{ap}^{t} versus MMSE_{ext}^{t} and the curve for MMSE_{ap}^{t+1} versus MMSE_{ext}^{t+1} is the convergence point of BP based iterative channel decoding and state estimation. As shown in the figure, the value of MMSE_{ap}^{t} and MMSE_{ext}^{t} corresponding to the cross-point are $1.0e+1.33$ and $1.0e+1.25$, respectively; and the value of MMSE_{ext}^{t} corresponding to the point without priori information from $\mathbf{y}(t)$, i.e, $\text{MMSE}_{ap}^{t}=1.0e+5$, is $1.0e+1.43$. Therefore, the gain of MMSE_{ext}^{t} for BP based iterative channel decoding and state estimation is $10*(1.43-1.25)=1.8\text{dB}$.

2. The gain of MMSE_{ext}^{t} from BP based iterative channel decoding and state estimation with three steps, step from $\mathbf{y}(t)$ to $\mathbf{y}(t+1)$, step from $\mathbf{y}(t+1)$ to $\mathbf{y}(t)$, step from $\mathbf{y}(t)$ to $\mathbf{y}(t+1)$, is close to the gain of MMSE_{ext}^{t} of convergence point.

   The trace of BP based iterative channel decoding and state estimation with the mentioned three steps is shown by arrows with blue color in the figure. The detail of these three steps is as below:

   (a) Step 1: from $\mathbf{y}(t)$ to $\mathbf{y}(t+1)$:

   As there is no priori information, the starting point is MMSE_{ap}^{t} with value $1.0e+5$; and the corresponding value of MMSE_{ext}^{t} $1e+1.43$.

   (b) Step 2: $\mathbf{y}(t+1)$ to $\mathbf{y}(t)$:

   We have MMSE_{ap}^{t+1} with value $1e+1.43$; and the corresponding value of MMSE_{ext}^{t+1} is $1e+1.34$

   (c) Step 3: $\mathbf{y}(t)$ to $\mathbf{y}(t+1)$:

   We have MMSE_{ap}^{t} with value $1e+1.34$; and the corresponding value of MMSE_{ext}^{t} is $1e+1.255$. Comparing with step 1, $10*(1.43-1.255)=1.75\text{dB}$ gain of MMSE_{ext}^{t} is obtained from these three steps. Comparing with the

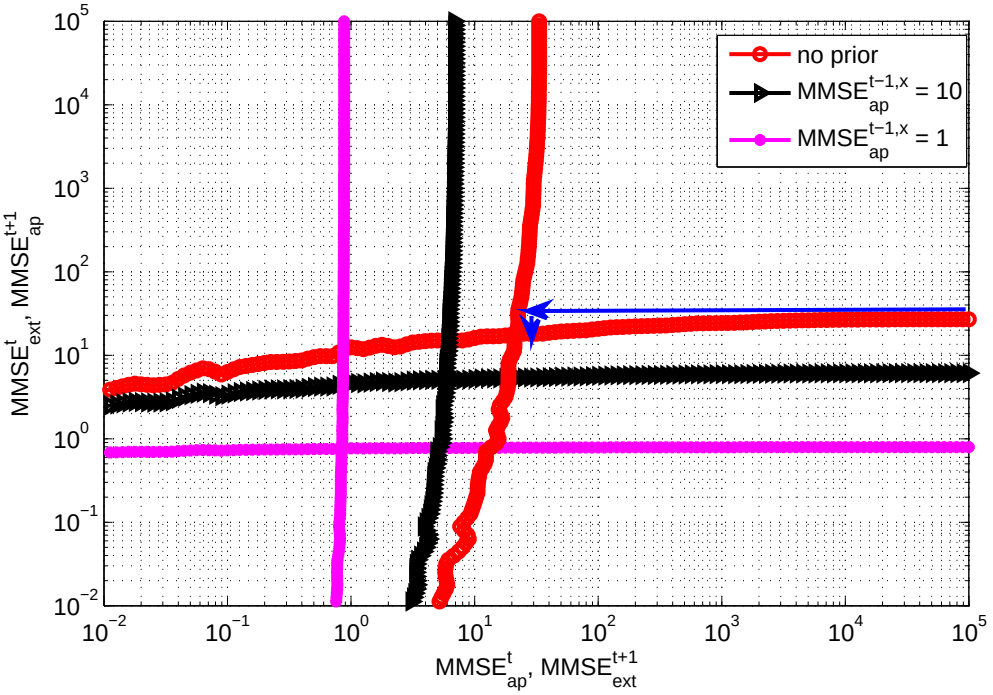

Figure 5.37: MSE-based transfer chart for iterative channel decoding and system state estimation with different $\text{MMSE}_{ap}^{t-1,x}$ and $E_b/N_0 = 5dB$

gain of 1.8dB for MMSE_{ext}^{t} from convergence point, the gain loss for BP based iterative channel decoding and state estimation with three steps is just $1.8 - 1.75 = 0.05$dB.

Therefore, we can implement BP based iterative channel decoding and state estimation with three steps, step from $\mathbf{y}(t)$ to $\mathbf{y}(t+1)$, step from $\mathbf{y}(t+1)$ to $\mathbf{y}(t)$, step from $\mathbf{y}(t)$ to $\mathbf{y}(t+1)$, to obtain the gain of MMSE_{ext}^{t} of convergence point.

When $\text{MMSE}_{ap}^{t-1,x}$ is equal to 1 and 10, BP based iterative channel decoding and state estimation cannot improve the performance of state estimation. This is because with small $\text{MMSE}_{ap}^{t-1,x}$ the priori information from $\mathbf{x}(t)$ is dominant in predicting $\mathbf{y}(t+1)$. Therefore, the gain of extrinsic information from using the prediction of $\mathbf{y}(t)$ in channel decoder at time slot t is negligible in predicting $\mathbf{y}(t+1)$.

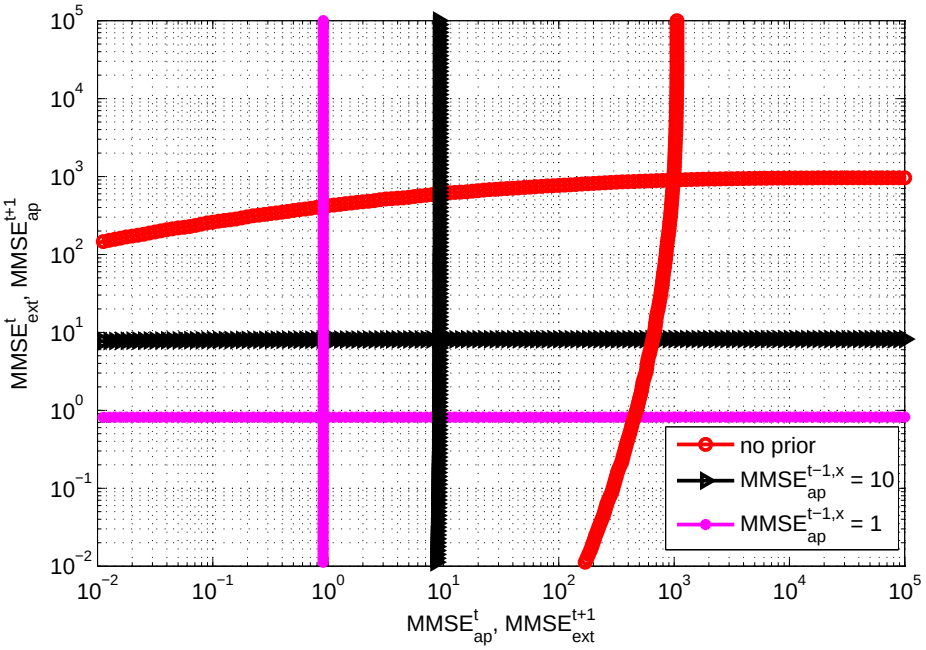

Figure 5.38: MSE-based transfer chart for iterative channel decoding and system state estimation with different $\text{MMSE}_{ap}^{t-1,x}$ and $E_b/N_0 = 3dB$

The MSE-based transfer charts for E_b/N_0 equal to 3dB and 1dB are shown in Figure 5.38 and 5.39, respectively. From these two figures we can have similar observations as that for E_b/N_0 equal to 5dB.

5.7.4 Performance Analysis for Kalman Filtering based Heuristic Approach

We can also utilize this framework to evaluate the gain obtained by utilizing the redundancy of system dynamics in assisting the estimation of system observation for Kalman filtering based heuristic approach mentioned in section 3.3. In the Kalman filtering based heuristic approach, the prediction of $\mathbf{y}(t)$ is used as priori information for $\mathbf{b}(t)$ in order to improve the performance of channel decoding. Instead of using extrinsic information of channel decoder to obtain soft estimate of $\mathbf{y}(t)$, the total information generated by channel decoder including priori information and extrinsic information is used to obtain hard estimate of $\mathbf{y}(t)$. The corresponding performance

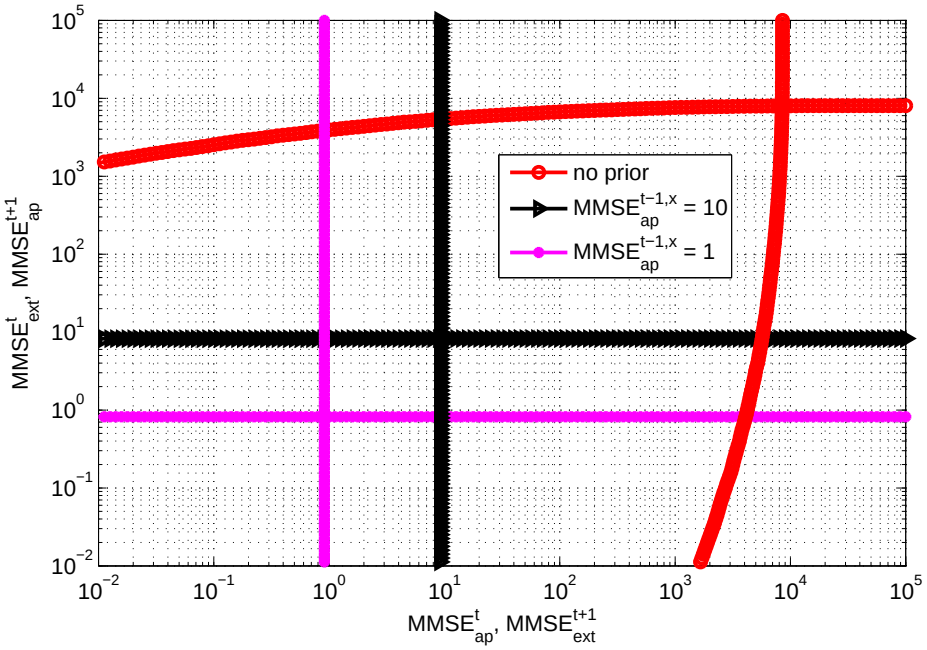

Figure 5.39: MSE-based transfer chart for iterative channel decoding and system state estimation with different $\mathrm{MMSE}_{ap}^{t-1,x}$ and $E_b/N_0 = 1dB$

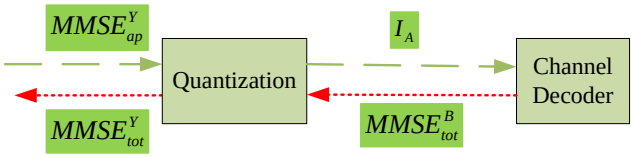

Figure 5.40: Model for message passing between state estimator and channel decoder

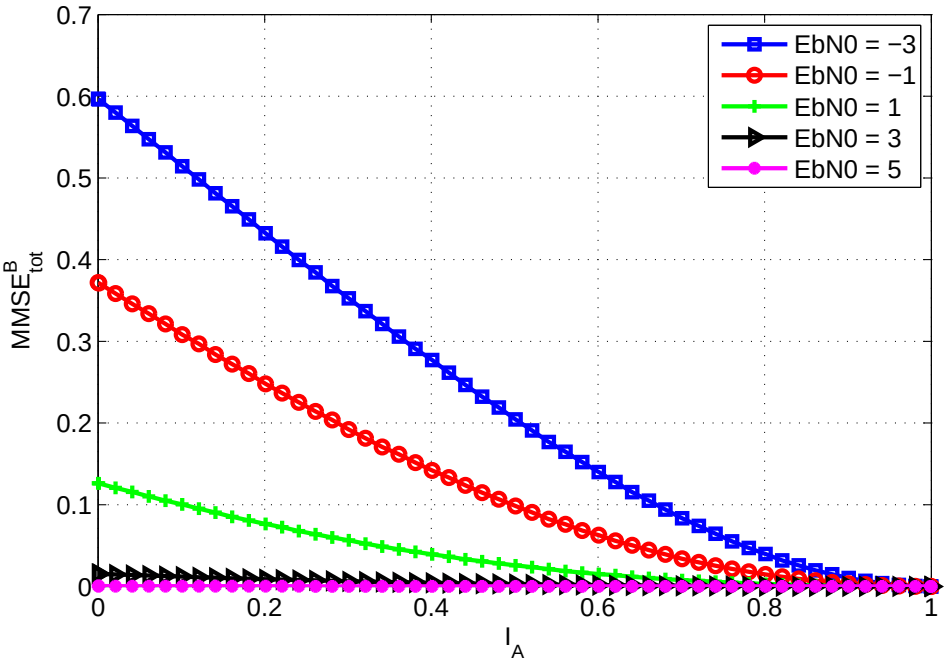

Figure 5.41: MSE curve for channel decoder

evaluation framework for Kalman filtering based heuristic approach is shown in Figure 5.40. Similarily with BP based channel decoding and state estimation, the priori information from $\mathbf{y}(t)$ is modeled with $S_{\pi,t}$ equal to $\text{MMSE}_{ap}^{Y}\mathbf{I}_K$ and the distribution of $\mathbf{y}_{\pi,t}$ is $f_{\mathbf{y}_\pi}$; then, the priori information for $\mathbf{b}(t)$ is represented by mutual information I_A. The total information from channel decoder for the estimate of $\mathbf{b}(t)$ is modeled by $\text{MMSE}^{B}tot$, which means the MMSE of estimate $\mathbf{b}(t)$ based on total information from channel decoder.

Figure 5.41 shows the relationship between total information from channel decoder in terms of MMSE MMSE_{tot}^{B} and priori information in terms of mutual information I_A. Figure 5.42 illustrates the relationship between MMSE_{ap}^{Y} and MMSE_{tot}^{Y}. As shown in Figure 5.24, the prediction of $\mathbf{y}(t)$ cannot provide priori information for channel decoder when MMSE_{ap}^{Y} is equal to $1.0e+5$. Therefore, when MMSE_{ap}^{Y} is equal to $1.0e+5$, the corresponding MMSE_{tot}^{Y} is based on all information from channel decoder without priori information from $\mathbf{y}(t)$. Then, we can set the value of MMSE_{tot}^{Y}

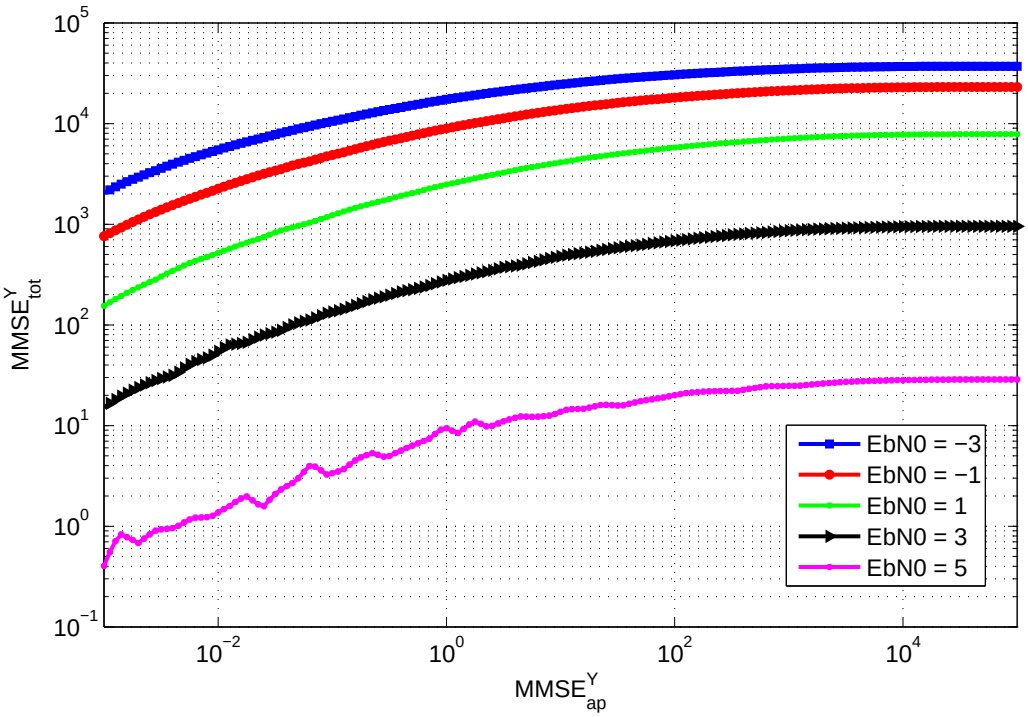

Figure 5.42: MMSE_{tot}^{Y} with different MMSE_{ap}^{Y} and E_b/N_0

corresponding to MMSE_{ap}^{Y} equal to $1.0e+5$ as a reference MMSE_{tot}^{Y}. For other MMSE_{ap}^{Y} the gain can be obtained by comparing its MMSE_{tot}^{Y} with this reference MMSE_{tot}^{Y}. The gain of MMSE_{tot}^{Y} with different MMSE_{ap}^{Y} and E_b/N_0 is shown in Figure 5.43.

5.8 Conclusions

In this chapter we have presented the proposed MSE-based transfer chart performance analysis framework for BP based channel decoding and state estimation. We also show how to utilize the proposed MSE-based transfer chart to evaluate:

1. The gain of utilizing the prediction of $\mathbf{y}(t)$ to assist channel decoding for BP based channel decoding and state estimation;

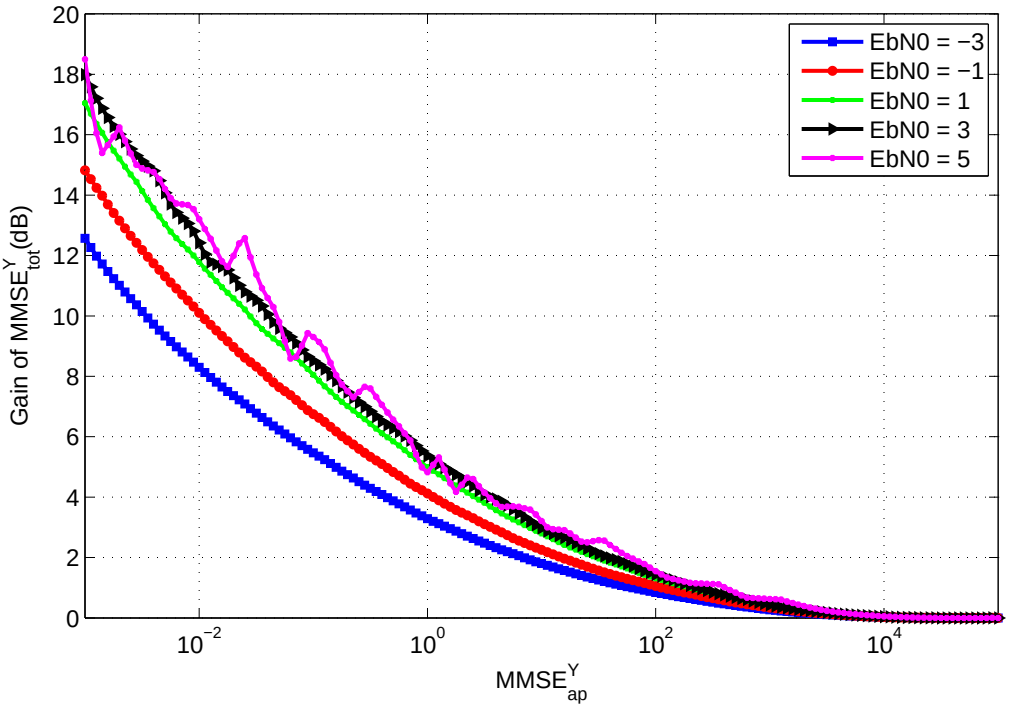

Figure 5.43: Gain of MMSE^Y_{tot} with different MMSE^Y_{ap} and E_b/N_0

2. the performance of BP based sequential channel decoding and state estimation over time slots with channel condition modeled by E_b/N_0;

3. the performance of BP based iterative channel decoding and state estimation over two time slots;

4. the gain of utilizing the prediction of $\mathbf{y}(t)$ to assist channel decoding for Kalman filtering based heuristic approach for state estimation.

Chapter 6

Conclusions and Future Work

6.1 Summary of Contributions

In this dissertation we study *the decoding procedure (including the demodulation procedure) for the messages with no or weak channel coding protection in the context of NCS with stringent delay requirement.* We propose to utilize the redundancy of the system dynamics to protect the reliability of the uncoded or weakly encoded messages. The system dynamics are considered as a 'nature encoding' similar to convolution code, due to its redundancy in time.

Firstly, for systems with or without explicit channel coding, a decoding procedures based on Pearl's Belief Propagation (BP), in a similar manner to Turbo processing in traditional data communication systems, is proposed. Numerical simulations have demonstrated the validity of the schemes, using a linear model of electric generator dynamic system. One disadvantage of this proposed scheme is that there is error propagation at low SNR especially for Kalman Filtering based heuristic approach.

Secondly, we propose a quickest detection based error propagation detection scheme to detect error propagation online. Then we combine this proposed error propagation detection scheme with the proposed system dynamics assisted channel decoding and state estimation algorithm to improve its robustness. The numerical

results show that error propagation does not happen and consistent performance gain is observed in the proposed system dynamics based channel decoding and state estimation together with error propagation detection.

Finally, we propose to use MSE-based transfer chart evaluate the performance of BP based channel decoding and state estimation. We focus on two models, BP based **sequential** and **iterative** channel decoding and state estimation. The first model can be used to evaluate the performance of sequential channel decoding and state estimation over time slots; and the second model can be used to evaluate the performance of iterative channel decoding and state estimation over two time slots. The numerical results show that MSE-based transfer chart can provide much insight about the performance of the proposed BP based channel decoding and state estimation algorithm.

6.2 Future Work

In this dissertation we propose to utilize the time-domain redundancy of system dynamics to assist channel decoding; and propose an mse-based transfer performance evaluation framework to jointly evaluate the performance of estimator and channel decoder. In the future, more research work in the following areas can be performed.

1. Performance gain from system dynamics assisted channel decoding for estimator discarding erroneous packets.

   As shown in subsection 5.7.4 there is also gain from using system dynamics to assist channel decoding on the condition that the prediction is correct in probabilistic manner. The framework to utilize system dynamics assisted channel decoding for estimator discarding erroneous packets is shown in Fig.6.1. Estimator which discards erroneous packet is not impacted by communication noise from estimates of system observation; therefore, estimator can provide correct prediction for channel decoder in probabilistic manner resulting in

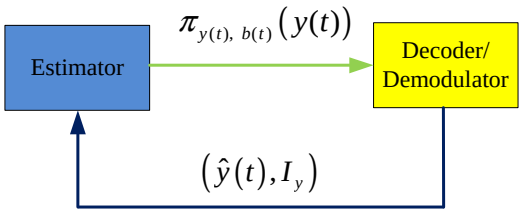

Figure 6.1: Framework of system dynamics assisted channel decoding for estimator discarding erroneous packets

decrease of packet drop rate. For an estimator with different packet drop rate it is worth exploring the performance gain in terms of packet drop rate from system dynamics assisted channel decoding.

Bibliography

Alexander, H. L. (1991). State estimation for distributed systems with sensing delay. *Proc. SPIE*, 1470:103–111. 8

Alexander, P. D., Reed, M. C., and Schlegel, C. B. (1999). Iterative multiuser interference reduction: Turbo cdma. *IEEE Trans. Commun*, 47(7):1008–1014. 5, 19

Ashikhmin, A., Kramer, G., and ten Brink, S. (2004). Extrinsic information transfer functions: model and erasure channel properties. *IEEE Trans. Inf. theory*, 50(1):2657–2673. 16, 58

Bai, J., Eyisi, E., Qiu, F., Xue, Y., and Koutsoukos, X. (2012). Optimal cross-layer design of sampling rate adaptation and network scheduling for wireless networked control systems. In *Cyber-Physical Systems (ICCPS), 2012 IEEE/ACM Third International Conference on*, pages 107–116. 10

Benedetto, S., Divsalar, D.and Montorsi, G., and Pollara, F. (1998). Serial concatenation of interleaved codes: performance, analysis, design, and iterative decoding. *IEEE Trans. Inform. Theory*, 44(3):909–926. 15

Berrou, C., Glavieux, A., and Thitimajshima, P. (1993). Near shannon limit error-correcting coding and decoding. turbo codes. *Proc. Int. Conf. Communications*. 5, 19, 28

Bhattad, K. and Narayanan, K. R. (2007). An mse-based transfer chart for analyzing iterative decoding schemes using a gaussian approximation. *IEEE Trans. Inf. theory*, 53(1):22–38. 16, 29, 56, 58, 75, 79

Boggia, G., Camarda, P., Grieco, L., and Zacheo, G. (2008). Toward wireless networked control systems: An experimental study on real-time communications in 802.11 wlans. In *Factory Communication Systems, 2008. WFCS 2008. IEEE International Workshop on*, pages 149–155. 2

Branicky, M. (1997). Stability of hybrid systems: state of the art. In *Decision and Control, 1997., Proceedings of the 36th IEEE Conference on*, volume 1, pages 120–125 vol.1. 13

Branicky, M. S., Phillips, S. M., and Zhang, W. (2000). Stability of networked control systems: Explicit analysis of delay. In *Proc. Amer. Contr. Conf.*, page 2352C2357. 13

Chamaken, A. and Litz, L. (2010). Joint design of control and communication in wireless networked control systems: A case study. In *American Control Conference (ACC), 2010*, pages 1835–1840. 10

Chen, S.and Lee, H., Chen, C., Huang, H., and Luo, C. (2007). Wireless sensor network system by separating control and data path (scdp) for bio-medical applications. In *Microwave Conference, 2007. European*, pages 430–433. 2

Chen, S.-L., Lee, H.-Y., Chen, C.-A., Huang, H.-Y., and Luo, C.-H. (2009). Wireless body sensor network with adaptive low-power design for biometrics and healthcare applications. *Systems Journal, IEEE*, 3(4):398–409. 2

Chen, W., Chen, L., Chen, Z., and Tu, S. (2005). A realtime dynamic traffic control system based on wireless sensor network. In *Parallel Processing, 2005. ICPP 2005 Workshops. International Conference Workshops on*, pages 258–264. 2

Chen, Z., Weng, J., Yang, X., and Feng, J. (2011). Irrigation pumping station wireless measurement and control system based on zigbee and 3g network. In *Internet Technology and Applications (iTAP), 2011 International Conference on*, pages 1–5. 2

Chiuso, A. and Schenato, L. (2008). Information fusion strategies from distributed filters in packet-drop networks. In *Decision and Control, 2008. CDC 2008. 47th IEEE Conference on*, pages 1079–1084. 10

Cover, T. M. and Thomas, J. A. (1991). *Elements of information theory*. Wiley. 11, 59

Duan, Z. and Li, X. (2011). Lossless linear transformation of sensor data for distributed estimation fusion. *Signal Processing, IEEE Transactions on*, 59(1):362–372. 10

Duan, Z. S., Li, X. R., and Yang, M. (2007). Why are more sensors better in estimation fusion? In *Proc. 2007 Int. Colloquium Information Fusion*, pages 173 –179. 10

Elias, P. (1955). Coding for noise channels. *IRE conv. Rept. Pr. 4*, pages 37–47. 15

Fresia, M., Perez-Cruz, F., Poor, H. V., and Verdu, S. (2010). Joint source and channel coding. *IEEE Signal Processing Magzine*, 27(6):104–113. 15, 17, 59

Gallager, R. G. (1963). *Low-density parity-check codes*. MIT Press, Cambridge, MA. 15, 16, 57, 62

Garcia-Frias, J. and Villasenor, J. D. (1997). Combining hidden markov source models and parallel concatenated codes. *IEEE Commun. Lett.*, 1(7):111–113. 15, 17, 59

Garcia-Frias, J. and Villasenor, J. D. (1998). Turbo decoding of hidden markov sources with unknown parameters. *Proc. of IEEE Data Compression Conf.* 15, 17, 59

Garcia-Frias, J. and Villasenor, J. D. (2001). Joint turbo decoding and estimation of hidden markov models. *IEEE J. Select. Areas Commun.*, 19(9):1671–1679. 15, 17, 59

Garcia-Frias, J. and Zhao, Y. (2001). Data compression of unknown single and correlated binary sources using punctured turbo codes. *Proc. of 39th Annu. Allerton Conf. Communications, Computing and Control*. 15, 17, 59

Garcia-Frias, J. and Zhao, Y. (2002). Compression of binary memoryless sources using punctured turbo codes. *IEEE Commun. Lett.*, 6(9):394–396. 15, 17, 59

Garcia-Frias, J. and Zhong, W. (2003). Ldpc codes for compression of multi-terminal sources with hidden markov correlation. *IEEE Commun. Lett.*, 7(3):115–117. 15, 17, 59

Garcia-Frias, J., Zhong, W., and Zhao, Y. (2003). Turbo-like codes for source and joint source-channel coding. *Proc. of 3rd Int. Symp. Turbo Codes and Related Topics*. 15, 17, 59

Godoy, E., Scorzoni, F., and Porto, A. J. V. (2012). Evaluating serial zigbee devices for application in wireless networked control systems. In *IECON 2012 - 38th Annual Conference on IEEE Industrial Electronics Society*, pages 3176–3181. 2

Gong, S., Li, H., Lai, L., and Qiu, R. (2011). Decoding the 'nature encoded' messages for distributed energy generation control in microgrid. In *Communications (ICC), 2011 IEEE International Conference on*, pages 1–5. 33, 38

Guo, D., Shamai, S., and Verdú, S. (2005). Mutual information and mimimum mean-square error in gaussian channels. *IEEE Trans. Inf. theory*, 51(4):1261–1281. 16, 17, 58, 62, 63, 80

Gupta, V., Chung, T. H., Hassibi, B., and Murray, R. M. (2006). On a stochastic sensor selection algorithm with applications in sensor scheduling and sensor coverage. *Automatica*, 42(2):251–260. 10

Gupta, V., Dana, A., Hespanha, J., Murray, R., and Hassibi, B. (2009). Data transmission over networks for estimation and control. *Automatic Control, IEEE Transactions on*, 54(8):1807–1819. 9, 10

Gupta, V., Hassibi, B., and Murray, R. M. (2007a). Optimal lqg control across packet-dropping links. *System and Control Letters*, 56(6):439–446. 12

Gupta, V., Martins, N., and Baras, J. (2007b). Stabilization using multiple sensors over analog erasure channels. In *Modeling and Optimization in Mobile, Ad Hoc and Wireless Networks and Workshops, 2007. WiOpt 2007. 5th International Symposium on*, pages 1–7. 12

Han, D. and Lim, J. (2010). Smart home energy management system using ieee 802.15.4 and zigbee. *Consumer Electronics, IEEE Transactions on*, 56(3):1403–1410. 2

Heegard, C. and Wicker, S. (1999). *Turbo coding*. Kluwer International Series in Engineering and Computer Science. Kluwer Academic, Boston. 15

Imer, O. C., Yuksel, S., and Basar, T. (2006). Optimal control of dynamical systems over unreliable communication links. *Automatica*, 42(9):1429–1440. 8, 60

Jing, C., Shu, D., and Gu, D. (2007). Design of streetlight monitoring and control system based on wireless sensor networks. In *Industrial Electronics and Applications, 2007. ICIEA 2007. 2nd IEEE Conference on*, pages 57–62. 2

Kang, M., Ke, Y., and Li, J. (2011). Implementation of smart loading monitoring and control system with zigbee wireless network. In *6th IEEE Conference on Industrial Electronics and Applications (ICIEA)*, pages 907–912. 2

Kim, Y., Evans, R., and Iversen, W. (2008). Remote sensing and control of an irrigation system using a distributed wireless sensor network. *Instrumentation and Measurement, IEEE Transactions on*, 57(7):1379–1387. 2

Larsen, T., Andersen, N., Ravn, O., and Poulsen, N. (1998). Incorporation of time delayed measurements in a discrete-time kalman filter. In *Decision and Control, 1998. Proceedings of the 37th IEEE Conference on*, volume 4, pages 3972–3977 vol.4. 8

Lee, S., Park, J., Ha, K., and Lee, K. (2008). Wireless networked control system using ndis-based four-layer architecture for ieee 802.11b. In *IEEE International Workshop on Factory Communication Systems*, pages 101–104. 2

Lin, H. and Antsaklis, P. (2004). Persistent disturbance attenuation properties for networked control systems. In *Decision and Control, 2004. CDC. 43rd IEEE Conference on*, volume 1, pages 953–958 Vol.1. 13

Lin, H. and Antsaklis, P. J. (2005). Stability and hinf performance preserving scheduling policy for networked control systems. In *In Proc. of the 16th World Congress of Int. Federation of Automat. Contr.* 13

Lin, H., Zhai, G., and Antsaklis, P. (2003). Robust stability and disturbance attenuation analysis of a class of networked control systems. In *Decision and Control, 2003. Proceedings. 42nd IEEE Conference on*, volume 2, pages 1182–1187 Vol.2. 13

Liu, Q., Wang, X., and Rao, N. S. V. (2012). Fusion of state estimates over long-haul sensor networks under random delay and loss. In *INFOCOM, 2012 Proceedings IEEE*, pages 2686–2690. 10

Liu, X. and Goldsmith, A. (2004). Kalman filtering with partial observation losses. In *Decision and Control, 2004. CDC. 43rd IEEE Conference on*, volume 4, pages 4180–4186 Vol.4. 8

Ma, X., Djouadi, S., and Charalambous, C. (2011). Optimal filtering over uncertain wireless communication channels. *Signal Processing Letters, IEEE*, 18(6):359–362. 8

Ma, X., Djouadi, S., Kuruganti, T., Nutaro, J., and Li, H. (2009). Optimal estimation over unreliable communication links with application to cognitive radio. In *Decision and Control, 2009 held jointly with the 2009 28th Chinese Control Conference. CDC/CCC 2009. Proceedings of the 48th IEEE Conference on*, pages 4062–4067. 9

Ma, X., Djouadi, S., Kuruganti, T., Nutaro, J., and Li, H. (2010). Control and estimation through cognitive radio with distributed and dynamic spectral activity. In *American Control Conference (ACC), 2010*, pages 289–294. 9

Ma, X., Djouadi, S., and Li, H. (2012). State estimation over a semi-markov model based cognitive radio system. *Wireless Communications, IEEE Transactions on*, 11(7):2391–2401. 9

Machowski, J., Bialek, J. W., and Bumby, J. R. (2008). *Power system dynamics: stability and control*. Wiley. 31

Martins, N., Dahleh, M., and Elia, N. (2006). Feedback stabilization of uncertain systems in the presence of a direct link. *Automatic Control, IEEE Transactions on*, 51(3):438–447. 12

Matveev, A. and Savkin, A. (2003). The problem of state estimation via asynchronous communication channels with irregular transmission times. *Automatic Control, IEEE Transactions on*, 48(4):670–676. 8

McEliece, R., MacKay, D., and Cheng, J. (1998). Turbo decoding as an instance of pearl's 'belief propagation' algorithm. *IEEE Journal on selected areas in communications*, 16(2):140–152. 23

Mei, Z. and Wu, L. (2006). Joint source-channel decoding of huffman codes with ldpc codes. *J. Electron.*, 23(6):806–809. 15, 17, 59

Minero, P., Coviello, L., and Franceschetti, M. (2013). Stabilization over markov feedback channels: the general case. *Automatic Control, IEEE Transactions on*, 58(2):349–362. 12, 59

Minero, P., Franceschetti, M., Dey, S., and Nair, G. (2009). Data rate theorem for stabilization over time-varying feedback channels. *Automatic Control, IEEE Transactions on*, 54(2):243–255. 12, 59

Mo, Y., Garone, E., Casavola, A., and Sinopoli, B. (2011). Stochastic sensor scheduling for energy constrained estimation in multi-hop wireless sensor networks. *Automatic Control, IEEE Transactions on*, 56(10):2489–2495. 10

Moayedi, M., Foo, Y., and Soh, Y. (2010). Adaptive kalman filtering in networked systems with random sensor delays, multiple packet dropouts and missing measurements. *Signal Processing, IEEE Transactions on*, 58(3):1577–1588. 9

Montestruque, L. and Antsaklis, P. (2002a). Model-based networked control systems: necessary and sufficient conditions for stability. In *10th Mediterranean Conference on Control and Automation*. 14

Montestruque, L. and Antsaklis, P. (2002b). State and output feedback control in model-based networked control systems. In *Decision and Control, 2002, Proceedings of the 41st IEEE Conference on*, volume 2, pages 1620–1625 vol.2. 14

Montestruque, L. and Antsaklis, P. (2003a). On the model-based control of networked systems. *Automatica*, 39(10):1837C1843. 14

Montestruque, L. and Antsaklis, P. (2003b). Stability of model-based networked control systems with time-varying transmission times. In *Proc. Amer. Contr. Conf.*, volume 5, page 4119C4124. 14

Montestruque, L. and Antsaklis, P. (2004). Stability of model-based networked control systems with time-varying transmission times. *Automatic Control, IEEE Transactions on*, 49(9):1562–1572. 14

Mostofi, Y. and Murray, R. (2004). Effect of time-varying fading channels on control performance of a mobile sensor. In *Sensor and Ad Hoc Communications and Networks, 2004. IEEE SECON 2004. 2004 First Annual IEEE Communications Society Conference on*, pages 317–324. 60

Mostofi, Y. and Murray, R. (2009a). Kalman filtering over wireless fading channels. *Special Issue on Control with Limited Information, International Journal of Robust and Nonlinear Control*, 19:1993–2015. 9

Mostofi, Y. and Murray, R. (2009b). Kalman filtering over wireless fading channels - how to handle packet drop. *Special Issue on Control with Limited Information, International Journal of Robust and Nonlinear Control*, 19:1993–2015. 9, 60

Mostofi, Y. and Murray, R. (2009c). To drop or not to drop: Design principles for kalman filtering over wireless fading channels. *Automatic Control, IEEE Transactions on*, 54(2):376–381. 3, 9, 60

Nahi, N. (1969). Optimal recursive estimation with uncertain observation. *Information Theory, IEEE Transactions on*, 15(4):457–462. 8

Nair, G. N. and Evans, R. J. (2004). Stabilizability of stochastic linear systems with finite feedback data rates. *SIAM J. Control Optimiz.*, 43(2):413C436. 12, 59

Nesic, D. and Teel, A. (2004). Input-output stability properties of networked control systems. *Automatic Control, IEEE Transactions on*, 49(10):1650–1667. 14

Nilsson, J., Bernhardsson, B., and Wittenmark, B. (1998). Stochastic analysis and control of real-time systems with random time delays. *Automatica*, 34(1):57–64. 8

Pan, X., Cuhadar, A., and Banihashemi, A. H. (2006). Combined source and channel coding with jpeg2000 and rate-compatible low-density parity-check codes. *IEEE Trans. Signal Processing*, 54(3):1160–1164. 15, 17, 59

Pearl, J. (1988). *Probabilistic reasoning in intelligent systems: networks of plausible inference*. Morgan Kaufmann, San Mateo, CA. 23

Pu, L., Wu, Z., Bilgin, A., Marcellin, M. W., and Vasic, B. (2007). Ldpc-based iterative joint source-channel decoding for jpeg2000. *IEEE Trans. Image Processing*, 16(2):577–581. 15, 17, 59

Quevedo, D., Ahlen, A., and Ostergaard, J. (2010). Energy efficient state estimation with wireless sensors through the use of predictive power control and coding. *Signal Processing, IEEE Transactions on*, 58(9):4811–4823. 10

Quevedo, D., Ostergaard, J., and Ahlen, A. (2013). Power control and coding formulation for state estimation with wireless sensors. *Control Systems Technology, IEEE Transactions on*, PP(99):1–1. 10

Ramzan, N., Wan, S., and Izquierdo, E. (2007). Joint source-channel coding for wavelet-based scalable video transmission using an adaptive turbo code. *J. Image Video Processing*, 2007(1):1–12. 15, 17, 59

Refaat, T., Daoud, R., Amer, H., and Makled, E. (2010). Wifi implementation of wireless networked control systems. In *Networked Sensing Systems (INSS), 2010 Seventh International Conference on*, pages 145–148. 2

Richardson, T. and Urbanke, R. (2001). The capacity of low-density parity check codes under message passing decoding. *IEEE Trans. Inform. Theory*, 47:599–618. 23

Schenato, L. (2008). Optimal estimation in networked control systems subject to random delay and packet drop. *Automatic Control, IEEE Transactions on*, 53(5):1311–1317. 8, 60

Schenato, L., Sinopoli, B., Franceschetti, M., Poolla, K., and Sastry, S. (2007). Foundations of control and estimation over lossy networks. *Proceedings of the IEEE*, 95(1):163–187. 60

Shannon, C. E. (1948). A mathematical theory of communication. *Bell Syst. Tech. J.* 11

Sinopoli, B., Schenato, L., Franceschetti, M., Poolla, K., Jordan, M., and Sastry, S. (2004). Kalman filtering with intermittent observations. *Automatic Control, IEEE Transactions on*, 49(9):1453–1464. 8, 12, 60

Smith, S. and Seiler, P. (2003). Estimation with lossy measurements: jump estimators for jump systems. *Automatic Control, IEEE Transactions on*, 48(12):2163–2171. 8

Song, J. (2010). Greenhouse monitoring and control system based on zigbee wireless senor network. In *2010 International Conference on Electrical and Control Engineering (ICECE)*, pages 2785–2788. 2

Song, Y. H., Park, J. H., Lee, K. Z., and Lee, S. (2009). Performance evaluation of wireless networked control system using time-triggered ieee 802.15.4. In *ICCAS-SICE*, pages 2187–2191. 2

Tatikonda, S. and Mitter, S. (2004). Control over noisy channels. *Automatic Control, IEEE Transactions on*, 49(7):1196–1201. 11, 59

ten Brink, S. (1999). Convergence of iterative decoding. *Electron. Lett.*, 35(1):1117–1118. 16, 58, 62, 63

ten Brink, S. (2000). Iterative decoding trajectories of parallel concatenated codes. *Proc. 3rd IEEE/ITG Symp. Source and Channel Coding*, pages 75–80. 16, 58, 62, 63

ten Brink, S. (2001). Convergence behavior of iteratively decoded parallel concatenated codes. *IEEE Trans. Commun*, 49(10):1727–1737. 16, 58, 62, 63

Tüchler, M., Koetter., R., and Singer, A. C. (2002). Turbo equalization: principles and new results. *IEEE Trans. Commun*, 50(5):754–767. 5, 19

Vembu, S., Verdu, S., and Steinberg, Y. (1995). The source-channel separation theorem revisited. *IEEE Trans. Inform. Theory*, 41(1):44–54. 15

Walsh, G., Ye, H., and Bushnell, L. (2002). Stability analysis of networked control systems. *Control Systems Technology, IEEE Transactions on*, 10(3):438–446. 14

Xu, Y. and Hespanha, J. (2004). Optimal communication logics in networked control systems. In *Decision and Control, 2004. CDC. 43rd IEEE Conference on*, volume 4, pages 3527–3532 Vol.4. 9, 10

Xu, Y. and Hespanha, J. (2005). Estimation under uncontrolled and controlled communications in networked control systems. In *Decision and Control, 2005 and 2005 European Control Conference. CDC-ECC '05. 44th IEEE Conference on*, pages 842–847. 10

Xy, Y. and Hespanha, J. (2005). Estimation under uncontrolled and controlled communications in networked control systems. In *Decision and Control, 2005 and 2005 European Control Conference. CDC-ECC '05. 44th IEEE Conference on*, pages 842–847. 9

Yang, C., Wu, J., Zhang, W., and Shi, L. (2013). Schedule communication for decentralized state estimation. *Signal Processing, IEEE Transactions on*, 61(10):2525–2535. 10

Yen, B. X., Hop, D. T., and Yoo, M. (2013). Redundant transmission in wireless networked control system over ieee 802.15.4e. In *Information Networking (ICOIN), 2013 International Conference on*, pages 628–631. 2

Yin, L., Lu, J., and Wu, Y. (2002). Ldpc-based joint source and channel coding scheme for multimedia communications. *Proc. of 8th Int. Conf. Communication Systems*. 15, 17, 59

Yook, J., Tilbury, D., and Soparkar, N. (2002). Trading computation for bandwidth: reducing communication in distributed control systems using state estimators. *Control Systems Technology, IEEE Transactions on*, 10(4):503–518. 10

You, K. and Xie, L. (2011). Minimum data rate for mean square stabilizability of linear systems with markovian packet losses. *Automatic Control, IEEE Transactions on*, 56(4):772–785. 12, 59

Zhai, G., Hu, B., Yasuda, K., and Michel, A. (2002). Qualitative analysis of discrete-time switched systems. In *American Control Conference, 2002. Proceedings of the 2002*, volume 3, pages 1880–1885 vol.3. 13

Zhang, W., Branicky, M., and Phillips, S. (2001). Stability of networked control systems. *Control Systems, IEEE*, 21(1):84–99. 13

Zhang, W. and Branicky, M. S. (2001). Stability of networked control systems with time-varying transmission period. In *in Allerton Conf. Communication, Contr. and Computing*. 14

Zhao, Y. and Garcia-Frias, J. (2002). Joint estimation and data compression of correlated non-binary sources using punctured turbo codes. *Proc. of Conf. Information Sciences and Systems*. 15, 17, 59

Zhao, Y. and Garcia-Frias, J. (2005). Joint estimation and compression of correlated nonbinary sources using punctured turbo codes. *IEEE Trans. Commun.*, 53(3):385–390. 15, 17, 59

Appendix

Appendix A

Derivation of Equations

A.1 Derivation of Key Steps in the Pearl's BP

In the following derivation part, we will use the following two basic equations, where $\mathcal{N}(x, \mu, \sigma)$ is the probability density function of Gaussian distribution with expectation μ and variance σ at x:

$$\begin{aligned} & \int_{-\infty}^{\infty} \mathcal{N}(\mathbf{x}, \mathbf{m}_1, \mathbf{\Sigma}_1)\mathcal{N}(\mathbf{y}, \mathbf{C}\mathbf{x}, \mathbf{\Sigma}_2)d\mathbf{x} \\ \propto \; & \mathcal{N}(\mathbf{y}, \mathbf{C}\mathbf{m}_1, \mathbf{C}\mathbf{\Sigma}_1\mathbf{C}^T + \mathbf{\Sigma}_2), \end{aligned} \tag{A.1}$$

and

$$\mathcal{N}(\mathbf{x}, \mathbf{m}_1, \mathbf{\Sigma}_1)\mathcal{N}(\mathbf{x}, \mathbf{m}_2, \mathbf{\Sigma}_2) \propto \mathcal{N}(\mathbf{x}, \mathbf{m}_3, \mathbf{\Sigma}_3), \tag{A.2}$$

where the variance is given by

$$\mathbf{\Sigma}_3 = (\mathbf{\Sigma}_1^{-1} + \mathbf{\Sigma}_2^{-1})^{-1}, \tag{A.3}$$

and the expectation is given by

$$\mathbf{m}_3 = \mathbf{\Sigma}_3(\mathbf{\Sigma}_1^{-1}\mathbf{m}_1 + \mathbf{\Sigma}_2^{-1}\mathbf{m}_2). \tag{A.4}$$

Below is the notation used throughout the derivation:

$$\begin{aligned}
\pi_{\mathbf{x}_{t-1},\mathbf{x}_t}(\mathbf{x}_{t-1}) &= \mathcal{N}(\mathbf{x}_{t-1}, \mathbf{x}_{\pi_x,t-1}, P_{\pi_x,t-1}) \\
\pi_{\mathbf{x}_{t-1},\mathbf{y}_{t-1}}(\mathbf{x}_{t-1}) &= \mathcal{N}(\mathbf{x}_{t-1}, \mathbf{x}_{\pi_y,t-1}, P_{\pi_y,t-1}) \\
\pi_{\mathbf{y}_t,\mathbf{b}_t}(\mathbf{y}_t) &= \mathcal{N}(\mathbf{y}_t, \mathbf{y}_{\pi,t}, S_{\pi,t}) \\
\pi_{\mathbf{x}_t}(\mathbf{x}_t) &= \mathcal{N}(\mathbf{x}_t, \mathbf{x}_{l,t}, P_{l,t}) \\
\pi_{\mathbf{y}_t}(\mathbf{y}_t) &= \mathcal{N}(\mathbf{y}_t, \mathbf{y}_{l,t}, S_{l,t}) \\
\lambda_{\mathbf{y}_t,\mathbf{x}_t}(\mathbf{x}_t) &= \mathcal{N}(\mathbf{x}_t, \mathbf{x}_{\lambda_y,t}, P_{\lambda_y,t}) \\
\lambda_{\mathbf{x}_t,\mathbf{x}_{t-1}}(\mathbf{x}_{t-1}) &= \mathcal{N}(\mathbf{x}_{t-1}, \mathbf{x}_{\lambda_x,t-1}, P_{\lambda_x,t-1}) \\
\lambda_{\mathbf{b}_t,\mathbf{y}_t}(\mathbf{y}_t) &= \mathcal{N}(\mathbf{y}_t, \mathbf{y}_{\lambda,t}, S_{\lambda,t}) \\
\mathrm{BEL}(\mathbf{x}_t) &= \mathcal{N}(\mathbf{x}_t, \mathbf{x}_{\mathrm{BEL},t}, P_{\mathrm{BEL},t}) \\
p(\mathbf{x}_t|\mathbf{x}_{t-1}) &= \mathcal{N}(\mathbf{x}_t, A\mathbf{x}_{t-1} + B\mathbf{u}_{t-1}, \Sigma_p).
\end{aligned}$$

1. Step 1: $\mathbf{x}_{t-1} \rightarrow \mathbf{y}_{t-1}$: we have

$$\begin{aligned}
& \pi_{\mathbf{x}_{t-1}}(x_{t-1}) \\
= & \int_{-\infty}^{\infty} p(\mathbf{x}_{t-1}|\mathbf{x}_{t-2})\pi_{\mathbf{x}_{t-2},\mathbf{x}_{t-1}}(\mathbf{x}_{t-2})d\mathbf{x}_{t-2} \\
= & \mathcal{N}(\mathbf{x}_{t-1}, \mathbf{x}_{l,t-1}, P_{l,t-1}),
\end{aligned} \tag{A.5}$$

where the expectation is given by

$$\mathbf{x}_{l,t-1} = A\mathbf{x}_{\pi_x,t-2} + B\mathbf{u}_{t-2}, \tag{A.6}$$

and the variance is given by

$$\begin{aligned} P_{l,t-1} &= A \times P_{\pi_x,t-2} \times A^T + \Sigma_p \\ \pi_{\mathbf{x}_{t-1},\mathbf{y}_{t-1}}(\mathbf{x}_{t-1}) &= \pi_{\mathbf{x}_{t-1}}(x_{t-1})\lambda_{\mathbf{y}_{t-1},\mathbf{x}_{t-1}}(\mathbf{x}_{t-1}) \\ &= \mathcal{N}(\mathbf{x}_{t-1}, \mathbf{x}_{l,t-1}, P_{l,t-1}) \times 1 \\ &= \mathcal{N}(\mathbf{x}_{t-1}, \mathbf{x}_{\pi_y,t-1}, P_{\pi_y,t-1}) \qquad \text{(A.7)} \end{aligned}$$

where

$$\mathbf{x}_{\pi_y,t-1} = \mathbf{x}_{l,t-1}; P_{\pi_y,t-1} = P_{l,t-1}. \qquad \text{(A.8)}$$

2. Step 2: $\mathbf{y}_{t-1} \rightarrow \mathbf{b}_{t-1}$:

$$\begin{aligned} \pi_{\mathbf{y}_{t-1}}(\mathbf{y}_{t-1}) &= \int_{-\infty}^{\infty} p(\mathbf{y}_{t-1}|\mathbf{x}_{t-1})\pi_{\mathbf{x}_{t-1},\mathbf{y}_{t-1}}(\mathbf{x}_{t-1})d\mathbf{x}_{t-1} \\ &= N(\mathbf{y}_{t-1}, \mathbf{y}_{l,t-1}, S_{l,t-1}) \qquad \text{(A.9)} \end{aligned}$$

where

$$\begin{aligned} \mathbf{y}_{l,t-1} &= C \times \mathbf{x}_{\pi_y,t-1}; \\ S_{l,t-1} &= C \times P_{\pi_y,t-1} \times C^T + \Sigma_o \end{aligned}$$

$$\begin{aligned} \pi_{\mathbf{y}_{t-1},\mathbf{b}_{t-1}}(\mathbf{y}_{t-1}) &= \pi_{\mathbf{y}_{t-1}}(\mathbf{y}_{t-1}) \times 1 \\ &= N(\mathbf{y}_{t-1}, \mathbf{y}_{\pi,t-1}, S_{\pi,t-1}) \qquad \text{(A.10)} \end{aligned}$$

where

$$\begin{aligned} \mathbf{y}_{\pi,t-1} &= \mathbf{y}_{l,t-1}; \\ S_{\pi,t-1} &= S_{l,t-1} \qquad \text{(A.11)} \end{aligned}$$

3. : Step 4: $\mathbf{y}_{t-1} \rightarrow \mathbf{x}_{t-1}$: we have

$$\begin{aligned}
\lambda_{\mathbf{y}_{t-1},\mathbf{x}_{t-1}}(\mathbf{x}_{t-1}) &= \gamma_{\mathbf{y}_{t-1}}(\mathbf{x}_{t-1}) \\
&= \int_{-\infty}^{\infty} \lambda_{\mathbf{b}_{t-1},\mathbf{y}_{t-1}}(\mathbf{y}_{t-1}) p(\mathbf{y}_{t-1}|\mathbf{y}_{x-1}) \\
&= \mathcal{N}(\mathbf{x}_{t-1}, \mathbf{x}_{\lambda_y,t-1}, P_{\lambda_y,t-1}), \qquad \text{(A.12)}
\end{aligned}$$

where the expectation is given by

$$\mathbf{x}_{\lambda_y,t-1} = C^{-1} \times \mathbf{y}_{\lambda,t-1}, \qquad \text{(A.13)}$$

and the variance is given by

$$P_{\lambda_y,t-1} = C^{-1}(S_{\lambda,t-1} + \Sigma_o) \times (C^{-1})^T. \qquad \text{(A.14)}$$

4. Step 5: $\mathbf{x}_{t-1} \rightarrow \mathbf{x}_t$: we have

$$\begin{aligned}
\pi_{\mathbf{x}_{t-1},\mathbf{x}_t}(\mathbf{x}_{t-1}) &= \pi_{\mathbf{x}_{t-1}}(x_{t-1}) \times \lambda_{\mathbf{y}_{t-1},\mathbf{x}_{t-1}}(\mathbf{x}_{t-1}) \\
&= \mathcal{N}(\mathbf{x}_{t-1}, \mathbf{x}_{\pi_x,t-1}, P_{\pi_x,t-1}), \qquad \text{(A.15)}
\end{aligned}$$

where the variance is given by

$$P_{\pi_x,t-1} = (P_{l,t-1}^{-1} + P_{\lambda,t-1}^{-1})^{-1}, \qquad \text{(A.16)}$$

and the expectation is given by

$$\begin{aligned}
\mathbf{x}_{\pi_x,t-1} &= P_{\pi_x,t-1} \times (P_{l,t-1}^{-1} \times \mathbf{x}_{l,t-1} \\
&+ P_{\lambda,t-1}^{-1} \mathbf{x}_{\lambda,t-1}).
\end{aligned}$$

The belief is thus given by

$$\begin{aligned} \mathrm{BEL}\mathbf{x}_{t-1} &= \alpha \times 1 \times \lambda_(\mathbf{y}_{t-1}, \mathbf{x}_{t-1})(\mathbf{x}_{t-1}) \\ &\times \pi_{\mathbf{x}_{t-1}}(\mathbf{x}_{t-1}) \\ &= \mathcal{N}(\mathbf{x}_{t-1}, \mathbf{x}_{\mathrm{BEL},t-1}, P_{\mathrm{BEL},t-1}), \end{aligned} \tag{A.17}$$

where the variance is given by

$$P_{\mathrm{BEL},t-1} = (P^{-1}_{\lambda_y,t-1} + P^{-1}_{l,t-1})^{-1}, \tag{A.18}$$

and the expectation is given by

$$\begin{aligned} \mathbf{x}_{\mathrm{BEL},t-1} &= P_{\mathrm{BEL},t-1} \times (P^{-1}_{\lambda_y,t-1} \times \mathbf{x}_{\lambda_y,t-1} \\ &+ P^{-1}_{l,t-1} \times \mathbf{x}_{l,t-1}). \end{aligned} \tag{A.19}$$

5. Step 10: $\mathbf{x}_t \rightarrow \mathbf{x}_{t-1}$, we have

$$\begin{aligned} \lambda_{\mathbf{x}_t,\mathbf{x}_{t-1}}(\mathbf{x}_{t-1}) &= \gamma_{\mathbf{x}_t}(\mathbf{x}_{t-1}) \\ &= \int_{-\infty}^{\infty} \lambda_{\mathbf{y}_t,\mathbf{x}_t}(\mathbf{x}_t) p(\mathbf{x}_{t-1}|\mathbf{y}_{t-1}) d\mathbf{x}_t \\ &= \mathcal{N}(\mathbf{x}_{t-1}, \mathbf{x}_{\lambda_x,t-1}, P_{\lambda_x,t-1}), \end{aligned} \tag{A.20}$$

where the variance is given by

$$\begin{aligned} P_{\lambda_x,t-1} &= A^{-1}(\Sigma_p + P_{\lambda_y,t})(A^{-1})^T \\ \mathbf{x}_{\lambda_x,t-1} &= A^{-1}\mathbf{x}_{\lambda_y,t} - A^{-1}B \times \mathbf{u}_{t-1}. \end{aligned} \tag{A.21}$$

6. Step 11: $\mathbf{x}_{t-1}$ update

$$\begin{aligned} \mathrm{BEL}\mathbf{x}_{t-1} &= \alpha \times \lambda_{\mathbf{x}_t,\mathbf{x}_{t-1}}(\mathbf{x}_{t-1}) \times \lambda_{\mathbf{y}_{t-1},\mathbf{x}_{t-1})(\mathbf{x}_{t-1}} \times \pi_{\mathbf{x}_{t-1}}(\mathbf{x}_{t-1}) \\ &= N(\mathbf{x}_{t-1}, \mathbf{x}_{\mathrm{BEL},t-1}, P_{\mathrm{BEL},t-1}) \end{aligned} \tag{A.22}$$

where

$$P_{\mathrm{BEL},t-1} = (P^{-1}_{\lambda_y,t-1} + P^{-1}_{\lambda_x,t-1} + P^{-1}_{l,t-1})^{-1}$$

and

$$\begin{aligned} \mathbf{x}_{\mathrm{BEL},t-1} &= P_{\mathrm{BEL},t-1} \times (P^{-1}_{\lambda_y,t-1} \times \mathbf{x}_{\lambda_y,t-1} \\ &+ P^{-1}_{\lambda_x,t-1} \times \mathbf{x}_{\lambda_x,t-1} + P^{-1}_{l,t-1} \times \mathbf{x}_{l,t-1}) \\ \pi_{\mathbf{x}_{t-1},\mathbf{y}_{t-1}}(\mathbf{x}_{t-1}) &= \pi_{\mathbf{x}_{t-1}}(\mathbf{x}_{t-1}) \lambda_{\mathbf{x}_t,\mathbf{x}_{t-1}}(\mathbf{x}_{t-1}) \\ &= N(\mathbf{x}_{t-1}, \mathbf{x}_{\pi_y,t-1}, P_{\pi_y,t-1}) \end{aligned} \tag{A.23}$$

$$\tag{A.24}$$

where

$$P_{\pi_y,t-1} = (P^{-1}_{\lambda_x,t-1} + P^{-1}_{l,t-1})^{-1}$$

and

$$\mathbf{x}_{\pi_y,t-1} = P_{\pi_y,t-1} \times (P^{-1}_{\lambda_x,t-1} \times \mathbf{x}_{\lambda_x,t-1} + P^{-1}_{l,t-1} \times \mathbf{x}_{l,t-1})$$

Vita

Shuping Gong was born in Yiyang, P.R. China. He received his B.S. degree in electrical engineering from Hainan University in 2004, and his M.S. degree in electrical engineering from University of Electronic Science and Technology of China in 2007. From 2007 to 2008, he worked as an assistant engineer at Huawei Technologies Co. Ltd, Shenzhen, P.R. China. He started his Ph.D. study at The University of Tennessee, Knoxville, in January 2009. His current interests include integration of wireless communication into Smart Grid and Cognitive Radio. Shuping is one of the recipient of the Best Paper Awards of IEEE ICC in 2011. From January to August 2012, he worked as a student intern at Broadcom. Then, he joined Broadcom and became a Staff II engineer. He will complete his Doctor of Philosophy degree in Electrical Engineering in December 2013.